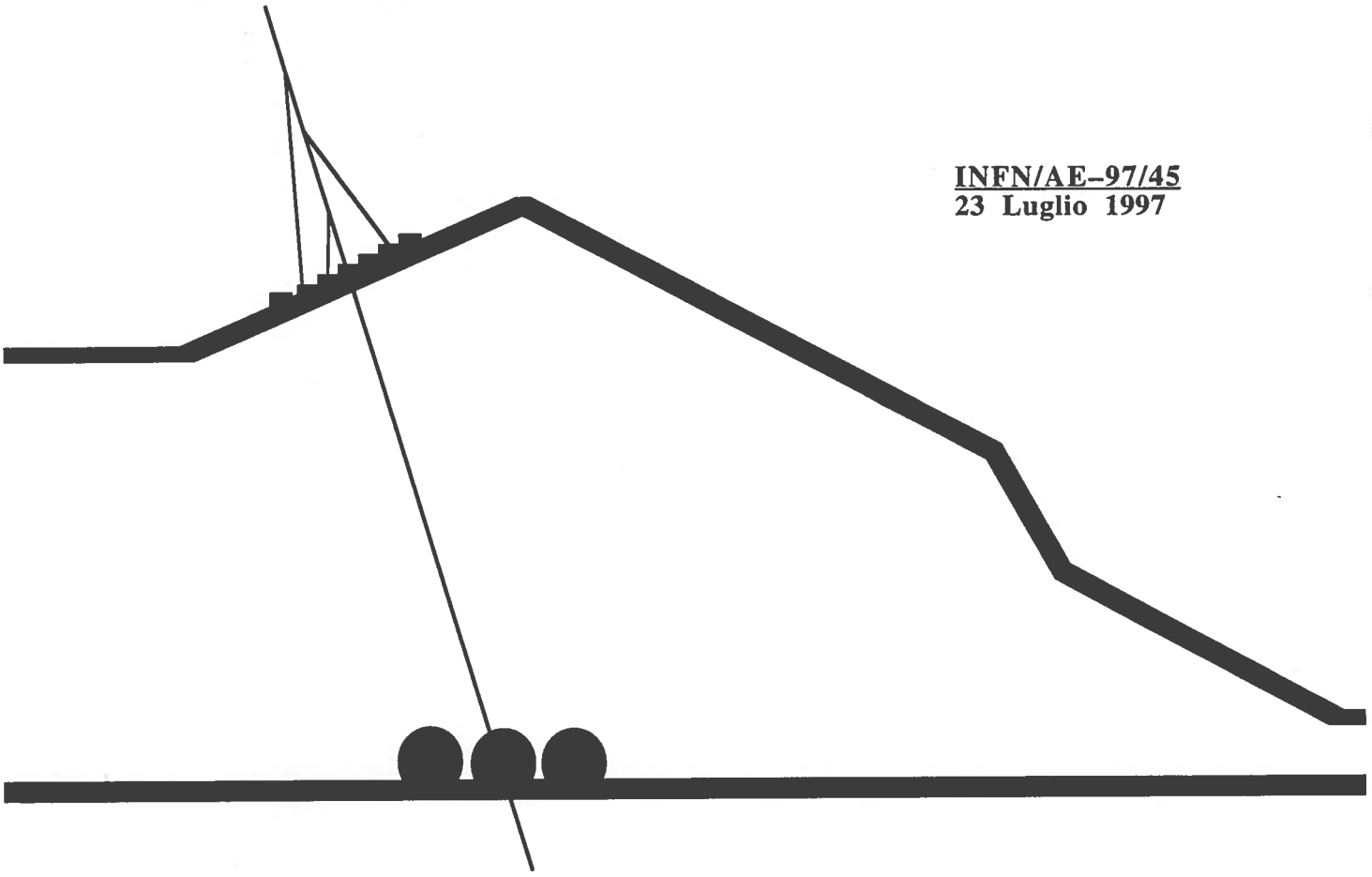

INFN/AE-97/45
23 Luglio 1997

DPMJET version II.3 and II.4

J. Ranft

INFN - Laboratori Nazionali del Gran Sasso

Published by ***SIS–Pubblicazioni***
dei Laboratori Nazionali di Frascati

INFN – Istituto Nazionale di Fisica Nucleare
Laboratori Nazionali del Gran Sasso

INFN/AE–97/45
23 Luglio 1997

DPMJET versions II.3 and II.4

Sampling of hadron–hadron, hadron-nucleus and nucleus-nucleus interactions at Cosmic Ray energies according to the Dual Parton Model

Description of the model and code manual

J. Ranft)[1]
INFN Laboratorio Nazionale del Gran Sasso

DPMJET is based on the DTUNUC model, which was written together with H.–J. Möhring. It uses parts of the DTUJET code written together with P.Aurenche, F.W.Bopp, A.Capella, R.Engel, K.Hahn, D.Pertermann and J.Tran Thanh Van. It uses the HADRIN code written together with K.Hänßgen and the DECAY code written together with S.Ritter and K.Hänßgen. The present version of the formation zone intranuclear cascade in the target and projectile nuclei and the model for diffractive events was written together with S.Roesler. Nuclear evaporation, Fermi break–up, γ–deexcitation and residual nuclei were implemented together with A.Ferrari, S.Roesler and P.Sala. DPMJET was introduced together with G.Battistoni and C.Forti into the cosmic ray cascade code HEMAS–DPM and applied to problems of the cosmic ray cascade. DPMJET uses the JETSET code due to T. Sjöstrand and collaborators, the lepto code due to G.Ingelman, A.Edin and J.Rathsman, the DIAGEN code due to Shmakov, Uzhinskii and Zadoroshny and the qel code due to P.Lipari.

Abstract

The dual parton model provides a unique picture for the calculation of cross sections for hadron–hadron, hadron–nucleus and nucleus–nucleus interactions and for the description of particle production in hadron–hadron, hadron–nucleus and nucleus–nucleus collisions at high energies. The two–component Dual Parton Model is used with multiple soft chains and multiple minijets at each elementary interaction. Within this model the high–energy projectile undergoes a multiple scattering process as formulated in Glauber's approach; particle production is realised by the fragmentation of colorless parton–parton chains constructed from the quark content of the interacting hadrons. DPMJET–II.3 and II.4 includes the cascading of secondaries within the target as well as projectile nuclei which is suppressed by the formation time concept. The excitation energy of the remaining target and projectile nuclei is calculated and using this nuclear evaporation is included into the model.

At lab energies below $3 - 5$ *GeV* hadron–nucleus collisions are described within the conventional formation zone intranuclear cascade picture; thus the model may be applied down to such energies. The present formulation of minijet production allows to use the model up to primary energies of 10^{21} eV (per nucleon) in the lab. frame.

DPMJET can also be applied to neutrino nucleus collisions. It extends the neutrino–nucleon models qel (quasi elastic neutrino interactions) and lepto (deep inelastic neutrino nucleon collisions) to neutrino collisions on nuclear targets.

)[1] *J.Ranft, e–mail: Johannes.Ranft@cern.ch and ranft@hpcalc.lnf.infn.it*

1 Introduction

The DPMJET–II.2 event generator [1] was described in detail before [1, 2]. Here, the main topic will be the extension of this model up to energies of $\sqrt{s} = 2000$ TeV, the resulting model will be refered to as DPMJET–II.3 or DPMJET–II.4. These two versions differ mainly by the versions of the Lund code JETSET they use. Since starting with the 1997 version PYTHIA–6.1 (now in DOUBLE PRECISION) (in which JETSET is contained) the names of all routines and common blocks are changed, the two versions of DPMJET should not be mixed. The extension to higher energies is done by calculating the minijet component of the model using new parton distribution functions, the GRV–LO parton distributions [3] (this is the new default) and the CTEQ4 parton distributions [4], which are both available in a larger Bjorken–x range than the MRS(D-) parton distributions, which were the default in DPMJET–II.2 and DTUJET–93 [5]. These new parton distributions describe the data measured in the last years at the HERA Collider.

A hadron production model to be used for simulations at accelerator and Cosmic Ray energies should use all possible information from fixed target experiments and collider experiments at accelerators. There might be large differences on what is considered important: Best studied at accelerators is the central region in hadron–hadron collisions. For studying the Cosmic Ray cascade, the main interest is in the forward fragmentation region of hadron–nucleus and nucleus–nucleus collisions.

DPMJET–II simulates hadron production in the framework of the Dual Parton Model with emphasis as well in the central as in the fragmentation region. Important for simulations in a wide energy range and with many different targets and projectiles are two aspects of multiparticle production:

(i)The change of particle production with energy, starting from the region well studied at present accelerator experiments.

(ii)The dependence of particle production on the nuclear target (and projectile).

A model for hadronic and nuclear interactions should provide the basic hadronic interaction term for the hadron cascade. It should provide the cross sections for hadron–hadron, hadron–nucleus and nucleus–nucleus collisions as function of the energy. Secondary π^0 and η mesons are the source of the electromagnetic shower, secondary $\pi^{\pm}$ and $K^{\pm}$ mesons are the source of Muons and the source of Neutrinos produced by the cascade. Secondary charmed mesons are the source for prompt Muons and Neutrinos. The model should work from the pion production threshold up to the highest possible primary energies.

Soft multiparticle production characterizing hadronic interactions at supercollider or Cosmic Ray energies cannot be understood purely within theoretical approaches provided by perturbative QCD. The nonperturbative soft component of hadron production, which is responsible for all of hadron production at low energies is still acting at higher energies.

The energy dependence of hadron production has so far been best studied in hadron–hadron collisions.

Using basic ideas of the dual topological unitarization scheme [6, 7] the Dual Parton Model (DPM) (a recent review is given in Ref.[8]) has been very successfully describing soft hadronic processes.

Observations like rapidity plateaus and average transverse momenta rising with energy, KNO scaling violation, transverse momentum–multiplicity correlations and *minijets* pointed out, that soft and hard processes are closely related. These properties were understood within the two–component Dual Parton Model [9, 10, 11, 12, 13, 14, 5].

The hard component is introduced applying lowest order of perturbative hard constituent scattering [15]. Single diffraction dissociation is represented by a triple–pomeron exchange (high mass single diffraction) and a low mass component.

The Dual Parton model provides a framework not only for the study of hadron–hadron interactions, but also for the description of particle production in hadron–nucleus and nucleus–nucleus collisions at high energies. Within this model the high energy projectile undergoes a multiple scattering as formulated in Glaubers approach; particle production is again realized by the fragmentation of colorless parton–parton chains constructed from the quark content of the interacting hadrons.

The first successfull applications of the Monte Carlo version of the dual parton model (DPM) to hadron–nucleus [16, 17] and nucleus–nucleus [18, 19, 20] collisions also demonstrated that the cascade of created secondaries in the target (and projectile) nuclei contributes significantly to particle production in the target (and projectile) fragmentation regions. On the other hand, it is known for many years that a naive treatment of intranuclear cascade processes on the basis of elementary cross sections overestimates the particle yields, if the incident energy significantly exceeds five or ten GeV [21, 22].

This problem may be solved by introducing the concept of a formation zone [23, 24] suppressing in a natural way the cascading of high–energy secondaries. The Monte Carlo model includes intranuclear cascade processes of the created secondaries combined with the formation time concept since the first version of DPMJET–II. The

FZIC (formation zone intranuclear cascade) was also introduced for the projectile nucleus and in addition the nuclear evaporation and fragmentation of the residual nucleus was introduced into DPMJET–II [25, 26].
In the following we briefly sketch the basic ideas of the model and mention the most important ingredients; for a more detailed description of the model as applied in the code we refer to Refs. [16, 17, 27, 28, 29, 30, 31, 32, 33, 34, 25, 26, 35, 36, 37].

In Section 2 we will describe the basic physical concepts of the Dual Parton Model as used in DPMJET–II. Furthermore, we discuss the implementation of the minijet component. The minijet component is of prime importance to implement the model at the highest energies. In Section 3 we compare the model to data and in Section 4 we discuss the properties of the model at the highest energies. In both these Sections we present only material obtained with DPMJET–II.3 and –II.4. At energies below $\sqrt{s} = 1$ to 2 TeV it is not to be expected, that the model has changed so strongly, that comparisons given in former papers would have become invalid. Section 5 gives a description of the DPMJET–II code. Further more technical details about the DPMJET–II code are given in some Appendices. Appendix A desribes the DPMJET–II test program, the particle codes used, the input cards for the test program and sample inputs. Appendix B discusses the event history and the event common block HKKEVT. Minor problems are discussed in Appendices C and D.

2 Basic physical concepts of the Dual Parton Model

2.1 The energy dependence of multiparticle production and the two–component Dual Parton Model for hadron–hadron collisions

The soft input cross section in our unitarization scheme is described by the supercritical pomeron

$$\sigma_s = g^2 s^{\alpha(0)-1} \tag{1}$$

with g being the effective proton–pomeron coupling constant and $\alpha(0)$ the pomeron intercept. The corresponding pomeron–trajectory is given by $\alpha(t) = \alpha(0) + \alpha' t$.

The supercritical pomeron was used in the two–component DPM from the beginning [9], while the so called minijet models use the critical pomeron with $\alpha(0) = 1$ from Durand and Pi [38] over Gaisser and Halzen [39] , SIBYLL [40] up to HIJING [41]. A large part of the differences between the results of these models and the DPM–results is due to this different starting point. In all fits of the pomeron parameters to cross section data , we get consistently better fits with the supercritical pomeron than with the critical one. *These better fits to the supercritical pomeron are our main argument for the continuous presence of the soft component to multiparticle production up to the highest energies.*

Besides the supercritical soft (Fig.1(a)) and the hard pomeron (Fig.1(b)) we introduce graphs with pomeron–pomeron couplings. Provided that the pomeron–pomeron coupling constant Γ is small in comparison with other couplings, such as g, it is sufficient to consider the expansion in Γ only up to first order [10] . Thus a correction to the pure pomeron–exchange is represented by the triple–pomeron graph (Fig. 1(c)). included with an input cross section

$$\sigma_{TP} = \frac{2}{16\pi} \frac{g^3 \Gamma}{b_{TP}} ln \frac{s}{s_0} \tag{2}$$

where b_{TP} is the slope $b_{TP} = b^0_{TP} + 2\alpha' ln(s)$ and $s_0 = 100$ GeV^2.

In Table 1 we give the model parameters obtained in a fit using the two modern parton structure functions.

The simplest cut of the triple–pomeron (Fig. 1(c)) corresponds to a high mass single diffractive interaction. High mass diffraction is a comparatively rare process. High mass means that the diffractively excited system should not be a well defined hadron resonance. We also describe high mass double diffractive processes again to first order introducing loop graphs (Fig. 1(d)), with a cross section

$$\sigma_L = \frac{1}{16\pi} \frac{g^2 \Gamma^2}{2 b_{DD}} (ln^2 \frac{s}{s_0} + ln^2 \frac{s'_0}{s} - 2 ln^2 \frac{5}{20}) \tag{3}$$

with b_{DD} being the slope parameter $b_{DD} = 2\alpha' ln(s)$, $s_0 = 400$ GeV^2, and $s'_0 = 25$ GeV^2.

The input cross section for semihard multiparticle production σ_h is calculated applying the QCD improved parton model, the details are given in Ref.[9, 12, 13, 42].

$$\sigma_h = \sum_{i,j} \int_0^1 dx_1 \int_0^1 dx_2 \int d\hat{t} \; \frac{1}{1+\delta_{ij}} \frac{d\sigma_{QCD,ij}}{d\hat{t}} \; f_i(x_1, Q^2) f_j(x_2, Q^2) \; \Theta(p_\perp - p_{\perp thr}) \tag{4}$$

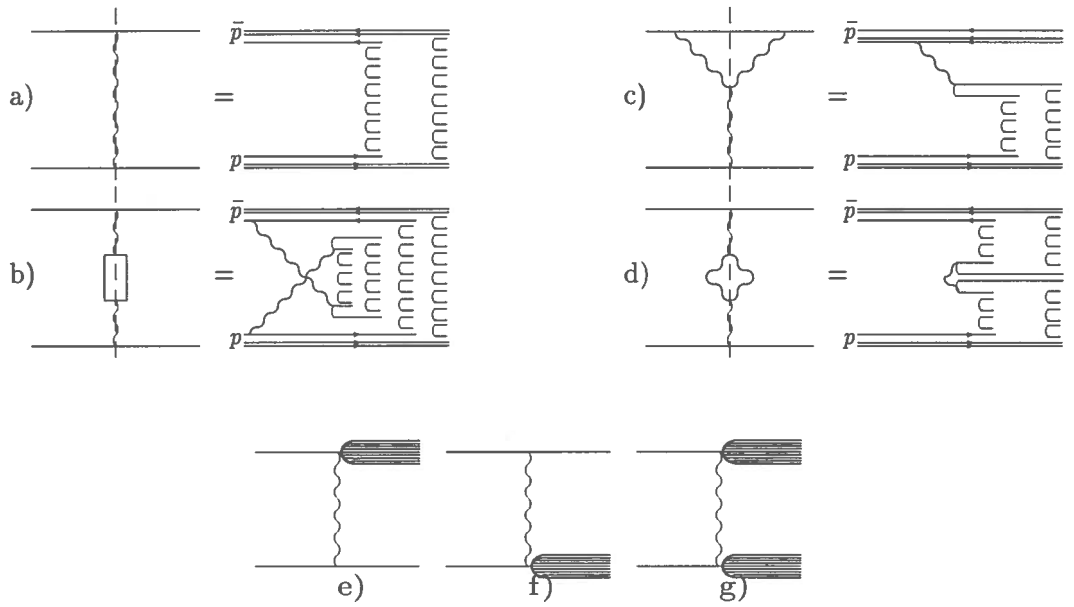

Figure 1: Diagrams and the corresponding cut graphs for the exchange of a) one soft pomeron, b) one hard pomeron, and c) one triple–pomeron (high mass single diffraction). Fig. d) shows one cut pomeron–loop graph (high mass double diffraction). Low mass single diffractive processes (e),(f) and low mass double diffractive processes (g) are introduced via a two–channel eikonal formalism

$f_i(x, Q^2)$ are the structure functions of partons with the flavor i and scale Q^2 and the sum i, j runs over all possible flavors. To remain in the region where perturbation theory is valid, we use a low $p_\perp$ cut–off $p_{\perp_{thr}}$ for the minijet component. Furthermore, since we calculate $\sigma_{QCD,ij}$ in lowest-order QCD perturbation theory we multiply the hard input cross section σ_h with a K factor in the range of 1.5 to 2. A hard interaction leads to a chain system shown in Fig. 1(b).

The momentum fractions of the constituents at the ends of the different chains are sampled using the exclusive parton distribution, which has the form for an event with n_s soft and $n_h (n_h \geq 1)$ hard pomerons

$$\rho(x_1, ..., x_{2n_s}, ..., x_{2n_s+2+n_h}) \sim \frac{1}{\sqrt{x_1}} \left(\prod_{i=3}^{2n_s+2} \frac{1}{\sqrt{x_i}} \right) x_2^{1.5} \prod_{i=2n_s+3}^{2n_s+2+n_h} g(x_i, Q_i) \delta(1 - \sum_{i=1}^{2n_s+2+n_h} x_i). \tag{5}$$

The distributions $g(x_i, Q_i)$ are the distribution functions of the partons engaged in the hard scattering. The Regge behaviour of the soft valence quark x–distributions is $x^{-0.5}$, the term $1/\sqrt{x_1}$ refers to the valence quark at the end of a soft valence chain. The Regge behaviour of a diquark x–distribution is $x^{1.5}$, the term $x_2^{1.5}$ refers to the x–distribution of the valence diquark at the end of a soft valence chain. The Regge behaviour of soft sea–quark x–distributions agrees to the one of the valence quarks, it is also $x^{-0.5}$. The terms $1/\sqrt{x_i}$ refer to the sea–quarks and sea–antiquarks at the end of soft sea chains.

Here one remark is in order. In the previous papers [10, 5], we did use terms $1/x_i$ for the soft sea–quarks and antiquarks. A corresponding formula with $1/x_i$ is also given in the Dual Parton Model review [8]. The use of this different behaviour for the soft sea–quark x–distributions was certainly motivated by the behaviour of the deep inelastic x–distributions for sea–quarks, but it is not correct for the soft sea quarks. The correct Regge behaviour of soft sea quarks was already discussed in an Appendix to the paper of Capella and Tran Thanh Van [43] and it is also given for instance in [44]. It is easy to check that at low energies, typical for fixed target experiments, the correct form $1/x$ or $1/\sqrt{x}$ is not very important, the behaviour is mainly determined by the low x cut–off of the structure functions.But for our goal, to study the Feynman x_F–distributions of hadrons at the highest energies in the fragmentation region, it is essential to use the correct form $1/\sqrt{x}$.

Soft(s), hard(h), high mass single diffractive(TP), and high mass double diffractive(L) processes are treated simultaneously within an eikonal unitarization scheme using the impact parameter representation

$$\chi_i(B, s) = \frac{\sigma_i(s)}{8\pi b_i} \exp[-\frac{B^2}{4b_i}], \qquad i = s, h, TP, L \tag{6}$$

normalized by

$$\int 2\chi_i(B,s)\,d^2B = \sigma_i \tag{7}$$

with b_h energy independent, $b_s = b_{TP} = b_L = b + \alpha' log(s)$. The exclusive cross section for l_c cut soft pomerons, m_c cut hard pomerons, n_c cut triple–pomeron graphs and p_c cut loop graphs is given by

$$\sigma(l_c, m_c, n_c, p_c, B, s) = \frac{(2\chi_s)^{l_c}}{l_c!}\frac{(2\chi_h)^{m_c}}{m_c!}\frac{(-2\chi_{TP})^{n_c}}{n_c!}\frac{(-2\chi_L)^{p_c}}{p_c!}\exp[-2\chi(B,s)] \tag{8}$$

with

$$\chi(B,s) = \chi_s(B,s) + \chi_h(B,s) - \chi_{TP}(B,s) - \chi_L(B,s). \tag{9}$$

The total and elastic cross section are given by

$$\sigma_{tot} = 4\pi\int_0^\infty BdB(1-\exp[\chi(B,s)]),\quad \sigma_{el}(B,s) = \frac{1}{4}[\sigma_{tot}(B,s)]^2. \tag{10}$$

Diffractive processes characterized by the excitation of an initial hadron to intermediate resonances (low mass diffractive interactions) are introduced via a two channel eikonal formalism. As suggested in Ref.[10] a new coupling λ modifies the three graphs given in Fig. 1(e-g) and leads to a modification of each graph with l soft, m hard, n triple–pomeron, and p loop exchanges.

The calculation of the minijet cross sections was easy before the HERA measurements of the parton structure functions al very small Bjorken–x. The structure functions in the Eighties were assumed to behave at small x like $1/x$. For the calculation of the minijet component we did use an energy independent cut–off , usually $p_{\perp thr}$ = 2 to 3 GeV/c.

Since the HERA measurements, the structure functions are known to behave at small x like $1/x^\alpha$ with α between 1.35 and 1.5. The minijet production is dominated by very small x values, therefore the minijet cross section calculated with the new structure functions rise very steeply with energy. We found already 1993 [5] with the MRS[D-] structure function [45] at the LHC energy a minijetcross section about 10 times larger than the total cross section at this energy. And we realized, that the model has become inconsistent and wrong at these energies.

What was inconsistent and wrong: The input minijet cross sections σ_h, which we put into the unitarization scheme are inclusive cross sections normalized to $n_{minijets}\sigma_{inel}$, where $n_{minijets}$ is the multiplicity of minijets. The physical processes, which contribute to this inclusive cross section, if we use parton distributions with Lipatov behaviour ($1/x^\alpha$), are $2 \to n$ parton processes. $2 \to n$ processes give a contribution to σ_h equal to $n\sigma_{2\to n}$. If we treat this huge cross section as σ_h in the usual way in the eikonal unitarization scheme we replace it by $n/2$ simultaneuos $2 \to 2$ parton processes, this is the inconsistency. What we should really use in the unitarization, but what we do not know how to compute reliably at present would be

$$\sigma_h = \sum_n \sigma_{2\to n} \tag{11}$$

The way to remove this inconsistency is to make in the two component DPM the threshold for minijet production $p_{\perp thr}$ energy dependent in such a way, that at no energy and for no PDF the resulting σ_h is much bigger than the total cross section. Then at least we have a cross section, which is indeed mainly the cross section of a $2 \to 2$ parton process at this level, the parton–parton scattering with the largest transverse momentum. We can get back to the real $2 \to n$ processes and recover the minijets with smaller transverse momenta via parton showering. One possible form for this energy dependent cut off is [5]:

$$p_{\perp thr} = 2.5 + 0.12[\lg_{10}(\sqrt{s}/\sqrt{s_0})]^3 \quad [\mathrm{GeV/c}],\quad \sqrt{s_0} = 50\mathrm{GeV}. \tag{12}$$

The resulting σ_h are smaller or not much larger than the total cross sections resulting after the unitarization for all PDF's. **Now we are again consistent.**

There are further features of the minijet component worth mentioning. We use as first described in [42] at $p_{\perp thr}$ the continuity requirement for the *soft* and *hard* chain end $p_\perp$ distributions. Physically, this means, that we use the soft cross section to cut the singularity in the minijet $p_\perp$ distribution. But note, that this cut moves with rising collision energy to higher and higher $p_\perp$ values. This procedure has besides cutting the singularity more attractive features:

(i) The model results (at least as long as we do not violate the consistency requirement described above) become somewhat independent from the otherwise arbitrary $p_\perp$ cut–off. This was already demonstrated with DTUJET90 [10] and cut–offs of 2 and 3 GeV/c.

(ii)The continuity between soft and semihard physics is emphasized, there is no basic difference between soft and semihard chains besides the technical problem, that perturbative QCD allows only to calculate the semihard component.

(iii) With this continuity in mind we feel free to call all chain ends, whatever their origin in the model, minijets, as soon as their $p_\perp$ exceeds a certain value, say 2 GeV/c.

Table 1: DTUJET97 model parameters obtained with an energy dependent $p_{\perp thr}$.

PDF set	$g^2(mb)$	$\alpha(0)$	α' $[GeV^{-2}]$	b $[GeV^{-2}]$	b_h $[GeV^{-2}]$	λ
GRV–LO	55.6	1.049	0.324	1.12	1.76	0.567
CTEQ4M	57.5	1.045	0.371	0.97	1.46	0.566

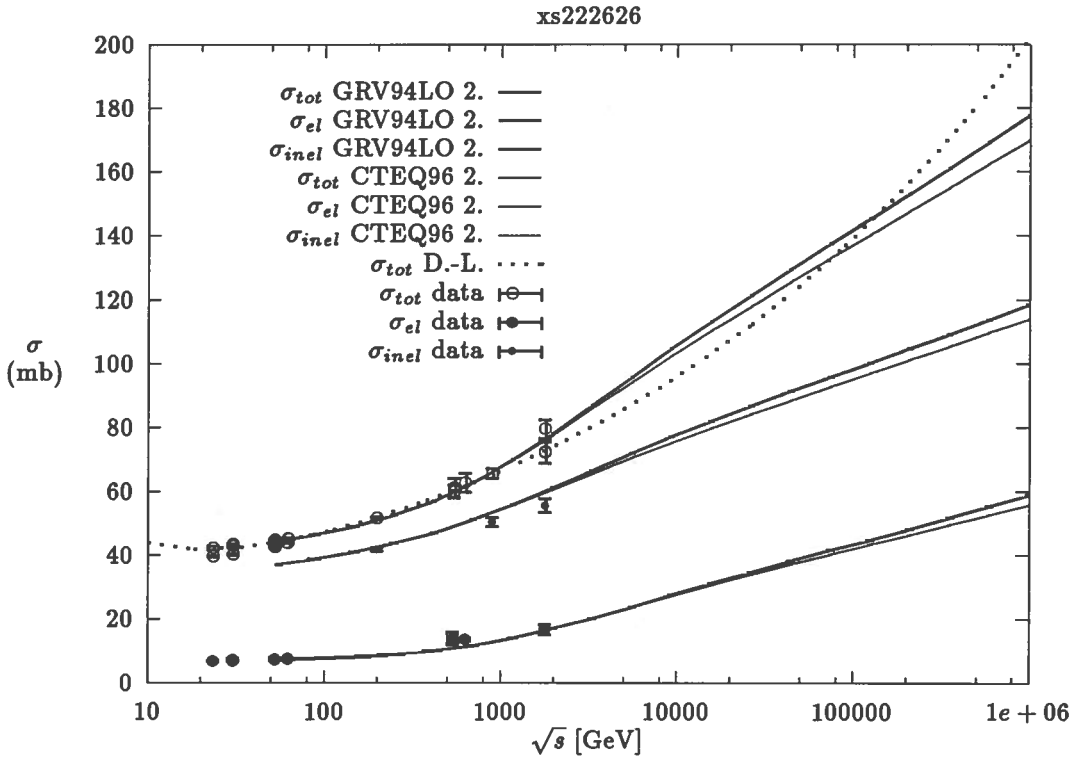

Figure 2: Total, inelastic and elastic $p\bar{p}$ and pp cross sections as function of the center of mass energy $\sqrt{s}$. The model results obtained using the GRV–LO parton distributions [3] and the CTEQ4 parton distributions [4] are compared to the Donnachie–Landshoff fit for the total cross section [46] and to data [47, 48, 49, 50, 51, 52, 53, 54, 55]

We turn now to the fit of the Pomeron parameters with the energy dependent $p_\perp$ cut–off given above. To describe the high energy particle production we have to determine the free parameters of the model, i.e. the proton-Pomeron coupling constant g, the effective soft Pomeron intercept $\alpha(0)$, the slope of the Pomeron trajectory α', the slope parameters b and b_h and the excitation coupling constant λ. This has been done by a global fit to all available data of total, elastic, inelastic, and single diffractive cross sections in the energy range from ISR to collider experiments as well as to the data on the elastic slopes in this energy range. Since there are some differences in the hard parton distribution functions at small x values resulting in different hard input cross sections we have to perform separate fits for each set of parton distribution functions.

We get good fits using the two PDF's already mentioned. In Table 1 we give the parameters obtained in the fit. The values obtained for $\alpha(0)$ demonstrate again that the fits result in a supercritical Pomerom. In Fig. 2 we plot the fitted cross sections obtained with the two PDF's together with the data. Furthermore we compare the total cross sections obtained with the popular Donnachie–Landshoff fit [46].

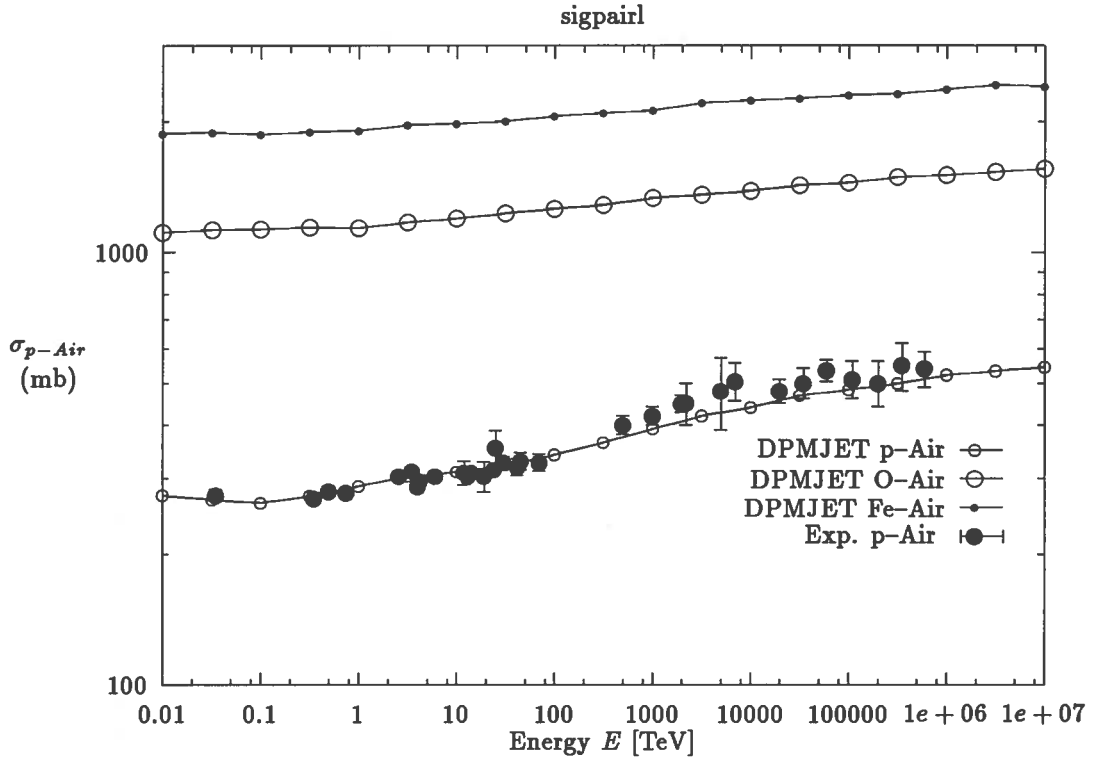

Figure 3: The inelastic cross section σ_{p-Air} calculated by DPMJET–II.3 as function of the laboratory collision energy (from 0.02 TeV up to 1.E7 TeV) compared to experimental data collected by Mielke et al. [56]. Given are also the DPMJET–II.3 predictions for the O–Air and Fe–Air cross sections as function of the collision energy per projectile nucleon. All of these cross sections are of relevance for cosmic ray studies.

In Fig.3 we present also the cross sections for p–Air, O–Air and Fe–Air which are relevant for calculating the Cosmic Ray cascade as function of the lab energy from 0.02 TeV to 1.E9 TeV. The DPMJET cross sections are compared to the experimental data collected by Mielke et al. [56].

2.2 The Dual Parton Model for hadron production in hadron–nucleus and nucleus–nucleus collisions

The first successfull applications of the Monte Carlo version of the dual parton model (DPM) to hadron–nucleus [16, 17] and nucleus–nucleus [18, 19, 20] collisions also demonstrated that the cascade of created secondaries in the target (and projectile) nuclei contributes significantly to particle production in the target (and projectile) fragmentation regions. On the other hand, it is known for many years that a naive treatment of intranuclear cascade processes on the basis of elementary cross sections overestimates the particle yields, if the incident energy significantly exceeds five or ten GeV [21, 22].
This problem may be solved by introducing the concept of a formation zone [23, 24] suppressing in a natural way the cascading of high–energy secondaries. The Monte Carlo model includes intranuclear cascade processes of the created secondaries combined with the formation time concept since the first version DTUNUC.
In the following we briefly sketch the basic ideas of the model and mention the most important ingredients; for a more detailed description of the model as applied in the code we refer to Refs. [16, 17, 27, 28, 30, 31, 33, 57, 25, 26, 37].

2.2.1 The Monte Carlo realization of the dual parton model DPMJET for hadron-nucleus and nucleus-nucleus collisions

The model starts from the impulse approximation for the interacting nuclei – i.e. with a frozen discrete spatial distribution of nucleons sampled from standard density distributions [58]. The primary interaction of the incident high–energy projectile proceeds via totally n elementary collisions between $n_p = n_A$ and $n_t = n_B$

nucleons from the projectile (for incident hadrons $n_p = 1$) and the target nuclei, resp. Actual numbers n, n_p and n_t are sampled on the basis of Glauber's multiple scattering formalism using the Monte Carlo algorithm of Ref.[58].

The Glauber model, which is part of DPMJET–II allows to calculate the inelastic hadron–nucleus cross sections. What we need for this calculation is the nuclear geometry and the elementary hadron–nucleus scattering amplitude parametrized as follows:

Energy dependent quantities enter the Glauber approach via the profile function of elastic hadron-nucleon scattering,

$$\gamma_{hN}(b) = \frac{1}{2\pi ip}\int d^2q \exp(i\vec{q}\cdot\vec{b}) f_{hN}(\vec{q}), \tag{13}$$

i.e. the amplitude of elastic hadron-nucleon scattering in the impact parameter representation (with $\vec{q}$ denoting the lateral, i.e. two-dimensional momentum transfer). In their Monte Carlo realization of Glauber's approach Shmakov et al. [58] apply the high-energy approximation of the profile function,

$$\gamma_{hN}(b) = \frac{\sigma_{hN}^{tot}}{4\pi a}\left(1 - i\frac{\Re f_{hN}(0)}{\Im f_{hN}(0)}\right) e^{-\frac{b^2}{2a}}, \tag{14}$$

with parameters σ^{tot}, a and $\rho = \Re f_{hN}(0)\ /\ \Im f_{hN}(0)$ appropriate for the description of nucleus-nucleus interactions at energies of several GeV per nucleon. (This parametrization corresponds to a differential cross section $d\sigma/dt \simeq \sigma_{tot}\exp(a\cdot t)$ with $t \simeq -\vec{q}^2$.)

However, the energy dependence of the elastic hadron-nucleon scattering amplitudes will influence the properties of hadron–nucleus and nucleus–nucleus scattering. In particular, the number of individual high-energy hadron-nucleon interactions (n, n_A, n_B) will increase with rising energy, hence the multiplicity will increase stronger than to be expected from the energy dependence of single hadron-hadron interactions.

Guided by the data collected in Ref. [59], we apply the following parametrizations for the slope parameter a : $a = 8.5\ (1 + 0.065\ln s)$ for nucleon-nucleon collisions above $s = 50$ GeV^2, $a = 6.2\ (1 + 0.13\ln s)$ for nucleon-nucleon collisions below $s = 50$ GeV^2 and $a = 6.0\ (1 + 0.065\ln s)$ for $\pi-$ and K–nucleon collisions. We use for the ratio ρ of the real and imaginary part of the elastic scattering amplitude: $\rho = -0.63 + 0.175\ln\sqrt{s}$ for the energy region $3.0 \leq \sqrt{s} \leq 50.$ and $\rho = 0.1$ in the energy region $\sqrt{s} \geq 50$ GeV in nucleon-nucleon scattering and $\rho = 0.01$ for $\pi-$ and K–nucleon scattering.

The energy dependence of the total cross sections is described by the fits of the Particle Data Group [60]; at energies beyond the range of the actual parametrization of the pp cross section the one for $\bar{p}p$ is applied and at energies even higher we use the total cross–sections as calculated by the two–component Dual Parton Model for hadron–hadron collisions, see also Fig.2.

The same information is also needed to construct the inelastic events and indeed usually each run of DPMJET starts with a calculation of the inelastic cross section.

Note that individual hadrons may undergo several interactions. Particle production in each elementary collision was desrcibed in DTUNUC by the fragmentation of two color–neutral parton–parton chains. In DPMJET also multiple soft chains and multiple minijets are considered. Those chains are constructed from the valence quark systems or – in the case of repeated scatterings of single hadrons – from sea–$q\bar{q}$ pairs and sea–$qq - \bar{q}\bar{q}$ pairs of the interacting hadrons.

For nucleus–nucleus collisions in the two–chain approximation the single particle densities are given by

$$\begin{aligned}
\frac{dN^{AB}}{dy} \;=\; & \frac{1}{\sigma_{AB}}\sum \sigma_{n_A,n_B,n}\{\Theta(n_B - n_A)[n_A(N^{qq^A - q_v^B} + N^{q_v^A - qq^B}) \\
& +(n_B - n_A)((1-\alpha)(N^{q_s^A - qq^B} + N^{\bar{q}_s^A - q_v^B}) + \alpha(N^{(q\bar{q})_s^A - qq^B} + N^{(qq)_s^A - q_v^B})) \\
& +(n - n_B)((1-2\alpha)(N^{q_s^A - \bar{q}_s^B} + N^{\bar{q}_s^A - q_s^B}) \\
& +\alpha(N^{q_s^A - (qq)_s^B} + N^{(qq)_s^A - q_s^B}) + \alpha(N^{\bar{q}_s^A - (\bar{q}\bar{q})_s^B} + N^{(\bar{q}\bar{q})_s^A - \bar{q}_s^B}))] \\
& +(A \to B)\}
\end{aligned} \tag{15}$$

Here n denotes the total number of inelastic collisions between n_A and n_B participating nucleons from the projectile and target nuclei and α is the rate of diquark pairs to $q - \bar{q}$ pairs in the proton sea .

The hadronization of single chains was handled originally by the Monte Carlo codes BAMJET [61, 62] and DECAY [63] or by the Lund code JETSET–7.3 [64]. Presently, BAMJET is practically never used any longer.

2.3 Important differences between the two–component Dual Parton Model and minijet models

There is no scientific reason, not to call the two–component Dual Parton Model (the two components are the soft pomeron and the hard pomeron or the minijets) also a minijet model. Minijet models too have a soft and a hard component. The reason not to use the term minijet model for DPMJET is connected with the fact that the name minijet model so far was only used for models which use a critical pomeron with an intercept of exactly one. In such a minijet scheme, it is then claimed, all the rise of the cross sections with energy is due to the rise of the minijet cross sections. This is not so in our model, therefore we avoid to use the name minijet model.

The supercritical pomeron was used in the two–component DPM from the beginning [9], while the so called minijet models use the critical pomeron with $\alpha(0) = 1$.

There are important differences which result from this different approach:

(i)Both kinds of models determine the free parameters of their model in a fit to total, inelastic and elastic cross sections. Both models obtain acceptable fits, we have reported even about the fits using a critical pomeron elsewhere [13], but of course, if at the end of the fit we treat the pomeron intercept $\alpha(0)$ as a free parameter instead to fix it to $\alpha(0) = 1$, the fit improves and in all situations (fits using different parton structure functions to calculate the minijet cross sections) we obtain the intercept larger than 1. namely $\alpha(0) \approx 1.07$. These better fits to the data are our main argument for the continuing presence and even rise of soft hadron production at the highest energies.

(ii)Due to these different starting points the chain structure of the models differ: In both models we have a pair of soft valence–valence chains (resulting from cutting one soft pomeron) and in both models we have minijets. Only in the two component Dual Parton Model we have in addition soft sea–sea chains with soft sea quarks at their ends. The number of these chains increases with energy and a substantial part of the rise of the multiplicity and rapidity plateau results from this mechanism.

(iii)The x–distributions of soft sea quarks are determined by the Regge behaviour, which is for soft sea as well as valence quarks like $1/\sqrt{(}x)$. The minijets are calculated from the deep inelastic structure functions with (depending on the parametrization for the structure functions used) a behaviour like $1/x$ or $1/x^{1.5}$. In the Dual Parton Model the Feynman x_F distributions resulting from fragmenting valence chain ends (which dominate at small energy) and from fragmenting soft sea chain ends do not differ, this is the source of the excellent Feynman scaling and the nearly energy independent spectrum weighted moments. In the minijet models all chains except the single valence chain pair, which dominates at low energy, are minijets with the much softer x–distribution. Therefore in these models Feynman scaling is more strongly violated and the spectrum weighted moments decrease more strongly with the collision energy. The rise of the minijet component in the Dual Parton Model leads of course to the same effect, this effect is however smaller, since not all of the rise of particle production is due to the minijets.

2.4 Realization of the intranuclear cascade process

2.4.1 The FZIC (formation zone intranuclear cascade)

The physical picture explaining the absence of the intranuclear cascade at high energies is the concept of the formation zone [24]. It has been introduced in analogy to the Landau-Pomeranchuk [23] effect, which explains the observation that electrons passing through material become more penetrating at high energies. For the formation zone of an electron with 4-momentum p and energy E upon radiation of a photon with 4-momentum k one obtains

$$\tau = \frac{E}{k \cdot p} = \frac{E}{m} \frac{1}{\omega_e}, \tag{16}$$

where ω_e is the frequency of the photon in the rest frame of the electron and E/m is the time dilatation factor from the electron rest frame to the laboratory. Within the quark model, the states being formed in the primary nucleon-nucleon interaction can be understood as consisting of valence quarks only, i.e without the full system of sea quarks, antiquarks, and gluons and have therefore a reduced probability for hadronic interactions inside the nucleus [27]. The formation zone concept can be translated to hadron production as follows [20]. We consider the formation zone cascade in the rest system of the target nucleus (laboratory system) and note that the formulation is not Lorentz invariant. Denoting the 4-momenta of the projectile hadron p_p and the secondary hadron p_s with

$$p_p = (E_p, 0, 0, \sqrt{E_p^2 - m_p^2}), \qquad p_s = (E_s, \vec{p}_{s\perp}, \sqrt{E_s^2 - m_s^2 - \vec{p}_{s\perp}^2}) \tag{17}$$

and replacing in Eq. (16) the electron momentum by p_p and the photon momentum by p_s, the hadron formation zone reads for $E_p \gg m_p$

$$\tau_{\rm Lab} = \frac{2E_s}{(m_p x)^2 + m_s^2 + p_{s\perp}^2}, \qquad x = \frac{E_s}{E_p}. \tag{18}$$

Since for most of the produced secondaries the term $(m_p x)^2$ can be neglected one can approximate

$$\tau_{\rm Lab} \approx \gamma_s \tau_s, \qquad \gamma_s = \frac{E_s}{m_s}. \tag{19}$$

In the rest system of the secondary hadron s, we define an average formation time τ_s needed to create a complete hadronic state [27, 20]

$$\tau_s = \tau_0 \frac{m_s^2}{m_s^2 + p_{s\perp}^2}. \tag{20}$$

τ_0 is a free parameter, which has to be determined by comparing particle production within the model to experimental data. Typical values are in the range from 1 fm/c to 10 fm/c (In Refs. [28, 1] τ_0 was fixed to $\tau_0 = 5$ fm/c whereas in Ref. [27] τ_0=1-2 fm/c was used.). The present version of DPMJET uses $\tau_0 = 5$ fm/c. For each secondary we sample a formation time τ from an exponential distribution [65] with an average value as given in Eq. (20). As it was described in [28], in our MC model we know the full space-time history of the collision. In any particular Lorentz frame we can follow the trajectories of the secondaries created in the hadronization of the chains in space and time. Due to relativistic time dilatation secondaries with high energies in the target rest system are mostly formed outside the target nucleus and are therefore not able to initiate intranuclear cascade processes. On the other hand, the lower the energy of the secondary hadronic system the higher is the probability to form a hadron inside the nucleus. These hadrons may therefore reinteract with spectator nucleons taking into account the nuclear geometry.

Secondaries are followed along straight trajectories and may induce intranuclear cascade processes if they reach the end of their formation zone inside either the target or the projectile nuclei; otherwise they leave the nucleus without interaction. Below 9 GeV inelastic secondary interactions are described by the Monte Carlo code HADRIN [66]. For the sampling of elastic nucleon–nucleon scattering below 4 *GeV* the parametrization of the HETC-KFA code [67, 68] was adopted; at higher energies and for all other particle species the parametrization

$$\frac{d\sigma}{dt} \propto \exp(-at),$$

is applied. Reinteractions of energetic secondaries beyond 9 GeV within the colliding nuclei are very rare and, therefore, neglected in DPMJET–II.

2.4.2 The nuclear excitation energy

The treatment of nuclear effects within the MC model has already been discussed in [28]. Since they are essential in calculating excitation energies of nuclei left after primary interactions and intranuclear cascade processes we summarize the basic ideas. Fermi momenta for nucleons as well as a simplified treatment of the nuclear potential are applied to control the generation of low-energy particles. Nucleon momenta are sampled from zero-temperature Fermi distributions

$$\frac{dN^{\rm n,p}}{dp} = N^{\rm n,p} \frac{3p^2}{(p_{\rm F}^{\rm n,p})^3}. \tag{21}$$

Here and in the following the indices "n" and "p" denote neutrons and protons, resp. The maximum allowed Fermi momenta of neutrons and protons are

$$p_{\rm F}^{\rm n,p} = \left[\left(\frac{N^{\rm n,p}}{V_A} \right) \frac{3h^3}{8\pi} \right]^{\frac{1}{3}} \tag{22}$$

with V_A being the volume of the corresponding nucleus with an approximate nuclear radius $R_A = r_0 A^{1/3}, r_0 =$ 1.29 fm. Modifications of the actual nucleon momentum distribution, as they would arise, for instance, taking the reduced density and momenta in the nuclear skin into consideration, effectively result in a reduction of the Fermi momenta as compared to those sampled from Eq. (22). This effect can be estimated by a correction factor

$\alpha^{\rm F}_{\rm mod}$ which modifies the Fermi-momenta. Results presented in this paper have been obtained with $\alpha^{\rm F}_{\rm mod}$=0.60. The depth of the nuclear potential is assumed to be the Fermi energy and the binding energy for outer shell nucleons

$$V^{\rm n,p} = \frac{(p_{\rm F}^{\rm n,p})^2}{2m_{\rm n,p}} + E^{\rm n,p}_{\rm bind}. \tag{23}$$

To extend the applicability of the model to the energy region well below 1 GeV an approximate treatment of the Coulomb-potential is provided. The Coulomb-barrier modifying the nuclear potential is calculated from

$$V_{\rm C} = \frac{e^2}{4\pi\epsilon_0 r_0} \frac{Z_1 Z_2}{(A_1^{1/3} + A_2^{1/3})} \tag{24}$$

with the mass numbers A_1, A_2 and charges Z_1, Z_2 of the colliding nuclei, i.e. with $A_1 = |Z_1| = 1$ for charged hadrons entering or leaving the target nucleus. e denotes the elementary charge and $r_0 = 1.29$ fm.

The excitation energy U of the residual nucleus with mass number $A_{\rm res}$ and charge $Z_{\rm res}$, i.e. the energy above the ground state mass $E_{0,\rm res}$, is given as

$$\begin{aligned} U &= E_{\rm res} - E_{0,\rm res}, \\ E_{0,\rm res} &= Z_{\rm res} m_{\rm p} + (A_{\rm res} - Z_{\rm res}) m_{\rm n} - E_{\rm bind}(A_{\rm res}, Z_{\rm res}). \end{aligned} \tag{25}$$

We calculate the binding energy $E_{\rm bind}(A_{\rm res}, Z_{\rm res})$ using the experimentally determined excess masses of all known (measured) nuclides and using mass formulae for nuclides far from the stable region, where no measurements are available. The excitation energy is obtained within our model from an explicit consideration of the effects of the nuclear potential (Eq. (23)) and the Coulomb energy (Eq. (24)), i.e. from corrections which are applied to the 4-momenta of the final state hadrons leaving the spectator nucleus. We modify the energies of these hadrons by the potential barrier and rescale the 3-momenta correspondingly. It is assumed that these corrections have to be applied to nucleons wounded in primary and secondary interactions and to those hadrons only, which are formed inside the spectator nucleus corresponding to the sampled formation time. Among these particles we find apart from the nucleons a small fraction of other baryons, which are assumed to move in a nucleon potential and mesons to which we apply an effective meson potential of 0.002 GeV. Due to energy-momentum conservation these corrections lead to a recoil momentum and, therefore, to an excitation of the residual nucleus. In addition, there is a further contribution to the recoil momentum of the residual nucleus arising from potential corrections applied to the momentum of the projectile hadron entering the nuclear potential and from cascade nucleons with kinetic energies below the nuclear potential which are therefore not able to escape the spectator nucleus.

2.4.3 Nuclear evaporation and fragmentation[25]

At the end of the intranuclear cascade the residual nucleus is supposed to be left in an equilibrium state, in which the excitation energy U is shared by a large number of nucleons. Such an equilibrated compound nucleus is supposed to be characterized by its mass, charge, and excitation energy with no further memory of the steps which led to its formation. The excitation energy can be higher than the separation energy, thus nucleons and light fragments (α,d,^{3}H, ^{3}He) can still be emitted: they constitute the low-energy (and most abundant) part of the emitted particles in the rest system of the residual nucleus, having an average energy of few MeV. The emission process can be well described as an evaporation from a hot system. The treatment starts from the formula of Weisskopf [69], that is an application of the detailed balance principle. The evaporation probability for a particle of type j , mass m_j, spin $S_j \cdot \hbar$, and kinetic energy E is given by

$$P_j(E)dE = \frac{(2S_j+1)m_j}{\pi^2\hbar^3} \sigma_{\rm inv} \frac{\rho_f(U_f)}{\rho_i(U_i)} E dE \tag{26}$$

where ρ's are the nuclear level densities ($\rho_f(U_f)$ for the final nucleus, $\rho_i(U_i)$ for the initial one), $U_i \equiv U$ is the excitation energy of the evaporating nucleus, $U_f = U - E - Q_j$ that of the final one, Q_j is the reaction Q for emitting a particle of type j from the original compound nucleus, and $\sigma_{\rm inv}$ is the cross section for the inverse process.

Eq. (26) must be implemented with a suitable form for the nuclear level density and the inverse cross sections. Many recipes have been suggested for both. In the original work of Dostrovsky [70], $\rho(U) \approx C \exp(2\sqrt{aU})$, with $a = A/8$ has been used for the level density dependence on the excitation energy U. This has led to a

simple form for the evaporation probability:

$$P_j(E)dE = \frac{(2S_j+1)m_j}{\pi^2\hbar^3}\sigma_{\rm inv}\frac{e^{2\sqrt{a(U-E-Q_j)}}}{e^{2\sqrt{aU}}}EdE. \tag{27}$$

In the same work, the inverse cross sections have been parametrized in a very simple way, so that expression (27) can be analytically integrated and used for MC sampling. The same formulation is used in this work with, however, a different choice of a as it will be discussed later.

The total width for neutron emission can be found by integrating Eq. (26) between zero and the maximum possible ejectile energy $(U - Q_j)$

$$\Gamma_j = \frac{(2S_j+1)m_j}{\pi^2\hbar^2}\int_0^{(U-Q_j)}\sigma_{\rm inv}(E)\frac{\rho_f}{\rho_i}EdE. \tag{28}$$

The same applies to charged particles, where the integration actually goes from some effective Coulomb barrier where $\sigma_{\rm inv}$ drops to zero, up to the maximum energy.

The evaporative process is in competition with another equilibrium process, that is fission [71]. For the fission probability, a statistical method can be used [69, 72]: obtaining for the total fission width

$$\Gamma_{\rm F} = \frac{1}{2\pi}\frac{1}{\rho_i(U)}\int_0^{(U-B_{\rm F})}\rho_{\rm F}(U-B_{\rm F}-E)dE \tag{29}$$

where $B_{\rm F}$ is the fission barrier, and $\rho_{\rm F}(U_{\rm F}) \approx C\exp\left(2\sqrt{a_{\rm F}U_{\rm F}}\right)$, the level density of the fissioning nucleus at the saddle point, where the excitation energy $U_{\rm F}$ is given by the initial one minus the fission barrier.

We follow the prescriptions of Atchison [73] to calculate the quantities entering Eq. (29), except, again, for the level density parameter $a_{\rm F}$.

In both $\rho_{\rm F}(U)$ and $\rho(U)$ we use the so-called backshifted level density, using $U - \Delta$ rather than U, where Δ is the pairing energy. Moreover, $\tilde{a} = a/A$, and $\tilde{a}_{\rm F} = a_{\rm F}/A$ are found to be all but constant parameters: they possess a dependence on A and Z, due to shell and deformation effects, and a dependence on excitation energy. Both effects have been experimentally observed, and have been subject of many phenomenological and theoretical investigations (see [74, 75, 76, 77, 78, 79]). Here the N and Z dependence of Ref. [74] is used, and complemented with the energy dependence prescription of Ignatyuk [75, 76]

$$\begin{aligned} a &= A\cdot[\bar{a}\cdot f(U) + \tilde{a}\cdot(1-f(U))] \\ \bar{a} &= a_0 + 9.17\times10^{-3}\cdot[S_{\rm Z}(Z)+S_{\rm N}(N)] \\ \tilde{a} &= 0.154 - 6.3\times10^{-5}\cdot A \\ f(U) &= \frac{1-e^{-0.054\cdot(U-\Delta)}}{0.054\cdot(U-\Delta)} \end{aligned} \tag{30}$$

where according to [74], a_0 is given by 0.142 MeV^{-1} and 0.12 MeV^{-1} for undeformed and deformed nuclei respectively, and $S_{\rm Z}(Z)$ and $S_{\rm N}(N)$ are the shell correction terms for protons and neutrons. The unit of energy used throughout Eq. (30) is MeV.

The level density at the saddle point $\rho_{\rm F}$ is different from that of the nucleus in its ground state. From comparison to experimental data, it turns out that $a_{\rm F}$ is greater than the a used for evaporation of about 10% at low excitation energies, and the two a's become equal at large excitation energies. We use $a_{\rm F} \approx 1.08a$, with a smooth A dependence. After fission occurs, the two fragments are treated like independent residual nuclei with their own excitation and can possibly emit further particles.

For light nuclei, the statistical assumptions and the sequential emission scheme underlying the classical evaporation models become less and less applicable, because:

- Already moderate excitation energies can represent a substantial fraction of the (total) binding energy of such nuclei.
- The level structure of such nuclei is usually highly specific and anyway level spacings can be comparable with the excitation energy.
- The "evaporation" of light fragments other than p or n becomes meaningless, since the mass of the "evaporated" fragment can be comparable or even larger than the mass of the residual nucleus.

Therefore other deexcitation mechanisms are more suitable for these light residual nuclei. The one adopted for this calculations is the so called Fermi Break-up model [80, 81], where the excited nucleus is supposed to disassemble just in one step into two or more fragments, with branching given by plain phase space considerations. In particular, the probability for disassembling a nucleus of N neutrons, Z protons, and U excitation energy (total mass $M^* = U + M_{A,Z}$) into n fragments ($n \geq 2$) of the same total charge and baryon number, is given by:

$$W = \frac{g}{G}\left[\frac{V_{\rm br}}{(2\pi\hbar)^3}\right]^{n-1}\left(\frac{1}{M^*}\prod_{i=1}^{n} m_i\right)^{3/2}\frac{(2\pi)^{3(n-1)/2}}{\Gamma(\frac{3}{2}(n-1))}E_{\rm kin}^{3n/2-5/2} \tag{31}$$

where the spin factor g, and the permutation factor G are given by (n_j is the number of identical particles of jth kind)

$$g = \prod_{i=1}^{n}(2S_i+1), \qquad G = \prod_{j=1}^{k} n_j! \tag{32}$$

and $E_{\rm kin}$ is the total kinetic energy of all fragments at the moment of break-up. $V_{\rm br}$ is a volume of the order of the initial residual nucleus volume. Therefore, the final state are conveniently selected by means of a MC procedure, by evaluating such an expression for all possible combinations of fragments energetically allowed and making a random selection. We considered all combinations formed by up to six fragments, unless the residual "nucleus" is composed by A like particles (p or n), in which case it is disintegrated into A fragments according to phase space. All particle stable states with $A \leq 16$ have been included, plus the particle unstable levels with sizeable γ decay branching ratios. Also a few known particle unstable isotopes, like ^{8}Be, have been included and, if produced, are let to decay according to the experimental branching. Once the final state configuration has been selected, the kinematical quantities of each fragment are chosen according to n-body phase space distribution. Such a selection must be performed taking care to subtract from the available energy the Coulomb repulsion of all charged particles: the Coulomb energy is then added back to the charged particles alone, to simulate properly the effect of the Coulomb repulsion. In practice $E_{\rm kin}$ at disassembling will be given by:

$$E_{\rm kin} = U - \left(\sum_{i=1}^{n} m_i - M_{A,Z}\right) - B_{\rm Coul} \tag{33}$$

where it must be recalled that the emitted fragments can be in an excited state. The total Coulomb barrier $B_{\rm Coul}$ of the selected configuration is distributed to charged particles after disassembling, in their own c.m. system.

According to the picture of the compound nucleus like an equilibrated system determined only by its mass, charge and excitation energy, with no memory of previous steps of the interaction, Fermi Break-up is activated in the model every time the current compound nucleus has mass number $A \leq 17$, including possible light fission fragments. The fragmentation of higher mass compound nuclei is not yet included in the model. This process, although its cross section is quite small, is important when considering the distribution of residual nuclei, because it can produce isotopes very far both from the target mass and from the fission product distribution.

2.4.4 γ deexcitation of the residual nuclei[26]

At the end of the intranuclear cascade the prefragments are supposed to be left in an equilibrium state, characterized by their masses, charges, and excitation energies with no further memory of the steps which led to their formation. Since the excitation energies can be higher than the separation energies, nucleons and light fragments (α,d,^{3}H, ^{3}He) can still be emitted. A detailed account on the evaporation treatment which follows the intranuclear cascade was given in [25]. Furthermore, a model for high energy fission and a Fermi Break-up model for light nuclei where an excited prefragment is supposed to disassemble just in one step into two or more fragments were discussed in [25].

The evaporation stage ends when the nuclear excitation energy becomes lower than all separation energies for nucleons and fragments. This residual excitation energy is then dissipated through emission of photons. In reality, photon emission occurs even during the preequilibrium and evaporation stages, in competition with particle emission, but its relative probability is low, and it is presently neglected in the model.

γ-deexcitation proceeds through a cascade of consecutive photon emissions, until the ground state is reached. The cascade is assumed to be statistical as long as the excitation energy is high enough to allow the definition of a continuous nuclear level density. Below a (somewhat arbitrary) threshold, set at the pairing gap value, the cascade goes through transitions between discrete levels.

The statistical model formulation for the γ-ray emission probability is again similar to those for evaporation and fission [82, 83]

$$P(E_\gamma)dE_\gamma = \frac{\rho_f(U_f)}{\rho_i(U_i)} \sum_L f(E_\gamma, L)dE\gamma \tag{34}$$

where L is the multipolarity of the γ transition. The strength functions $f(E, L)$ can be either derived from photoabsorption cross sections or calculated from single-particle estimates of transition strengths. The former approach is more sophisticated but requires the knowledge of the resonance parameters for all isotopes; the latter approach is easier and sufficient for a first order estimate of the γ spectral distribution. We thus assume

$$f(E_\gamma, L) = c_L \cdot F_L(A) \cdot E_\gamma^{(2L+1)} \tag{35}$$

where $E_\gamma^{(2L+1)}$ is the energy dependence for multipolarity L. For the c_L coefficients we adopted the Weisskopf single particle estimates [84]. The $F_L(A)$ factors have been included to partially account for the many effects that bring to deviations from the single particle estimates. They are rough A dependent averages of the hindrance and enhancement factors given in [85]. Only E1, M1, and E2 transitions have been considered. The assumed level density ρ is the same as in the evaporation part described in [25], but the ratio of exponentials coming from the level densities has been approximated as first order expansion around $E_\gamma = 0$. This is equivalent to the assumption of a constant nuclear temperature at low excitation energies, which is often used in the analysis of photon emission following neutron capture [82, 86].

As a result, one obtains the expressions for the emission probabilities for the considered multipoles. Since competition between photon and particle emission is neglected at the present status of the model, only the relative values are of interest

$$\begin{aligned} P(L, E_\gamma)dE_\gamma &= \tilde{C}_L E_\gamma^{(2L+1)} e^{\frac{E_\gamma}{T}} dE_\gamma \\ \frac{\tilde{C}_{M1}}{\tilde{C}_{E1}} &= 0.31 A^{-\frac{2}{3}} \frac{F_{M1}(A)}{F_{E1}(A)} \\ \frac{\tilde{C}_{E2}}{\tilde{C}_{E1}} &= 7.2 \cdot 10^{-7} A^{\frac{2}{3}} \frac{F_{E2}(A)}{F_{E1}(A)} \ \text{MeV}^{-2} \end{aligned} \tag{36}$$

T is the nuclear temperature at the initial excitation energy U, taken as $U - \Delta = aT^2$, a being the usual level density constant (see Eq.15 of [25]) and Δ the pairing energy.

A first sampling is performed on the integrated photon emission probabilities to choose the character(electric or magnetic) and the multipole order of the emitted photon, and a second sampling is performed to determine the emission energy according to the selected multipolarity. For both steps the full energy range $0 \leq E_\gamma \leq U$ is used, even though the intrinsic limit of validity would be $0 \leq E_\gamma \leq (U - \Delta)$. After emission, all parameters are updated on the basis of the new excitation energy, and another statistical emission is performed, until the excitation energy falls below the preset "discrete level threshold". This threshold has been set to the pairing energy for even-even or odd mass nuclei; for odd-odd nuclei the threshold corresponds to the (known or approximated) first excited level.

For many isotopes the experimentally determined values of the first and second excited levels have been tabulated in the code, for the others a rotational-like structure is assumed, with level energy given by :

$$U_I = \frac{\hbar^2}{2\mathcal{I}} I(I+1) \tag{37}$$

where I is the level spin (integer for even-mass , half integer for odd mass nuclei, 0 or 1/2 for the ground state), and $\mathcal{I}$ is the nuclear moment of inertia, taken as 0.4 times that of a rigid body . The last steps of the γ cascade consist of δI=2 transitions among these rotational levels, down to the ground state. When known levels are tabulated, the cascade is forced to pass through them. All photons are emitted isotropically, since from the evaporation stage we have no information on the residual nucleus spin and polarization.

2.5 The Cronin effect

In nuclear collisions, the partons at the sea and valence chain ends carry transverse momenta from different sources: (i)The intrinsic parton transverse momentum in the hadron. (ii) A transverse (and longitudinal) momentum resulting from the Fermi motion of the nucleons inside the nucleon. These first two kinds of transverse momentum were implemented into DPMJET–II from the beginning. (iii) During the passage of

the chain end partons through nuclear matter, they suffer nuclear multiple scattering which changes (usually increases) their transverse momenta.
The multiple scattering of partons is known since a long time to be responsable for the so called *Cronin effect* [87] of particle production at large transverse momentum on nuclear targets. A similar enhancement of particle production in hadron–nucleus and nucleus-nucleus collisions compared to hadron–hadron collisions has been observed in many experiments already at rather modest $p_\perp$. (See for instance the review of experimental data of Schmidt and Schukraft [88] where the data of these $p_\perp$ ratios are collected in Figs.4.21 to 4.24.)
At large $p_\perp$ this effect can be studied calculating the parton scattering pertubatively. Our rather low $p_\perp$ sea chain ends might be considered as the low $p_\perp$ limit of perturbatively scattered partons. We apply to them multiple scattering taking into account their path length inside the nuclear matter and adjust the parameters in such a way, that the measured $p_\perp$ ratios at rising transverse momenta are approximately reproduced by the code DPMJET–II.

2.6 Diquark fragmentation

The fragmentation of diquarks is slightly more complicated than the fragmentation of a quark jet. There are two possibilities for the first fragmentation step. Either we get in the first step a baryon, which contains both quarks of the diquark or we get in the first step a meson containing only one of the two quarks and the baryon is produced in the following fragmentation step. This mechanism is well known, it is presented in the review on the Dual Parton Model [8] and it was investigated for instance in [89, 90]. This mechanism is also implemented under the name *popcorn* fragmentation in the Lund chain fragmentation model JETSET–7.3 [64, 91]. There seems to be largely agreement, that the two fragmentations each have the probability of about 50 percent. This mechanism has been implemented from the beginning in the BAMJET–fragmentation code [62, 61] used so far in DPMJET–II but this feature was not used in the past. Therefore, it was considered to be more safe, also to introduce JETSET, where this mechanism is well tested, into DPMJET–II as an alternative fragmentation model.
What happens in the model with the popcorn mechanism compared to the model without can be most easiely seen looking at the proton rapidity distribution in p–p collisions. The two maxima in the target and projectile fragmentation region of the proton rapidity distribution shift by about half a unity to the center, these maxima become wider and correspondingly the dip in the center is reduced.

2.7 Production of strange Particles

Studies of strangeness production within this model were given in [31, 33, 34]. Enhanced generation of strange particles, in particular of strange antibaryons, has been proposed as a signal for the formation of quark gluon plasma in dense hadronic matter [92, 93]. Recent data from experiments at the CERN SPS have already been interpreted within this scheme. However, we find it worthwhile to pursue the study of conventional models without QGP formation like the DPM before drawing final conclusions. The DPM is an independent string model. Since the individual strings are universal building blocks of the model, the ratio of *produced* strange particles over non–strange ones will be approximately the same in all reactions. However, since some strings contain sea quarks at one or both ends and since strange quarks are present in the proton sea, it is clear, that, by increasing the number of those strings, the ratio of strange over non–strange particles will increase. This will be the case for instance, when increasing the centrality in a nucleus–nucleus collision. It is obvious, that the numerical importance of the effect will depend on the assumed fraction of strange over non–strange quarks in the proton sea. The rather extreme case leading to a maximum increase of strangeness is to assume a SU(3) symmetric sea (equal numbers of u, d and s flavors). We express the amount of SU(3) symmetry of the sea chain ends by our parameter s^{sea} defined as $s^{sea} = 2 < s_s > /(< u_s > + < d_s >)$ where the $< q_s >$ give the average numbers of sea quarks at the sea chain ends. However, the above scenario has an important draw–back. Since an antiquark from the sea is always attached to a valence– or sea–quark on the opposite hemisphere, and since the only important strings at CERN–energies are those containing at least a diquark at one end, it will be impossible to obtain an enhancement of antibaryons. In fact, due to energy–momentum conservation, the ratio $\bar{\Lambda}/h^-$ will in fact decrease with increasing centrality. In an attempt to solve this problem, we allow the creation of $qq - \bar{q}\bar{q}$ pairs from the proton sea, leading to the production of strings of type $\bar{q}\bar{q} - \bar{q}$ or $\bar{q}\bar{q} - qq$ in which the production of strange antibaryons will be easier. The rate of diquark pairs to $q - \bar{q}$ pairs in the proton sea is assumed to be the same as the ratio of $q \rightarrow (qq)$ to $q \rightarrow q$ branching in the chain fragmentation.

The fragmentation of diquarks has been discussed in the last section.

2.8 Diffractive events

Single diffraction within the Dual arton Model was studied in detail and compared to experimental data in [32, 57]. Single diffraction dissociation is represented by a triple–Pomeron exchange (high mass single diffraction) and a low mass component (low mass simgle diffraction) [10].

Diffractive processes characterized by the excitation of an initial hadron to intermediate resonances (low mass diffractive interactions) are introduced via a two channel eikonal formalism.
High mass single diffractive events are sampled cutting the triple–Pomeron graph . The excited system consists of two chains stretched between the constituents of the excited hadron and a $q\bar{q}$–pair of the Pomeron emitted from the hadron at the upper vertex.

Corresponding to $M_D^2 = x_D s$ and to the known $1/M_D^2$–behaviour of the diffractive differential cross section $d^2\sigma_{sd}/dtdM_D^2$ we sample the sum of the momentum fractions of the $q\bar{q}$–pair $x_D = x_q + x_{\bar{q}}$ from a $1/x_D$–distribution. Assuming that inelastic diffraction dissociation puts virtual hadronic states on the mass shell we limit this selection by the coherence condition.

$$M_D^2/s \leq (m_p R)^{-1} \qquad \text{with} \qquad R \simeq m_\pi^{-1} \tag{38}$$

where $\sqrt{s}$ is the c.m. energy of the collision and R is the interaction radius.
An excited low mass single diffractive event is represented by a chain connected to the valence partons of one hadron. The invariant mass M_D is fixed in the same way as above.

2.9 Hadron–nucleus interactions below 5 *GeV*

For theoretical as well as technical reasons (kinematics) the application of the Dual Parton Model for the description of the primary inelastic interaction is limited to not too low energies well above 1 GeV. Therefore, the conventional intranuclear cascade picture is used for lab energies below 3 – 5 GeV: The projectile hadron collides with a single nucleon inside the target nucleus, created secondaries may induce cascading. Inelastic as well as elastic hadron–nucleon interactions are described in the same way as mentioned in the previous subsection. Note, that the extrapolation to nucleus–nucleus interactions below 5 GeV is not implemented in DPMJET–II.

2.10 Restrictions of DPMJET–II

DPMJET–II.4 0r –II.4 works for hadron–nucleus collisions above 50 MeV kinetic energy and nucleus–nucleus interactions above 5 GeV per nucleon.

Presently DPMJET–II is able to run up to energies of approximately 10^{21} eV in the lab system (or $\sqrt{s} =$ 2000 TeV).

3 Comparing DPMJET–II.3 to data

3.1 Comparing to data in hadron–hadron collisions

Before a model like DPMJET–II.3 can be used for anything, we have to demonstrate, that the model describes well enough the available data up to the highest energies. The parameters of the model as given in Table 1 are different from the parameters used in the previous version of the model, therefore, this agreement to the data is not trivial, even if the previous DPMJET version was quite succesful in this respect.

Table 2. Comparison of average multiplicities of produced hadrons in proton– proton collisions at 200 GeV. The experimental data are from Ref.[94].

Particle	DPMJET–II	Exp.[94]
n_{ch}	7.77	7.69 ± 0.06
n_-	2.88	2.85 ± 0.03
p	1.31	1.34 ± 0.15
n	0.65	0.61 ± 0.30
π^+	3.24	3.22 ± 0.12
π^-	2.61	2.62 ± 0.06
π^0	3.51	3.34 ± 0.24
K^+	0.28	0.28 ± 0.06
K^-	0.18	0.18 ± 0.05
K^0_S	0.22	0.17 ± 0.01
Λ	0.13	0.096 ± 0.01
$\bar{\Lambda}$	0.018	0.0136 ± 0.004
ρ^0	0.50	0.33 ± 0.06
$\bar{p}$	0.06	0.05 ± 0.02

We start with looking at data, which prove, that the average multiplicity and the particle content are well described. In Table 2 we compare to the very well known multiplicities of secondary hadrons in 200 GeV p–p collisions from Ref.[94]. In Table 3 we compare to multiplicities of secondary hadrons and hadron resonances in $\sqrt{s} = 27.5$ GeV p–p collisions from Ref.[95]. At higher energies (and in non-single diffractive $p\bar{p}$ collisions) there are pseudorapidity distributions from the UA–5 Collaboration [96] and from the CDF Collaboration [97]. In Fig.4 a very good agreement is found. Still in this and all previous versions of the model there is and was always a disagreement of the model with the UA–5 data at the highest pseudorapidity values, see Fig. 4. The model predicts systematically more particles at the largest pseudorapidities of the experiment. This disagreement (if the data would be correct) would of course be of importance, if one is interested in Cosmic Ray cascades, where the particle production in the fragmentation region is of main interest. Fortunately, a new independent measurement of the pseudorapidity distribution in the collider energy range became available recently [98]. In Fig. 5 the comparison with this new data is presented and we find a remarkable agreement with DPMJET–II.3 in the large pseudorapidity region.

Table 3. Comparison of average multiplicities of produced hadrons and hadron resonances in proton–proton collisions at $\sqrt{s} = 27.5$ GeV. The experimental data are from Ref.[95].

Particle	DPMJET–II	Exp.[94]
p	1.35	$1.20 \pm 0.097 \pm 0.022$
π^+	3.49	$4.10 \pm 0.11 \pm 0.15$
π^-	2.88	$3.34 \pm 0.08 \pm 0.12$
π^0	3.82	$3.87 \pm 0.12 \pm 0.16$
K^+	0.33	$0.331 \pm 0.016 \pm 0.007$
K^-	0.23	$0.224 \pm 0.011 \pm 0.004$
K^0_S	0.26	$0.232 \pm 0.011 \pm 0.004$
Λ	0.14	$0.125 \pm 0.008 \pm 0.008$
$\bar{\Lambda}$	0.027	$0.020 \pm 0.004 \pm 0.0008$
Σ^+	0.044	$0.048 \pm 0.015 \pm 0.004$
Σ^-	0.017	$0.0128 \pm 0.0061 \pm 0.0032$
Δ^{++}	0.26	$0.218 \pm 0.0031 \pm 0.013$
Δ^0	0.20	$0.141 \pm 0.0098 \pm 0.0089$
$\bar{\Delta}^{++}$	0.005	$0.013 \pm 0.0049 \pm 0.0049$
$\bar{\Delta}^0$	0.005	$0.0336 \pm 0.008 \pm 0.0006$
ρ^0	0.55	$0.385 \pm 0.018 \pm 0.038$
ρ^+	0.53	$0.552 \pm 0.083 \pm 0.046$
ρ^-	0.40	$0.355 \pm 0.058 \pm 0.033$
ω	0.46	$0.390 \pm 0.024 \pm 0.002$
η	0.31	$0.30 \pm 0.02 \pm 0.054$
K^{*+}	0.17	$0.132 \pm 0.016 \pm 0.002$
K^{*-}	0.11	$0.088 \pm 0.012 \pm 0.001$
K^{*0}	0.14	$0.119 \pm 0.021 \pm 0.002$
$\bar{K}^{*0}$	0.11	$0.0903 \pm 0.016 \pm 0.001$
ϕ	0.028	$0.019 \pm 0.0018 \pm 0.054$
$\bar{p}$	0.084	$0.063 \pm 0.002 \pm 0.001$

In Fig. 6 we compare the model with NA-22 data on the Feynman–x distribution of π^- produced in 250 GeV pp collisions.

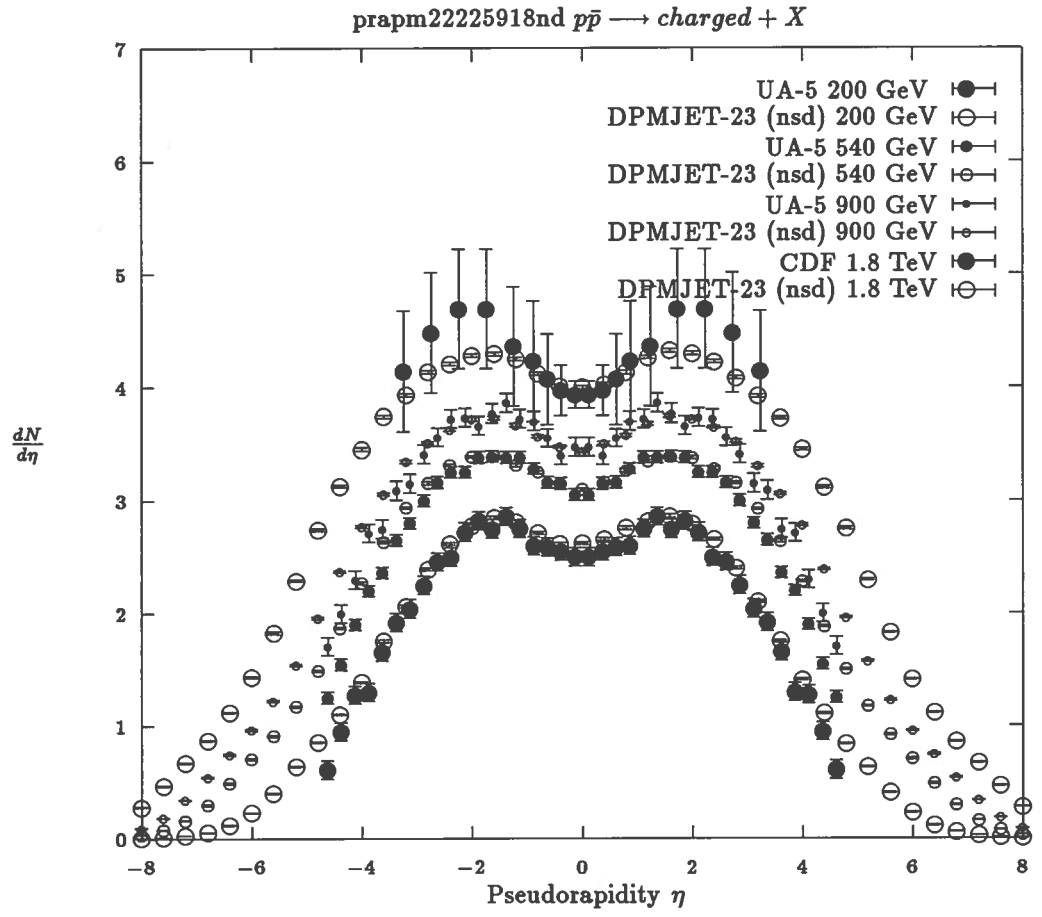

Figure 4: Pseudorapidity distributions of charged hadrons produced in nondiffractive $p\bar{p}$ collisions at $\sqrt{s} = 0.2$, 0.54, 0.9 and 1.8 TeV. The DPMJET–II.3 results are compared with data from the UA–5 Collaboration [96] and from the CDF Collaboration [97].

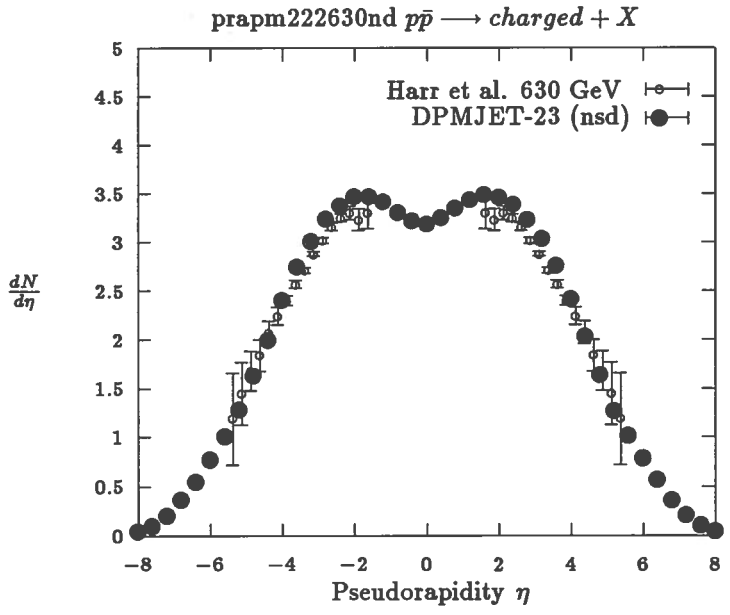

Figure 5: Pseudorapidity distributions of charged hadrons produced in nondiffractive $p\bar{p}$ collisions at $\sqrt{s} = 0.63$ TeV. The DPMJET–II.3 results are compared with recent data from Harr et al. [98].

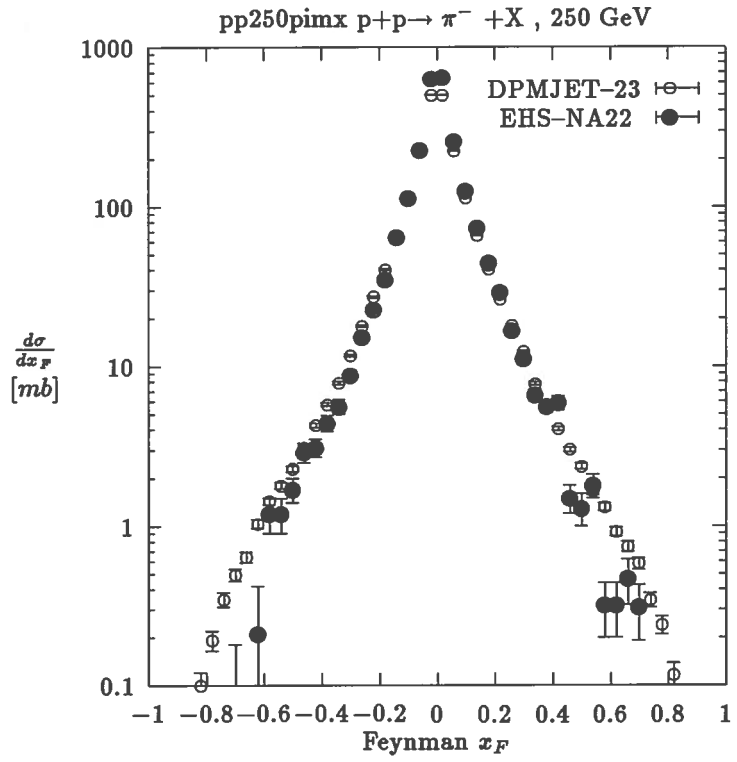

Figure 6: Comparison of Feynman–x distributions od π^- mesons produced in proton–proton collisions at 250 GeV. The experimental data are from the EHS–NA22 Collaboration [99].

3.2 Comparing to data in hadron–nucleus and nucleus–nucleus collisions

We turn to collisions with nuclei. In Fig. 7 The comparison is with the rapidity distribution of charged hadrons in p-Ar collisions at 200 GeV and in Fig. 8 we compare to rapidity distributions of negatively charged hadrons in central S–S and S–Ag collisions.

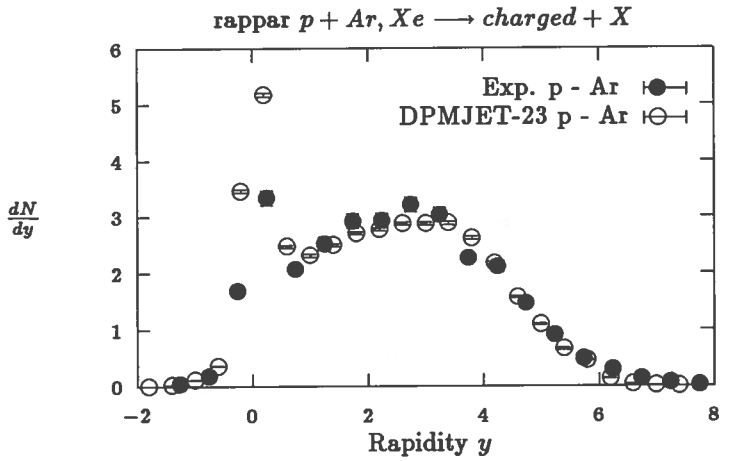

Figure 7: Charged particle rapidity distribution for p–Ar interactions. The DPMJET–II.3 results are compared with data [100].

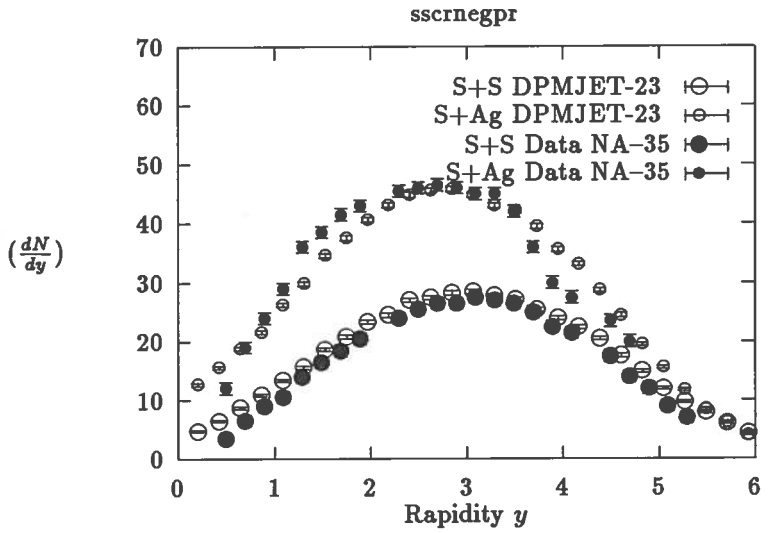

Figure 8: Rapidity distribution of negatively charged hadrons in central S–S ans S–Ag collisions. The results of DPMJET–II.3 are compared with data from the NA–35 Collaboration [101].

3.3 Comparing to data of hadron jet transverse energy distributions and particle transverse momentum distributions

The main new feature of DPMJET–II.3 is in the minijet component, therefore we should compare carefully with particle transverse momentum distributions and hadron–jet transverse energy distributions at collider energies.

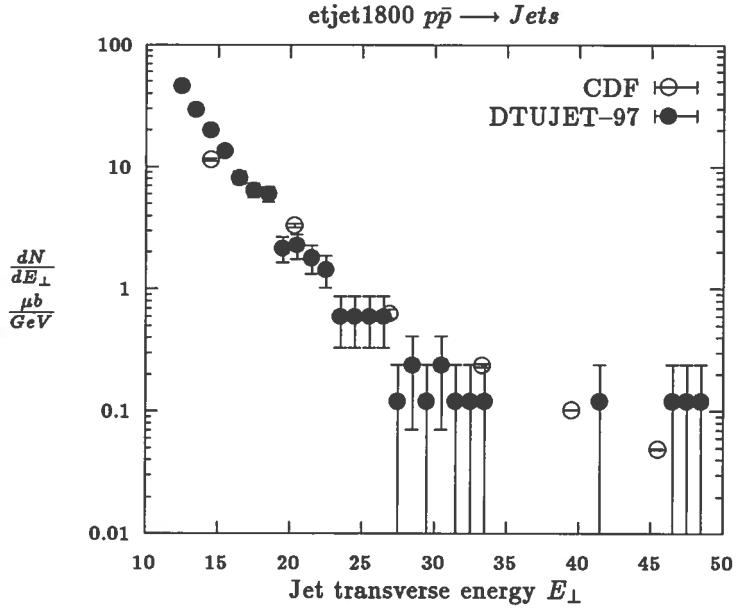

Figure 9: The jet transverse energy distribution is compared with data from the CDF–Collaboration [102]. The jets are found from the model events in the pseudorapidity region $|\eta| \leq 0.7$ using a jet finding algorithm.

In Fig.9 we compare hadron jet production in the model with data from the CDF–Collaboration [102]. The jets from the model are found out of the Monte Carlo events using a jet finding with the same parameters like the one used by the experiment. With a minimum bias Monte Carlo event generator it is of course not possible to obtain good statistics on the total transverse energy range of the experiment. We find good agreement of the jets in the model with the data up to $E_\perp = 30$ GeV/c.

Hadron transverse momentum distributions were measured by the UA–1 Collaboration [103]. In Fig.10 we compare the distributions at $\sqrt{s} = 200$ GeV and 900 GeV with DPMJET–II.3. The transverse momentum distribution up to larger $p_\perp$ was determined by the UA–1–MIMI Collaboration [104]. In Fig.11 we compare the model results with the parametrization of the data given by this experiment.

In Fig.12 we compare average transverse momenta as obtained from DPMJET–II.3 as function of the cms energy $\sqrt{s}$ with data collected by the UA–1 Collaboration. This plot gives at the same time the DPMJET predictions for the average transverse momenta up to $\sqrt{s} = 2000$ TeV. Average transverse momenta depend on the longitudinal variables, they differ if one chooses different pseudorapidity ranges. Therefore in Fig.12 the averages are presented for three different pseudorapidity windows.

Average transverse momenta change also with the multiplicity of the events. This feature is easy to understand qualitatively im models, where events with large multiplicity are mainly events with many minijets. In Fig.13 we compare these transverse momentum – multiplicity correlation for pions and antiprotons in the model with collider data [105].

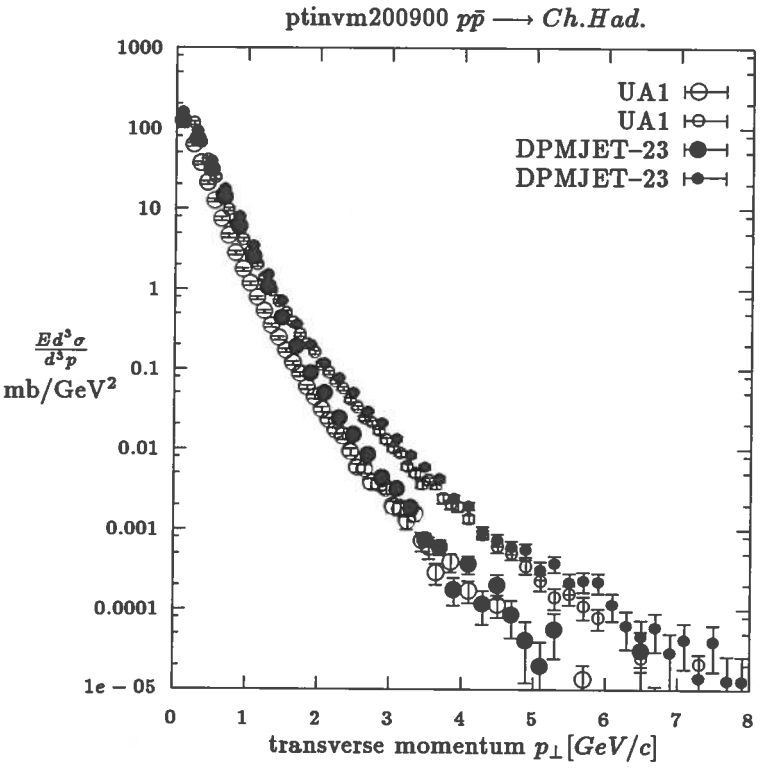

Figure 10: Comparison with transverse momentum cross sections at $\sqrt{e} = 0.2$ and -.9 TeV with collider data from the UA–1 Experiment [103].

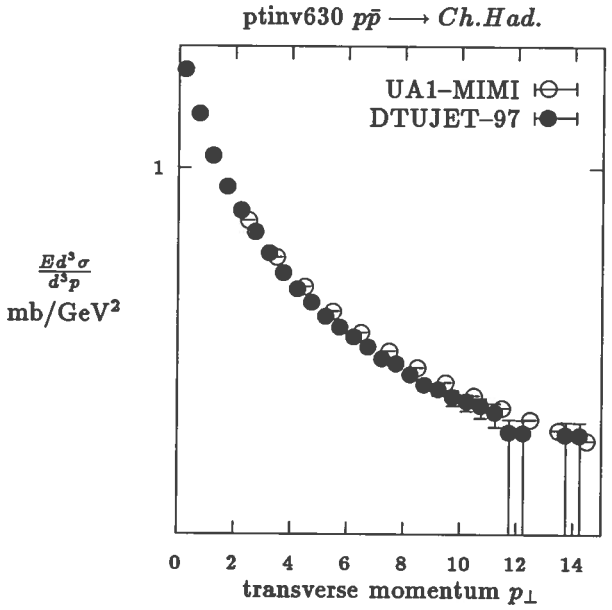

Figure 11: Comparison with transverse momentum cross sections at $\sqrt{e} = 0.63$ TeV with collider data from the UA–1 MIMI Collaboration [104]. The experimental date are represented by the parametrization given by the Experiment.

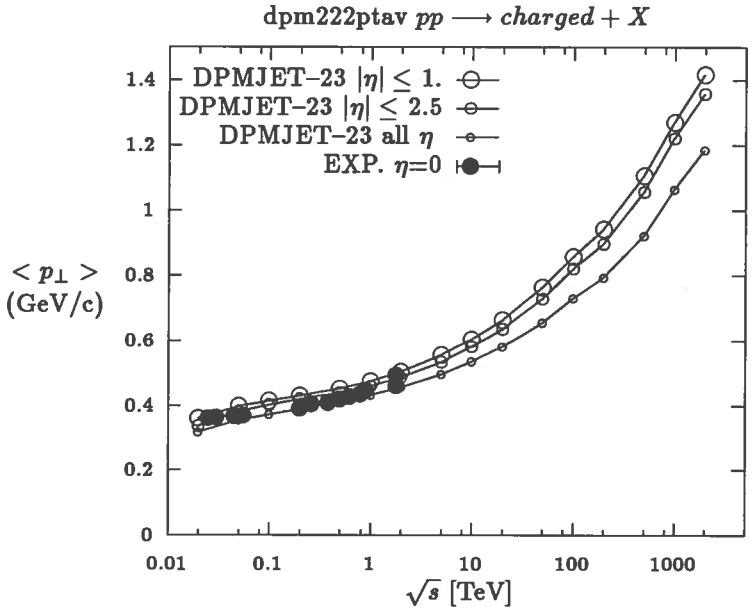

Figure 12: Average transverse momenta of charged secondaries produced in $p\bar{p}$ and pp collisions determined in three different pseudorapidity intervals as function of the center of mass energy $\sqrt{s}$ compared to date collected by the UA–1 Collaboration [103].

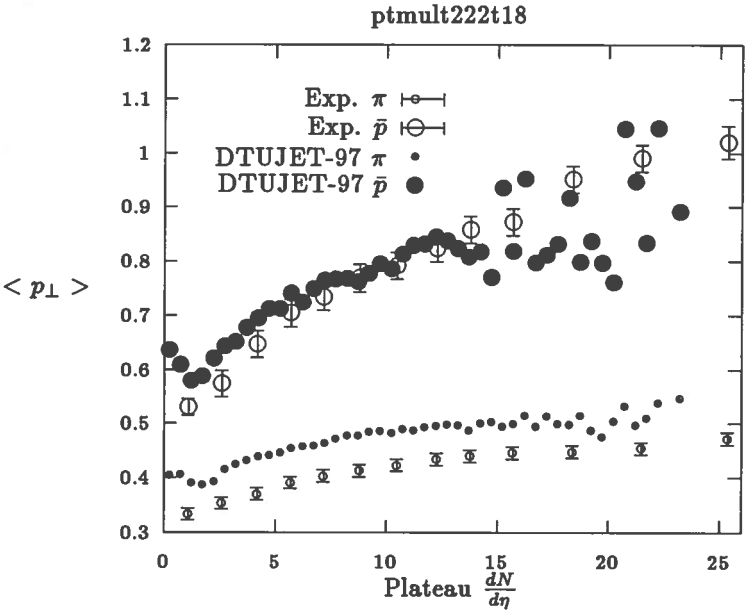

Figure 13: Comparison of the average transverse momentum–multiplicity correlation for secondary pions and antiprotons with collider data [105].

3.4 The fraction of strange hadrons

With rising energy the fraction of strange hadrons rises slowly. In Fig.14 the K/π ratio according to DPMJET–II.3 for pp or $p\bar{p}$ collisions is compared to data from the E735 Collaboration [105].

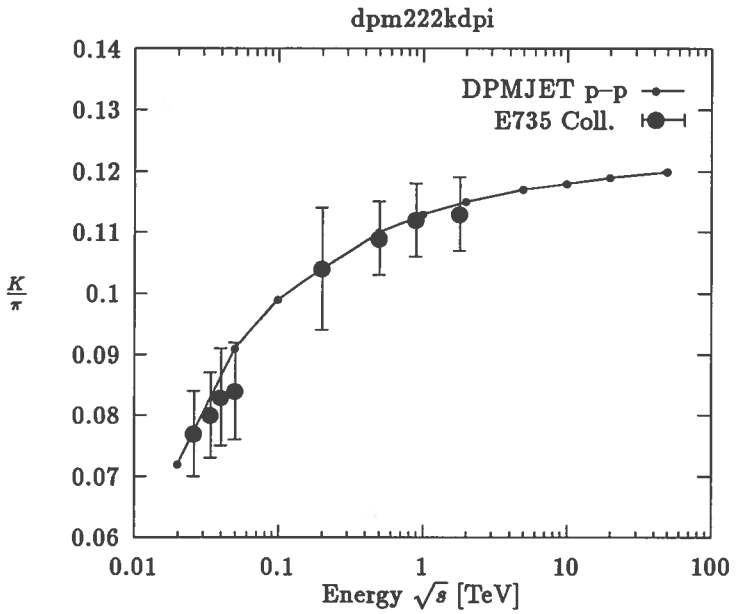

Figure 14: K/π ratios in $p\bar{p}$ collisions as function of the cms energy $\sqrt{s}$. The DPMJET–II.3 calculation is compared with data collected from the E735 Collaboration at Fermilab [105].

4 Properties of the model in the highest energy region

In Fig.15 the pseudorapidity distributions for charged hadrons are presented for energies between $\sqrt{s} = 1$ TeV and 2000 TeV. The width of the distributions increases like the logarithm of the energy and also the maximum of the curves rises like the logarithm of the energy. If we call the central region around the two maxima the plateau, then we find the width of this plateau hardly to change with energy. Fig.16 presents the rise of the total charged multiplicity with the cms energy $\sqrt{s}$.

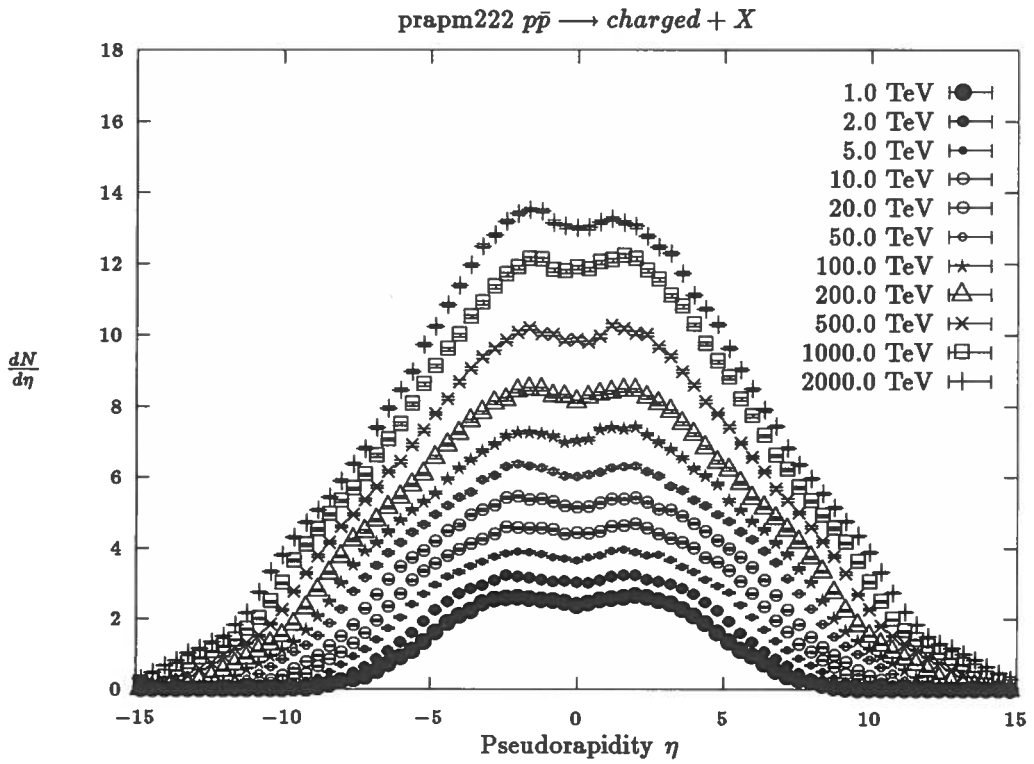

Figure 15: The development of the pseudorapidity distribution of charged hadrons produced in inelastic pp collisions in the in the center of mass energy range between $\sqrt{s}$=1 TeV and $\sqrt{s}$ = 2000 TeV.

In Fig.17 we present the change of the transverse momentum distribution in pp collisions with the cms energy $\sqrt{s}$. Between $\sqrt{s} = 1$ and 2000 TeV the distribution at large pt rises by approximately a factor 10^4. The corresponding rise of the average transverse momenta was already presented in Fig.12

Following for instance the basic discussion of [106], we introduce a variable x_{lab} similarly to Feynman–x_F, but this time in the lab–frame :

$$x_{lab} = \frac{E_i}{E_0} \tag{39}$$

E_i is the lab–energy of a secondary particle i and E_0 is the lab–energy of the projectile in a h–nucleus collision. We introduce x_{lab} distributions $F(x_{lab})$:

$$F_i(x_{lab}) = x_{lab} \frac{dN_i}{dx_{lab}} \tag{40}$$

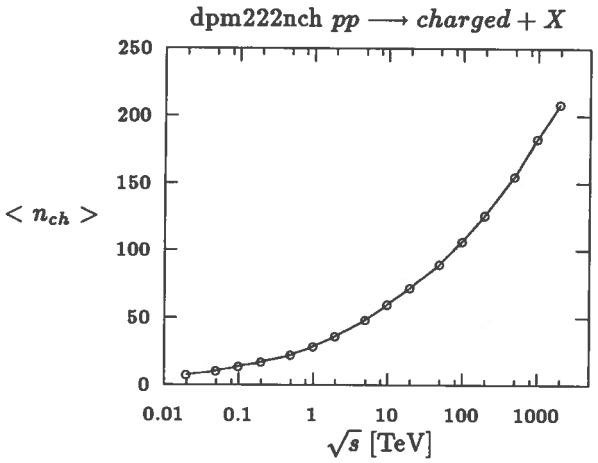

Figure 16: Rise of the charged multiplicity in inelastic pp collisions in the center of mass energy range between $\sqrt{s}$=0.02 TeV and $\sqrt{s}$ = 2000 TeV.

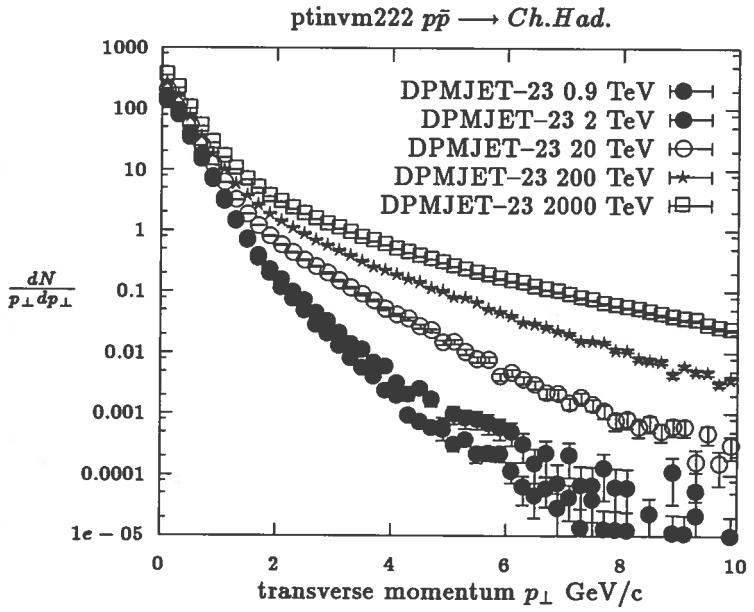

Figure 17: Transverse momentum distributions at center of mass energies $\sqrt{s}$ between 0.9 and 2000 GeV as calculated with DPMJET–II.3.

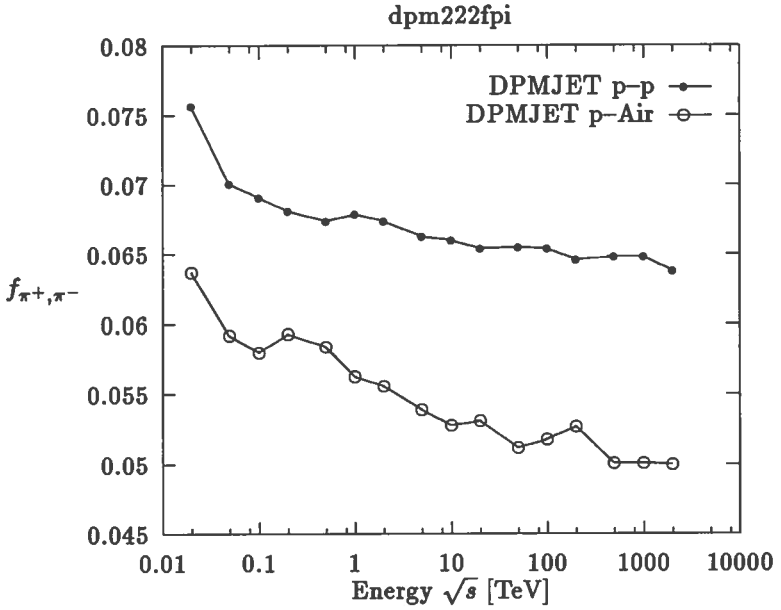

Figure 18: Spectrum weighted moments for pion production in pp and p–Air collisions as function of the (nucleon–nucleon) cms energy $\sqrt{s}$.

We note that the Feynman–x_F distribution at positive x_F in the projectile fragmentation region is a very good approximation to the x_{lab} distribution.

The cosmic ray spectrum–weighted moments in p–A collisions are defined as moments of the $F(x_{lab})$:

$$Z_i^{p-A} = \int_0^1 (x_{lab})^{\gamma-1} F_i^{p-A}(x_{lab}) dx_{lab} \tag{41}$$

Here $-\gamma \simeq -1.7$ is the power of the integral cosmic ray energy spectrum and A represents both the target nucleus name and its mass number.

The spectrum–weighted moments for nucleon–air collisions, as discussed in [106], determine the uncorrelated fluxes of energetic particles in the atmosphere.

We also introduce the energy fraction K_i^{p-A} :

$$K_i^{p-A} = \int_0^1 F_i^{p-A}(x_{lab}) dx_{lab} \tag{42}$$

As for x_{lab}, the upper limit for K is 1 in h–nucleus collisions.

In Fig.18 we present the spectrum weighted moments for pion production in pp and p–Air collisions as function of the cms energy $\sqrt{s}$ per nucleon. In Fig.19 The moments are given for charged Kaon production also in pp and p–Air collisions. The Kaon moments show stronger statistical fluctuations then the pion moments.

In Fig.20 we present again for pp anf p–Air collisions the energy fractions K for $B - \bar{B}$ (baryon - antibaryon) B (baryon) and charged pion production.

We find in DPMJET–II.3 all average values characterizing hadron production: the cross sections (Fig.2), the average transverse momenta (Fig.12) the charged multiplicities (Fig.16), and the moments in Figs. 18, 19 and 20 to change smoothly with energy in most cases just like the logarithm of the energy.

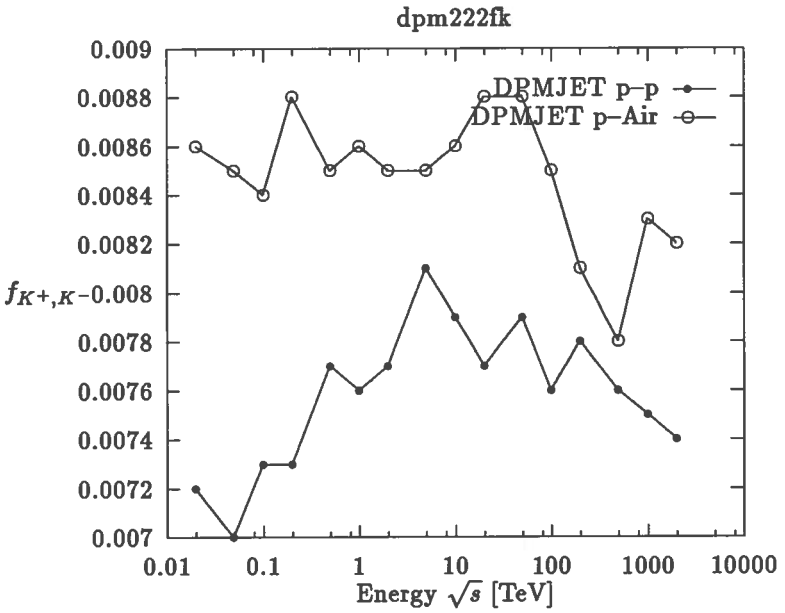

Figure 19: Spectrum weighted moments for Kaon production in pp and p–Air collisions as function of the (nucleon–nucleon) cms energy $\sqrt{s}$.

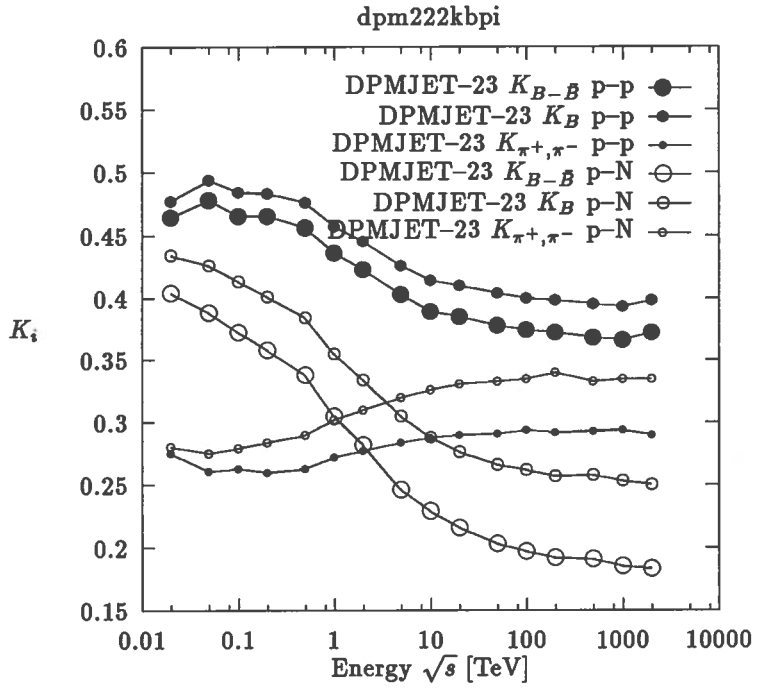

Figure 20: Laboratory energy fractions for $B - \bar{B}$, B and pion production in pp and p–Air collisions as function of the (nucleon–nucleon) cms energy $\sqrt{s}$.

5 Description of the DPMJET–II.3 and II.4 codes

5.1 Program Summary

Title of the program:	DPMJET–II.3,II.4
Computer:	UNIX Workstations
Program language:	FORTRAN-77
Number of program lines:	about 80,000 (in addition the Lund codes linked)
Other programs called: (included in DPMJET in modified form)	By DPMJET–II.3 as well as DPMJET–II.4 DIAGEN [58] Sampling of configurations for nucleus-nucleus interactions within the Glauber formalism BAMJET [62, 61] Sampling the hadronization of strings. This is no longer used, but still available. DECAY [63] Sampling the decay of hadron resonances. HADRIN [66] Sampling hadron-nucleon interactions below 5 GeV. parts of DTUJET [5, 107] Sampling of minijets and multiple soft chains. parts of FLUKA [108] Nuclear evaporation and residual nucleus module.
Other programs called:	Only by DPMJET–II.3 JETSET–7.3 [64] Sampling the hadronization of strings according to the Lund model [64] (privately converted to double precision compilation) qel [109] Quasi elastic neutrino–nucleon interaction.
Other programs called:	Only by DPMJET–II.4 PYTHIA–6.1 [64] Sampling the hadronization of strings according to the Lund model [64] (Double precision version of JETSET) (Note: routine and COMMON names changed) lepto–6.5 [110] Deep inelastic neutrino–nucleon interaction. Note: lepto–6.5 uses also JETSET–7.4.
Method of solution:	Monte Carlo event generator.

5.2 Description of the program DPMJET–II

The basic event generating unit of the code is the subroutine KKINC. Each call of this routine samples one inelastic hadron–nucleus or nucleus–nucleus interaction. Use and necessary initializations are described first in this section; a test program provided with the program package demonstrates the potential application. In the following subsection we discuss important model parameters and define their location in the code for potential user access. The basic structure of the supplied code is described in further subsections.

5.2.1 The event generator KKINC and its initialization

As already mentioned the code DPMJET–II uses several other programs. The initialization of the **BAMJET**[62, 61], **DECAY**[63] and **HADRIN**[66] codes requires *one single call* of the subroutines DPRIBL, DDATAR, DCHANT, DCHANH and DHADDE.
Calls to PRBLM2 and JDTU initialize the multi–Pomeron sampling and the sampling of minijets like in the DTUJET–93 [5, 107] code.
A call to LUNDIN initializes the JETSET-7.3 sampling of chain decay.
Further initializations and parameter definitions are provided in the routine DNINIT, via the named BLOCK DATA BLKDT1 and the subroutine DEFAUL(EPN,PPN). The routine DEFAUL has to be called before event generation, too. Besides other initializations this routine sets the parameters, characterizing the type of the actual interaction, for $\pi^+ Cu$ collisions at 200 GeV; EPN and PPN (output variables) give energy and momentum in the lab–system. Actual predefinition and locations of those parameters which might be changed potentially by the user are discussed in the following subsection.
Basic information for the application of the Glauber formalism according to the code **DIAGEN**[58] is generated by by the subroutine

SHMAKI (IP, IPZ, IT, ITZ, RPROJ, RTARG, PPN)

which requires the following input parameters defining the actual interaction:

IP, IPZ: nucleon number/atomic number of the projectile nucleus; set IP=IPZ=1 for incident hadrons;

IT, ITZ: nucleon number/atomic number of the target nucleus;

PPN: projectile momentum in GeV/c (per nucleon)

Since the calculations performed by SHMAKI are time consuming, in particular for heavy target nuclei, and in general have to be repeated for each different reaction type and energy, resp., the test program provided offers an option to prepare a data file 'GLAUBTAR.DAT' containing the necessary information for hadron–nucleus and nucleus–nucleus interactions to be considered. This file may be generated in a separate run of the test program using the option 'GLAUBERI' and GLAUBERA, compare Appendix A. The information from this file is read for a given projectile (projectile nucleus) (IP,IPZ) and target nucleus (IT, ITZ) by means of a subroutine call

CALL SHMAKF(IP,IPZ,IT,ITZ).

For the use of different target materials and or different projectiles in one calculation SHMAKF has to be called subsequently with the corresponding parameters (IP,IPZ,IT,ITZ). The information read from the file 'GLAUBTAR.DAT' is numbered internally by the index KKMAT=1,2,... according to the sequence of SHMAKF calls; up to 50 materials may be stored in the standard version of the program. If a larger number of materials is to be used the corresponding dimension in the common /DTUMAT/ has to be increased. (If the required data are not found in the file 'GLAUBTAR.DAT' the execution is stopped.)
After these initializations each call of the subroutine

KKINC (EPN, IT, ITZ, IP, IPZ, IPROJ, KKMAT, ITARG, NHKKH1, IREJ)

generates a single event. The input parameters not yet described have the following meaning:

IPROJ: projectile type for hadron–nucleus collisions;
DPMJET–II uses the naming and internal numbering conventions from the BAMJET [61, 62] and DECAY [63] codes which are listed in Table A–2 of Appendix A.1;

ITARG: Target type for hadron–hadron collisions;
DPMJET–II uses the naming and internal numbering conventions from the BAMJET [61, 62] and DECAY [63] codes which are listed in Table A–2 of Appendix A.1;

KKMAT: controls the access of the event generator to the information on the Glauber formalism:
KKMAT=0 : Glauber data expected from SHMAKI calculation;
KKMAT>0 : Glauber data expected from the KKMAT'th call of the subroutine SHMAKF.

NHKKH1: gives the position in the event COMMON HKKEVT, after which the final state particles
are recorded.

IREJ: IREJ = 1 indicates, that the event has been rejected
IREJ = 0 indicates, that the event is fine.

If DPMJET–II is used as event generator in a hadron cascade code, it is practical to write an interface routine. For the use of DPMJET–II in the Cosmic Ray cascade code HEMAS–DPM [36] there exists such an interface in the file dpmevt.f.

The following commands will cause the generator to sample one inelastic $\pi^+ Cu$ event at 200 GeV laboratory energy:

```
      CALL DMINIT(NCASES,EPN,PPN,NCOUNT,IGLAUB)

All of the following down to CALL SAMPPT is usually done within DMINIT

  *** BAMJET and DECAY initialization
        CALL DDATAR
        CALL DCHANT
  *** HADRIN initialization
        CALL DHADDE
        CALL DCHANH
  *** setting default parameters
        CALL DEFAUL(EPN,PPN)
        CALL DEFAUX(EPN,PPN)
  *** JETSET initialization
        CALL LUNDIN
  *** initialization of the random number generator supplied with DPMJET--II
        CALL RNDMST(12,34,56,78)
  *** initialization for the Glauber formalism by explicit calculation
  *** for the actual reaction (projectile/target/energy = pi+/Cu/200 GeV)
        IP=1
        IPZ=1
        IT=64
        ITZ=29
        PPN=200.
        CALL SHMAKI(IP,IPZ,IT,ITZ,RPROJ,RTARG,PPN)
  *** sampling of 1 event (pi+ has type IPROJ=13)
        IPROJ=13
        KKMAT=0
  *** initialization of the evaporation module
        CALL BERTTP
        CALL INCINI
  *** initialization of the unitarization
        CALL PRBLM2(CMENER)
  *** initialization of the hard scattering
        CALL JTDTU(0)
  *** initialization of the transverse momenta for soft scattering
        CALL SAMPPT(0,PT)


  *** generating one event
        CALL KKINC(EPN,IT,ITZ,IP,IPZ,IPROJ,KKMAT)}
        STOP
```

To use the information from the file 'GLAUBTAR.DAT' one has to call SHMAKF instead of SHMAKI and define KKMAT=1.

5.2.2 Information on the final state particles

During the generation of single events several entries are scored in the common blocks /HKKEVT/ and /EXTEVT/ characterizing subsequent stages of the sampling process: Information on initial state nucleons as well as on interacting partons and constructed parton chains, decaying resonances and final state particles is stored into these common blocks. It has the following structure, completely defined in Appendix B:

```
PARAMETER (NMXHKK=.....)
      COMMON /HKKEVT/ NHKK,NEVHKK,ISTHKK(NMXHKK),IDHKK(NMXHKK),
     &                JMOHKK(2,NMXHKK),JDAHKK(2,NMXHKK),
     &                PHKK(5,NMXHKK),VHKK(4,NMXHKK),WHKK(4,NMXHKK)
      COMMON /EXTEVT/ IDRES(NMXHKK),IDXRES(NMXHKK),NOBAM(NMXHKK),
     &                IDBAM(NMXHKK),IDCH(NMXHKK),NPOINT(10)
```

The entries are characterized by their status ISTHKK and type IDHKK as well as by the 4-momenta PHKK; additional pointers define 'parents' and 'daughters' of the actual entry. Final state particles are identified by their status ISTHKK(i)=1.
The structure of this common block closely follows the suggestions of Ref. [111, 112]; conventions for the description of the event history are described in some detail in Appendix B.2, followed by a sample event in Appendix B.3.

5.2.3 Important parameters of the code

In this subsection we summarize physical meaning and location of those parameters which may have a significant influence on observable quantities.

Sampling of x–values for partons

Parton x–values for a given hadron are sampled from distributions of the general form

$$q(x) \propto x^{-\alpha}(1-x)^{\beta},$$

subject to the reqirement that their sum is equal to one. The user has access to the β–parameters for valence quarks which have, however, only minor influence on the final results. They are set to the following default values:

$$\beta_v^{nuc} = 3.5, \qquad \beta_v^{mes} = 1.5;$$

for reasons of an optimal sampling efficiency $\beta_{sea} \equiv 0.0$. From standard Regge arguments the power in x is fixed to be $\alpha^{sea} = 1.0$ and $\alpha^{val} = 0.5$ for sea and valence quarks, resp.; these values may not be changed by the user.
Additionally, the x–values for partons of colliding projectile and target hadrons are correlated by the interaction mechanism within the DTU model: The constructed color–neutral parton–parton systems (chains) should aquire at least some minimum mass M_{min} to allow the fragmentation into final state hadrons,

$$M^2 \simeq x^{target} \cdot x^{project.} \cdot s \geq M_{min}^2;$$

otherwise the collision numbers sampled according to the Glauber formalism may be strongly biased. Therefore, lower cuts are defined for the sampling of x–values, $x^{min} = C/\sqrt{s}$, differing for valence quarks, diquarks and sea quarks, resp. To ensure minimum chain masses for valence–valence (v–v) systems the following values are set by default within DPMJET–II:

$$C_q^{val} = 1.0, \qquad C_{qq}^{val} = 2.0, \qquad C_{q/\bar{q}}^{sea} = 0.2$$

However, since these cuts are imposed for both the projectile and the target independently, lower (but still kinematically allowed) chain masses tend to be suppressed at least for v–v systems. This unwanted effect is partly corrected by resampling the x–value of the valence quark with the lowest kinematically allowed x_v^{min} if the mass of a v–v chain exceeds a certain value M_{vv}^{thr}. In a similar way the mass of sea–sea (s–s) systems may be required to exceed some minimum value,

$$M_{ss} \geq M_{ss}^{min}.$$

(Note that the s–s chains are only formed in nucleus–nucleus collisions.) The default values for the last mentioned parameters are

$$M_{vv}^{thr} = 6 \text{ GeV}, \qquad M_{ss}^{min} = 0.14 \text{ GeV}.$$

All the user accessible parameters discussed so far are located in the common block

```
      COMMON /XSEADI/ XSEACU,UNON,UNOM,UNOSEA, CVQ,CDQ,CSEA,SSMIMA,
     +                SSMIMQ,VVMTHR
```

with the following assignments:

β_v^{nuc} = UNON	β_v^{mes} = UNOM	
C_q^{val} = CVQ	C_{qq}^{val} = CDQ	$C_{q/\bar{q}}^{sea}$ = CSEA
M_{ss}^{min} = SSMIMA	$(M_{ss}^{min})^2$ = SSMIMQ	M_{vv}^{thr} = VVMTHR

Generation of transverse momenta for secondary hadrons

In the model there are two sources of transverse momenta for created secondaries. First the partons aquire an internal $p_\perp$ which is taken into account in the construction of parton–parton chains. The subsequent hadronization of the partonic chains is modelled by the JETSET code [64] (formerly the BAMJET code [62, 61] was used) which itself assignes to the created particles transverse momenta with respect to the jet axis.
Internal transverse momenta for partons are sampled within the subroutine SELPT (file DPMNUC3) according to the following distribution for the reduced transverse energy $E_s = E_\perp - m_p$,

$$\frac{dn}{dE_s} \propto E_s \exp\left(-\gamma^2 E_s/2\right) \tag{43}$$

with

$$p_\perp = \sqrt{E_s^2 + 2E_s m_p}, \qquad m_p = 0.94 \text{ GeV},$$

where the slope parameter $\gamma \equiv$ BB3 is defined directly in this routine (default value BB3=6.0). However, in the case of severe kinematical limitations for individual partons/chains this parameter may be modified in the sampling process.

Intranuclear cascade

There are two important parameters controlling the development of the intranuclear cascade which have been defined in the previous section: The formation time τ_0 of created secondary hadrons, and the factor α_{mod}^F scaling the Fermi momenta of nucleons. With increasing τ_0 the number of cascade generations and the number of low-energy particles will be reduced; α_{mod}^F provides the possibility for a certain modification of the momentum distribution for low–energy nucleons.
Additionally, the maximum number of cascade generations KTAUGE (by default 25) may be reset by the user to estimate the influence of the intranuclear cascade. In particular, the cascade is switched off by the choice KTAUGE=0.
In the code the corresponding parameters are defined in the common blocks

```
      COMMON /TAUFO/  TAUFOR,KTAUGE,ITAUVE
      COMMON /NUCIMP/ PRMOM(5,248),TAMOM(5,248),...,
     +                PREBIN,TAEBIN,FERMOD,ETACOU
```

where $\tau_0 \equiv$ TAUFOR and $\alpha_{mod}^F \equiv$ FERMOD. The option ITAUVE determines whether the $p_\perp$–dependent definition of the formation time (ITAUVE=1) or the constant value τ_0 (ITAUVE=2) are used; by default ITAUVE=1 (compare Section 2.2).

Lund JETSET fragmentation

The chain fragmentation according to the Lund model JETSET–7.3 is customized for the DPMJET–II needs by changing some of the Lund parameters in the initialization routine LUNDIN. More parameters are changed in the routine BAMLUN, where one JETSET fragmentation is called.
In LUNDIN we prevent furthermore the weak decays of all otherwise stable hadrons and the decay of the π^0 by setting the corresponding MDCY parameters equal to zero.

Baryon and strangeness production, Popcorn mechanism:

The popcorn mechanism in BAMJET and JETSET is controlled by the parameter p_{dB} (default: $p_{dB} = 0.2$).

```
      COMMON /POPCOR/ PDB,AJSDEF
```

In BAMJET p_{dB} gives the fraction of the diquarks fragmenting directly into baryons.
In JETSET $p_{dB} = 0.$ is used, to switch off the popcorn mechanism.
Sea SU(3) symmetry: The parameter s^{sea} = SEASQ (default: SEASQ = 0.5) controls the s-quark content at the sea–quark chain ends.

```
      COMMON /SEASU3/ SEASQ
```

Cronin effect: The parameters MKCRO (default: MKCRO = 1) and CRONCO (default: CRONCO = 0.64) control the multiple scattering of partons within nuclear matter, and thus the Cronin effect.

```
      COMMON /CRONIN/ CRONCO,MKCRON
```

MKCRON = 0 switches off the Cronin effect.
CRONCO is the parameter in the parton multiple scattering formula.

5.2.4 Structure of the supplied code

The DPMJET–II standard source code is stored in several FORTRAN files, listed in the following:

- dpmnuc1.f, dpmnuc2.f, dpmnuc3.f, dpmnuc4.f, dpmnuc5.f, dpmnuc6.f

  These modules contain all subroutines needed to describe the primary interaction according to the DPM as defined in the previous section. This includes the assignment of Fermi momenta to nucleons, construction of chains and monitoring their decay as well as the intranuclear cascade for generated secondaries.

- dpmtcbsh.f

  Contains the BAMJET [62, 61] and DECAY [63] routines for chain fragmentation, routines to test and call BAMJET as well as the routines from DIAGEN [58] for sampling the actual numbers of elementary collisions (i.e. n, n_p, n_t) according to the Glauber formalism.

- dpmhadri.f

  Includes the HADRIN [66] routines for event generation in hadron-nucleon collisions below 5 GeV as well as routines for the calculation of energy and reaction dependent cross sections.

- dpmnulib.f

  Contains few standard routines usually uneffected by further developments of the code, including the applied random number generator [113].

- dpmhist.f

  Contains the test program mentioned in the beginning of this subsection as well as a sample histogram routine producing line printer output for average multiplicities, rapidity and pseudo-rapidity distributions for generated particles.

- dpmdiff.f

  Contains the routines used to call single diffractive particle production.

- dpmlund.f

  Contains the routines nterfacing DPMJET–II with JETSET–7.3.

- dtu93luj.f (only in version DPMJET–II.3)

  Contains JETSET–7.3 privately transformed for compilation under double precision.

- pythia61.f (only in version DPMJET–II.4)

  Contains double precision version of JETSET combined with the PYTHIA–6.1 code.

- dpmsicha.f

  Contains the Regge exchange (single chain) contributions to the model.

- dpmdiqqq.f

  Contains contributions to the model with sea–diquarks at the chain ends.

- dpmevap2.f or dpmeva.f

  Contains the nuclear evaporation module. Please note, that the module DPMEVAP2 and the data file NUCLEAR.BIN can not be obtained from the author of DPMJET–II. The evaporation module from FLUKA [108] has to be obtained directly from the Authors of FLUKA (Dr. A.Ferrari and Dr. P.R.Sala, INFN, Sezione di Milano, I–20133 Milano, Italy). The DPMEVA module contains dummy routines, to enable to run DPMJET-II without changes without the DPMEVAP module. Of course DPMEVA performs no evaporation of the residual nucleus.

- dtu97lap.f or dpm97lap.f

Contains the calculation of the minijets.

Using the file dtu97lap.f the initialization of the minijets is done for one energy, given by the input cards. This version is used for stand–alone runs of the code, where each event is called for the same primary energy.

Using the file dpm97lap.f this initialization is done for all energies. This version is suitable to insert DPMJET–II into hadron cascade codes, where each event will be called at a new energy.

- dtu97pom.f or dpm97pom.f

  Contains the calculation of multiple chain production according to eikonal unitarization.

  Using the file dtu97pom.f the initialization of the two component Dual Parton Model (calculation of the exclusive multi Pomeron distribution) is done for one energy, given by the input cards. This version is used for stand–alone runs of the code, where each event is called for the same primary energy.

  Using the file dpm97pom.f this initialization is done for all energies. This version is suitable to insert DPMJET–II into hadron cascade codes, where each event will be called at a new energy.

  If the code is run repeatedly, it will be practical, to read these initialization tables, once calculated, from an external file.

- dtu97ctq.f

  Contains the last version of the CTEQ parton structure functions.

- dpmqeld.f

  Contains the qel code transformed to double precision and modified to use the Fermi momenta of the nucleons from DPMJET.

- lepto2.f (and jetset74.f)

  Contains the LEPTO–6.5 code in single precision, which uses the single precision jetset74.f. The lepto code has been modified to use PYTHIA routines from the double precision pythia61.f.

5.2.5 External input and output data files used

- GLAUBTAR.DAT, Unit 47

  Glauber model data, see input cards GLAUBERI, GLAUBERA.

- dtplapt3.dat, Unit 2

  Input data for the KMRS structure functions. These structure functions are no longer the default, therefore opening thes file is only needed, if one of these old structure functions is used.

- mrs92.dat, Unit 2

  Input data for the MRS structure functions. These structure functions are no longer the default, therefore opening thes file is only needed, if one of these old structure functions is used.

- NUCLEAR.BIN

  Binary file to read in nuclear data for use in the evaporation module.

- qel.evt

  Output file for the qel–events without the modifications of these events in DPMJET.

- lepto.evt

  Output file for the lepto–events without the modifications of these events in DPMJET.

5.2.6 Sequence of subroutine calls for event generation

1. The generator subroutine KKINC monitors the sampling of a single event by one call of KKEVT, repeated FOZOKA calls and call(s) of the subroutine FICONF.

2. The subroutine KKEVT performs the sampling of the primary projectile–target interaction. This includes

   - sampling of the actual nucleon coordinates and assignment of 'partners' in the n elementary interactions between n_p and n_t nucleons from the projectile and the target, resp., done in SHMAKO [58];
   - sampling of Fermi momenta of all nucleons in colliding nuclei in FER4M;
   - sampling of x-values for the appropriate quark systems (quarks, antiquarks and diquarks, resp.) from the interacting hadrons in the subroutine XKSAMP and assignment of quark flavors in FLKSAM;
   - construction of color neutral parton-parton chains in the subroutines KKEVVV, KKEVSV, KKEVVS, KKEVSS and further similar routines;
   - hadronization of chains via the BAMJET and DECAY codes (JETSET is called from within BAMJET), monitored by the subroutine HADRKK;
   - At energies below 3–5 GeV the code HADHAD is called as hadron–hadron event generator interfacing to the HADRIN code [66].
   - Diffractive events are generated using a call to SDIFF.

3. Alternatively the subroutines KKEVNU or KKEVLE treat the first step of the qel or lepto neutrino nucleus scattering.

   finally KKEVT, KKEVNU or KKEVLE returns the control to KKINC.

4. The intranuclear cascade is modeled by subsequent calls of FOZOKA for each secondary which did not leave the interacting nuclei. FOZOKA transports the particle either until the next interaction or until it leaves the nucleus.

5. The Routine FICONF is called to perform the evaporation step.

5.2.7 The test program DPMJET–II

The event generator itself is supplied together with a test program which may serve as an example for the application of the program. By a call of the subroutine DMINIT (included in the source file DPMNUC1) the main program DPMJET–II does the necessary initializations discussed above. It also allows the definition/modification of model parameters via input options explained in Appendix A.
The sample histogram routine DISTR (source file DPMHIST) generates line printer output for average multiplicities, rapidity and pseudorapidity distributions for created particles. The scoring procedure demonstrates how the information on the event history stored in the common /HKKEVT/ may be applied to extract the properties of the final state particles.

5.2.8 Remarks on the other codes applied in DPMJET–II: DIAGEN, BAMJET, DECAY, HADRIN and RNDM

All the external codes applied are well documented. The generator DIAGEN [58] samples configurations for nucleus-nucleus interactions in the framework of the Glauber model, i.e. spatial coordinates of nucleons in projectile and target nuclei, resp., as well as the actual numbers of 'elementary' interactions n, n_p and n_t (comp. sect. 2). DIAGEN routines are called via SHMAKI (initialization) and SHMAKO (sampling of configurations), both included in the file DPMTCBSH.
DPMJET–II calls BAMJET via routines which already perform Lorentz transformations and rotations of the events generated in BAMJET. The actual calling sequence is HADJET–CALBAM–DBAMJE. The JETSET code is called from inside BAMJET; HADJET is called from the HADRxx routines (module DPMNUC3) monitoring the hadronization of parton chains.
A modified version of the resonance decay routine is defined by the subroutine DECHKK treating the decay of resonances from the common /HKKEVT/.
The program HADRIN [66] for the description of hadron-nucleon interactions below 5 *GeV* is well tested against data [114]. In DPMJET–II it is called via the subroutine FHAD (file DPMHADRI).
The algorithm applied for the generation of uniform random numbers (function RNDM) was described in ref.

[113]. The generated sequence of pseudorandom numbers should be independent of the actual hardware (if a real number has at least 24 significant bits in the internal representation). This generator has a period of about 2^{144}. A few more comments and a test routine are provided in the source file DPMNULIB.

6 Summary

The model DPMJET–II.3/II.4 das been extended in energy up to lab energies of 10^{21} eV or $\sqrt{s} = 2000$ TeV.

In the present paper we report mainly about comparisons of this model with collider experiments.

Many of the published comparisons of former versions of the model to other aspects of experimental data should come out quite similar with the new versions of DPMJET–II, we mention especially the Feynman scaling behaviour of the model [1], the properties of the model at low energies

The test of the new version is however not yet completed. There are certainly more tests of the model needed for hadron–nucleus and nucleus–nucleus collisions (data from heavy ion experiments), for strangeness production, for secondary interactions of the produced particles and for the baryon stopping behaviour in nuclear collisions. Such tests are planned during the next year.

Acknowledgements

I thank first of all my collaborator Dr. H.–J. Möhring with whom together all previous versions of the code up to DTUNUC–1.03 were developped. The author thanks Y. Shmakov for supplying the DIAGEN code prior to publication. Furthermore, the support of CERN , the Department of Theoretical Physics in Lund, INFN, Sezione di Milano , INFN,LNF Frascati, LAPP Annecy, The University Santiago de Compostela and INFN, Lab. Naz. del Gran Sasso, where parts of the program were developped is acknowledged. The code in the versions described here was finalized at Gran Sasso. The author acknowledges the fruitful collaborations with P.Aurenche, G.Battistoni, F.Bopp, M.Braun, A. Capella, R.Engel, A.Ferrari, C.Forti, K.Hänßgen, K.Hahn, I.Kawrakov, C.Merino, N.Mokhov, H.J.Möhring, C.Pajares, D.Pertermann, S.Ritter, S.Roesler, P.Sala, G.R.Stevenson and J.Tran Thanh Van on the Dual Parton Model in general.

References

[1] J. Ranft: Phys. Rev. D 51 (1995) 64

[2] J. Ranft: DPMJET–II, a Dual Parton Model event generator for hadron–hadron, hadron–nucleus and nucleus–nucleus collisions, Proceedings of the second SARE workshop at CERN, 1995,ed. by G.R.Stevenson, CERN/TIS–RP/977–05, p. 144,, 1997

[3] M. Glück, E. Reya and A. Vogt: Z. Phys. C67 (1995) 433

[4] CTEQ-Collab.: H. L. Lai et al.: Phys. Rev. D55 (1997) 1280

[5] F. W. Bopp, D. Pertermann, R. Engel and J. Ranft,: Phys. Rev. D 49 (1994) 3236

[6] G. F. Chew and C. Rosenzweig: Nucl. Phys. B104 (1976) 290

[7] H.-M. Chan, J. E. Paton and S. T. Tsou: Nucl. Phys. B86 (1975) 479

[8] A. Capella, U. Sukhatme,Chung I Tan and J. Tran Thanh Van: Phys. Rep. 236 (1994) 225

[9] A. Capella, J. Tran Thanh Van and J. Kwiecinski: Phys. Rev. Lett. 58 (1987) 2015

[10] P. Aurenche, F. W. Bopp, A. Capella, J. Kwiecinski, M. Maire, J. Ranft and J. Tran Thanh Van: Phys. Rev. D45 (1992) 92

[11] F. W. Bopp, A. Capella, J. Ranft and J. Tran Thanh Van: Z. Phys. C C51 (1991) 99

[12] F. W. Bopp, D. Pertermann and J. Ranft: Z. Phys. C C54 (1992) 683

[13] R. Engel, F. W. Bopp, D. Pertermann and J. Ranft: Phys. Rev. D D46 (1992) 5192

[14] S. Roesler, R. Engel and J. Ranft: Z. Phys. C C59 (1993) 481

[15] B. L. Combridge, J. Kripfganz and J. Ranft: Phys. Lett. 70B (1977) 234

[16] J. Ranft and S. Ritter: Z. Phys. C C 20 (1983) 347

[17] J. Ranft and S. Ritter: Z. Phys. C C 27 (1985) 569

[18] H.-J. Möhring, J. Ranft and S. Ritter: Z. Phys. C C 27 (1985) 419

[19] J. Ranft : Phys. Lett. 188B (1987) 379

[20] J. Ranft : Z. Phys. C C 43 (1989) 439

[21] V.S.Barashenkov and V.D.Toneev: Moscow Atomisdat (1972)

[22] H.W. Bertini: Phys. Rev. 131 (1963) 1801

[23] L. Landau and I. Pomeranchuk: Dokl. Akad. Nauk SSR 92 (1953) 535, 734

[24] L. Stodolski: Proc. Vth Intern. Colloquium on Multiparticle Reactions Oxford (1975) 577

[25] A. Ferrari, J. Ranft, S. Roesler and P. R. Sala: Z. Phys. C70 (1996) 413

[26] A. Ferrari, J. Ranft, S. Roesler and P. R. Sala: Z. Phys. C71 (1996) 75

[27] J. Ranft: Phys. Rev. D37 (1988) 1842

[28] H.-J. Möhring and J. Ranft: Z. Phys. C52 (1991) 643

[29] I.Kawrakow, H.–J.Möhring and J.Ranft: Nucl. Phys. B A544 (1992) 471

[30] I.Kawrakow, H.–J.Möhring and J.Ranft: Z. Phys. C C56 (1992) 115

[31] H.–J. Möhring, J. Ranft, A. Capella and J. Tran Thanh Van: Phys. Rev. D47 (1993) 4146

[32] S. Roesler, R. Engel and J. Ranft: Z. Phys. C C59 (1993) 481

[33] J. Ranft, A. Capella and J. Tran Thanh Van: Phys. Lett. B320 (1994) 346

[34] A. Capella and J. Tran Thanh Van and J. Ranft: Nucl. Phys. B A 566 (1994) 511c

[35] G. Battistoni, C. Bloise, C. Forti, M. Greco, J. Ranft and A. Tanzini: Astroparticle Physics 4 (1996) 351

[36] G. Battistoni, C. Forti and J. Ranft: Astroparticle Phys. 3 (1995) 157

[37] G. Battistoni, C. Forti, J. Ranft and S. Roesler: Deviations from the superposition model in a Dual Parton Model with formation zone cascade in both projectile and target nuclei, preprint US-FT/29-96, (hep-ph/9606485), to appear in Astroparticle Phys., 1996

[38] L. Durand and H. Pi: Phys. Rev. Lett. 58 (1987) 303

[39] T.K. Gaisser and F. Halzen : Phys. Rev. Lett. 54 (1987) 1754

[40] R.S. Fletcher, T.K. Gaisser, P. Lipari and T. Stanev,: Phys. Rev. D50 (1994) 5710

[41] X. N. Wang and M. Gyulassy: Phys. Rev. D44 (1991) 3501

[42] K. Hahn and J. Ranft: Phys. Rev. D41 (1990) 1463

[43] A.Capella and J.Tran Thanh Van : Z. Phys. C C 10 (1981) 249

[44] A.B.Kaidalov and O.I.Piskunova : Z. Phys. C C 30 (1986) 145

[45] A. D. Martin, R. G. Roberts and W. J. Stirling: Phys. Rev. D47 (1993) 867

[46] A. Donnachie and P. V. Landshoff: Phys. Lett. B296 (1993) 227

[47] G. Arnison et al.: Phys. Lett. B128 (1983) 336

[48] UA4 Collab.: M. Bozzo et al.: Phys. Lett. B147 (1984) 385

[49] N. A. Amos et al.: Nucl. Phys. B262 (1985) 689

[50] UA4 Collab.: D. Bernard et al.: Phys. Lett. B198 (1987) 583

[51] UA5 Collab.: G. J. Alner et al.: Z. Phys. C32 (1986) 153

[52] E710 Collab.: N. A. Amos et al.: Phys. Lett. B243 (1990) 158

[53] CDF Collab.: F. Abe et al.: FERMILAB-PUB-93/234-E, 1993

[54] CDF Collab.: F. Abe et al.: Phys. Rev. D50 (1994) 5518

[55] CDF Collab.: F. Abe et al.: Phys. Rev. D50 (1994) 5550

[56] H.H.Mielke, M.Föller, J.Engler and J.Knapp : J.Phys. G 20 (1994) 637

[57] J. Ranft and S. Roesler: Z. Phys. C62 (1994) 329

[58] S.Yu.Shmakov,V.V.Uzhinskii andA.M.Zadoroshny: Comp.Phys.Comm. 54 (1989) 125

[59] R.Castaldi and G.Sanguinetti : Ann.Rev.Nucl.Part.Sci. 35 (1985) 351

[60] Particle Data Group: Phys. Rev. D45 (1992) 1

[61] S. Ritter: Comput. Phys. Commun. 31 (1984) 393

[62] J. Ranft and S. Ritter: Acta Phys. Pol. B 11 (1980) 259

[63] K. Hänssgen and S. Ritter: Comput. Phys. Commun. 31 (1984) 411

[64] T. Sjöstrand: Comp. Phys. Comm. 82 (1994) 74

[65] A. Bialas: Z. Phys. C26 (1984) 301

[66] K. Hänssgen and J. Ranft: Comput. Phys. Commun. 39 (1986) 37

[67] T.W. Armstrong, K.C. Chandler: Nucl. Sci. Eng. 49 (1972) 110

[68] P. Cloth, D. Filges, G. Sterzenbach, T.W. Armstrong, B.L. Colborn: KFA-Report, Jül-Spez-196, 1983

[69] V. F. Weisskopf: Phys. Rev. 52 (1937) 295

[70] I. Dostrovsky, Z. Fraenkel and G. Friedlander: Phys. Rev. 116 (1959) 683

[71] R. Vandenbosh and J. R. Huizenga: *Nuclear Fission* Academic Press New York 1973

[72] N. Bohr and J. A. Wheeler: Phys. Rev. 56 (1939) 426

[73] F. Atchison: preprint Jül-conf-34, in Proceedings of the Meeting on Targets for neutron beam spallation sources, KFA Jülich, Germany, ed. by G. Bauer, 1980

[74] A. Gilbert and A. G. W. Cameron: Can. J. Phys. 43 (1965) 1446

[75] A. V. Ignatyuk, G. N. Smirenkin and A. S. Tishin: Sov. J. Nucl. Phys. 21 (1975) 255

[76] A. V. Ignatyuk et al.: Sov. J. Nucl. Phys. 21 (1975) 612

[77] S. G. Mashnik: Acta Phys. Slov. 43 (1993) 86

[78] A. S. Iljinov and M. V. Mebel: Nucl. Phys. A543 (1992) 517

[79] S. Shlomo: Nucl. Phys. A539 (1992) 17

[80] E. Fermi: Prog. Theor. Phys. 5 (1950) 1570

[81] M. Èpherre and E. Gradsztajn: J. Physique 18 (1967) 48

[82] G. A. Bartholomew et al.: Advances in Nuclear Physics 7 (1975) 229

[83] I. Bergqvist and N. Starfelt: Progress in Nuclear Physics 11 (1970) 1

[84] D. H. Wilkinson: in Nuclear Spectroscopy B, ed. by F. Ajzenberg-Selove, Academic Press, New York, 1960

[85] P. M. Endt: Atomic Data and Nuclear Data Tables 26 (1981) 46

[86] W. Dilg, W. Schantl and H. Vonach: Nucl. Phys. A217 (1973) 269

[87] J. W. Cronin et al.: Phys. Rev. D 11 (1975) 3105

[88] H. R. Schmidt and J. Schukraft: GSI–preprint GSI–92–19, 1992

[89] U. Sukhatme, K. Lassila and R. Orava: Phys. Rev. D25 (1982) 2075

[90] B. Z. Kopeliovich and B. G. Zakharov: Z. Phys. C C43 (1989) 241

[91] B. Andersson, G. Gustafson and T. Sjöstrand: Physica Scripta 32 (1985) 574

[92] J. Rafelski and B. Müller: Phys. Rev. Lett. 48 (1982) 1066

[93] P. Koch, J. Rafelski and B. Müller: Phys. Rep. 142 (1986) 167

[94] M.Gazdzicki and O.Hansen : Nucl. Phys. B A 528 (1991) 754

[95] LEBC-EHS Collab.: M. Aguilar-Benitez et al.: Z. Phys. C50 (1991) 405

[96] UA5 Collab.: G. J. Alner et al.: Z. Phys. C33 (1986) 1

[97] CDF Collab.: F. Abe et al.: Phys. Rev. D41 (1990) 2330

[98] R. Harr and et al.: Pseudorapidity distribution of charged particles in $\bar{p}p$ collisions at $\sqrt{s} = 630$ GeV, Hep–ex/9703002, 1997

[99] NA22 Collab.: M. Adamus et al.: Z. Phys. C39 (1988) 311

[100] C. De Marzo et al.: Phys. Rev. D26 (1982) 1019

[101] NA35 Collaboration, presented by D.Röhrich at the QM93 Conference: Nucl. Phys. B A 566 (1994) 35c

[102] CDF Collab.: F. Abe et al.: Phys. Rev. Lett. 77 (1996) 438

[103] UA1 Collab.: C. Albajar et al.: Nucl. Phys. B335 (1990) 261

[104] G. Bocquet et al.: Phys. Lett. B366 (1996) 434

[105] E735 Collab.: T. Alexopolous et al.: University of Notre Dame, 1992

[106] T. K. Gaisser: *Cosmic Rays and Particle Physics,* Cambridge University Press, 1990

[107] P. Aurenche F. W. Bopp, D. Pertermann, R. Engel, J. Ranft and S. Roesler: Comput. Phys. Commun. 83 (1994) 107

[108] A.Fasso, A.Ferrari, J. Ranft and P.R.Sala: Proc. IV. Int. Conf. on Calorimetry in High Energy Physics La Biodola (Elba) (1993)

[109] P. Lipari: private communication (1997)

[110] G. Ingelman, A. Edin and J. Rathsman: DESY 96–057 (1996)

[111] G. Altarelli, R. Kleiss and C. Verzegnassi (Eds.): Z Physics at LEP 1, Vol. 3:Event generators and software CERN 89–08 v.3 (Sept. 1989) pp.327, 1989

[112] F. Carminati, O. DiRosa, B. van Eijk, I. Zacharov, D. Hatzifotiadou: Standard interfaces between modules of event generators using dynamical common structures, Proc. Large Hadron Collider workshop, CERN 90–10 vol. III(1990) CERN 90–10 vol. III (1990) pp. 52, 1990

[113] G. Marsaglia and A. Zaman: Florida State Univ. Preprint FSU–SCRI (1987), 1987

[114] K. Hänßgen and J. Ranft : Nucl. Sci. Eng. 88 (1984) 537

[115] C. Ciofi degli Atti and S. Simula: Phys. Rev. C 53 (1996) 1689

[116] H.–J.Möhring, J.Ranft, C.Merino and C.Pajares: Phys. Rev. D 47 (1993) 4142

[117] B. Blättel, G. Baym, L. L. Frankfurt, H. Heiselberg and M. Strikman: Phys. Rev. D D47 (1993) 2761

[118] B. Blättel, G. Baym, L. L. Frankfurt, H. Heiselberg and M. Strikman: Nucl. Phys. B A544 (1992) 479

[119] H. Heiselberg, B. Blättel, G. Baym, L. L. Frankfurt and M. Strikman: Phys. Rev. Lett. 67 (1991) 2946

[120] J. Kwieciński, A. D. Martin, R. G. Roberts and W. J. Stirling: Phys. Rev. D42 (1990) 3645

[121] J. Botts et al.: Phys. Lett. B304 (1993) 159

Appendix A :
The test program DPMJET–II

The test program demonstrates the application of the event generating routine KKINC and the extraction of information on the produced secondaries from the common block /HKKEVT/ (in the routine DISTR). Furthermore, it allows a simple redefinition of some important model parameters. It may also be used to prepare data files containing reaction specific information needed for the application of the Glauber formalism. In the case of event generation few standard histograms are constructed from sampled events.
All program activities are monitored by input options. Each input option is identified by a code word and either changes the default values of variables and/or demands some action. Tab. 1 summarizes the standard input options. All variables read from the input file have default values.

Table 2: The most important options read by the subroutine DMINIT

Option	Description
TITLE	next card is the run title
COMMENT	adds comments to the input data stream
PROJPAR	definition of the projectile
TARPAR	definition of the target
GLAUBERI	initialization of the Glauber formalism for hadron–nucleus interactions / data are written on unit 47
GLAUBERA	initialization of the Glauber formalism for nucleus–nucleus interactions / data are written on unit 47
HADRONIZ	selects BAMJET or JETSET fragmentation of chains
ENERGY	beam energy (GeV; per nucleon for nuclei)
MOMENTUM	beam momentum (GeV/c; per nucleon for nuclei)
CENTRAL	central A-A collisions forced
TAUFOR	definition of the formation time parameter
SEADISTR	monitors the x-behaviour of the quark distributions
SEASU3	defines s^{sea}
POPCORN	selects the popcorn mechanism
CRONINPT	selects the Cronin effect
XCUTS	monitors cuts for x–sampling
FERMI	monitors assignment of Fermi momenta to nucleons
SINGDIFF	controls the inclusion of single diffractive events
SINGLECH	include Regge (single chain) contribution
EVAPORAT	include nuclear evaporation
START	start event sampling for h–h, h–A or A–A collisions
NEUTRINO	start event sampling for qel neutrino collisions
LEPTOEVT	start event sampling for lepto neutrino collisions
STOP	stop the run
PARTICLE	print table of available particles and properties
POMTABLE	Write / Read a table for sampling multipomeron events

A.1: Description of input options and default parameters

Table A–2

Particle codes, SDUM is the parameter to be given on the PROJPAR input card. The internal codes and names were originally introduced by the BAMJET [62, 61] and DECAY [63] codes. These codes are also used by the FLUKA [108] and DTUJET [5, 107] codes.In the output of DPMJET, in COMMON HKKEVT, the particles are characterized with the PDG code, the internal code is given in the EXTEVT common. (Not all particles used internally are given in this Table.)

SDUM	internal code	internal name	particle	PDG number	charge	q1	q2	q3
PROTON	1	P	p^+	2212	1	2	2	1
APROTON	2	AP	$\bar{p}^-$	-2212	-1	-2	-2	-1
	3	E-	e^-	11	-1	0	0	0
	4	E+	e^+	-11	1	0	0	0
	5	NUE	ν_e	12	0	0	0	0
	6	ANUE	$\bar{\nu}_e$	-12	0	0	0	0
	7	GAM	γ	22	0	0	0	0
NEUTRON	8	NEU	n^0	2112	0	2	1	1
ANEUTRON	9	ANEU	$\bar{n}0$	-2112	0	-2	-1	-1
	10	MUE+	μ^+	-13	1	0	0	0
	11	MUE-	μ^-	13	-1	0	0	0
KAONLONG	12	K0L	K_L^0	130	0	0	0	0
PION+	13	PI+	π^+	211	1	2	-1	0
PION-	14	PI-	π^-	-211	-1	1	-2	0
KAON+	15	K+	K^+	321	1	2	-3	0
KAON-	16	K-	K^-	-321	-1	3	-2	0
LAMBDA	17	LAM	Λ^0	3122	0	0	0	0
ALAMBDA	18	ALAM	$\bar{\Lambda}^0$	-3122	0	0	0	0
KAONSHRT	19	K0S	K_S^0	310	0	0	0	0
SIGMA-	20	SIGM-	Σ^-	3112	-1	1	1	3

SDUM	internal code	internal name	particle	PDG number	charge	q1	q2	q3
SIGMA+	21	SIGM+	Σ^+	3222	1	2	2	3
SIGMAZER	22	SIGM0	Σ^0	3212	0	2	1	3
PIZERO	23	PI0	π^0	111	0	2	-2	0
KAONZERO	24	K0	K^0	311	0	1	-3	0
AKAONZER	25	AK0	$\bar{K}^0$	-311	0	3	-1	0
	31	ETA550	η	221	0	3	-3	0
	32	RHO+77	ρ^+	213	1	2	-1	0
	33	RHO077	ρ^0	113	0	2	-2	0
	34	RHO-77	ρ^-	-213	-1	1	-2	0
	35	OM0783	ω	223	0	0	0	0
	36	K*+892	K^{*+}	323	1	2	-3	0
	37	K*0892	K^{*0}	313	0	1	-3	0
	38	K*-892	K^{*-}	-323	-1	3	-2	0
	39	AK*089	$\bar{K}^{*0}$	-313	0	3	-1	0
	40	KA+125	K_1^+	10323	1	0	0	0
	41	KA0125	K_1^0	10313	0	0	0	0
	42	KA-125	K_1^-	-10323	-1	0	0	0
	43	AKA012	$\bar{K}_1^0$	-10313	0	0	0	0
	48	S+1385	Σ^{*+}	3224	1	0	0	0
	49	S01385	Σ^{*0}	3214	0	0	0	0
	50	S-1385	Σ^{*-}	3114	-1	0	0	0
	53	N*++12	Δ^{++}	2224	2	2	2	2
	54	N*+ 12	Δ^+	2214	1	2	2	1
	55	N*012	Δ^0	2114	0	2	1	1
	56	N*-12	Δ^-	1114	-1	1	1	1
	67	AN-12	$\bar{\Delta}^{--}$	-2224	-2	-2	-2	2
	68	AN*-12	$\bar{\Delta}^-$	-2214	-1	-2	-2	-1
	69	AN*012	$\bar{\Delta}^0$	-2114	0	-2	-1	-1

SDUM	internal code	internal name	particle	PDG number	charge	q1	q2	q3
	70	AN*+12	$\bar{\Delta}^{+}$	-1114	1	-1	-1	1
	95	ETA*	η'	331	0	0	0	0
	96	PHI	ϕ	333	0	3	-3	0
	97	TETA0	Ξ^{0}	3322	0	2	3	3
	98	TETA-	Ξ^{-}	3312	-1	1	3	3
	99	ASIG-	$\bar{\Sigma}^{-}$	-3222	-1	-2	-2	-3
	100	ASIG0	$\bar{\Sigma}^{0}$	-3212	0	-2	-1	-3
	101	ASIG+	$\bar{\Sigma}^{+}$	-3112	1	-1	-1	-3
	102	ATETA0	$\bar{\Xi}^{0}$	-3322	0	-2	-3	3
	103	ATETA+	$\bar{\Xi}^{+}$	-3312	1	-1	-3	-3
	104	SIG*+	Σ^{*+}	3224	1	2	2	3
	105	SIG*0	Σ^{*0}	3214	0	2	1	3
	106	SIG*-	Σ^{*-}	3114	-1	1	1	3
	107	TETA*0	Ξ^{*0}	3324	0	2	3	3
	108	TETA*	Ξ^{*-}	3314	-1	1	3	3
	109	OMEGA-	Ω^{-}	3334	-1	3	3	3
	110	ASIG*-	$\bar{\Sigma}^{*-}$	-3224	-1	-2	-2	-3
	111	ASIG*0	$\bar{\Sigma}^{*0}$	-3214	0	-2	-1	-3
	112	ASIG*+	$\bar{\Sigma}^{*}+$	-3114	1	-1	-1	-3
	113	ATET*0	$\bar{\Xi}^{*0}$	-3324	0	-2	-3	3
	114	ATET*+	$\bar{\Xi}^{*+}$	-3314	1	-1	-3	3
	115	OMEGA+	$\bar{\Omega}^{+}$	-3334	1	-3	-3	3
	116	D0	D^{0}	421	0	4	-2	0
	117	D+	D^{+}	411	1	4	-1	0
	118	D-	D^{-}	-411	-1	1	-4	0
	119	AD0	$\bar{D}^{0}$	-421	0	2	-4	0
	120	DS+	D_{s}^{+}	431	1	4	-3	0
	121	DS-	D_{s}^{-}	-431	-1	3	-4	0

SDUM	internal code	internal name	particle	PDG number	charge	q1	q2	q3
	122	ETAC	η_c	441	0	4	-4	0
	123	D*0	D^{*0}	423	0	4	-2	0
	124	D*+	D^{*+}	413	1	4	-1	0
	125	D*-	D^{*-}	-413	-1	1	-4	0
	126	AD*0	$\bar{D}^{*0}$	-423	0	2	-4	0
	127	DS*+	D_s^{*+}	433	1	4	-3	0
	128	DS*-	D_s^{*-}	-433	-1	3	-4	0
	129	CHI1C	χ_1^c	20443	0	4	-4	0
	130	JPSI	J/ψ	443	0	0	0	0
	131	TAU+	τ^+	-15	1	0	0	0
	132	TAU-	τ^-	15	-1	0	0	0
	133	NUET	ν_τ	16	0	0	0	0
	134	ANUET	$\bar{\nu}_\tau$	-16	0	0	0	0
	135	NUEM	ν_μ	14	0	0	0	0
	136	ANUEM	$\bar{\nu}_\mu$	-14	0	0	0	0
	137	LAMC+	Λ_c^+	4122	1	2	1	4
	138	XIC+	Ξ_c^+	4232	1	2	3	4
	139	XIC0	Ξ_c^0	4132	0	1	3	4
	140	SIGC++	Σ_c^{++}	4222	2	2	2	4
	141	SIGC+	Σ_c^+	4212	1	0	0	0
	142	SIGC0	Σ_c^0	4112	0	1	1	4
	143	S+	$\Xi_c'^+$	4322	1	0	0	0
	144	S0	$\Xi_c'^0$	4312	0	0	0	0
	145	T0	Ω_c^0	4332	0	3	3	4
	146	XU++	Ξ_{cc}^{++}	4422	2	2	4	4
	147	XD+	Ξ_{cc}^+	4412	1	1	4	4
	148	XS+	Ω_{cc}^+	4432	1	3	4	4
	149	ALAMC-	$\bar{\Lambda}_c^-$	-4122	1	-2	-1	4

SDUM	internal code	internal name	particle	PDG number	charge	q1	q2	q3
	150	AXIC-	$\bar{\Xi}_c^-$	-4232	1	-2	-3	-4
	151	AXIC0	$\bar{\Xi}_c^0$	-4132	0	-1	-3	-4
	152	ASIGC–	$\bar{\Sigma}_c^{--}$	-4222	-2	-2	-2	-4
	153	ASIGC-	$\bar{\Sigma}_c^-$	-4212	1	0	0	0
	154	ASIGC0	$\bar{\Sigma}_c^0$	-4112	0	-1	-1	-4
	155	AS-	$\bar{\Xi}_c^{\prime -}$	-4322	1	0	0	0
	156	AS0	$\bar{\Xi}_c^{\prime 0}$	-4312	0	0	0	0
	157	AT0	$\bar{\Omega}_c^0$	-4332	0	-3	-3	-4
	158	AXU–	$\bar{\Xi}_{cc}^{--}$	-4422	-2	-2	-4	-4
	159	AXD-	$\bar{\Xi}_{cc}^-$	-4412	1	-1	-4	-4
	160	AXS	$\bar{\Omega}_{cc}^-$	-4432	-1	-3	-4	-4
	161	C1*++	Σ_c^{*++}	4224	2	2	2	4
	162	C1*+	Σ_c^{*+}	4214	1	2	1	4
	163	C1*0	Σ_c^{*0}	4114	0	1	1	4
	164	S*+	Ξ_c^{*+}	4324	1	2	3	4
	165	S*0	Ξ_c^{*0}	4314	0	1	3	4
	166	T*0	Ω_c^{*0}	4334	0	3	3	4
	167	XU*++	Ξ_{cc}^{*++}	4424	2	2	4	4
	168	XD*+	Ξ_{cc}^{*+}	4414	1	1	4	4
	169	XS*+	Ω_{cc}^{*+}	4434	1	3	4	4
	170	TETA++	Ω_{ccc}^{*++}	4444	2	4	4	4
	171	AC1*–	$\bar{\Sigma}_c^{*--}$	-4224	2	-2	-2	-4
	172	AC1*-	$\bar{\Sigma}_c^{*-}$	-4214	-1	-2	-1	-4
	173	AC1*0	$\bar{\Sigma}_c^{*0}$	-4114	0	-1	-1	-4
	174	AS*-	$\bar{\Xi}_c^{*-}$	-4324	-1	-2	-3	-4
	175	AS*0	$\bar{\Xi}_c^{*0}$	-4314	0	-1	-3	-4
	176	AT*0	$\bar{\Omega}_c^{*0}$	-4334	0	-3	-3	-4
	177	AXU*–	$\bar{\Xi}_{cc}^{*--}$	-4424	-2	-2	-4	-4
	178	AXD*-	$\bar{\Xi}_{cc}^{*-}$	-4414	1	-1	-4	-4
	179	AXS*-	$\bar{\Omega}_{cc}^{*-}$	-4434	-1	-3	-4	-4
	180	ATET–	$\bar{\Omega}_{ccc}^{*--}$	-4444	-2	-4	-4	-4

All input records of DPMJET–II have the following form:

```
CODEWD, (WHAT(I), I = 1,6), SDUM
FORMAT (A8, 2X, 6E 10.0, A8)
```

In the following we describe the meaning of the corresponding variables for the standard input options in the same order as the code words CODEWD are listed in Tab. A–1.

Please note: further input options are described in the Appendices C and D.

We give also the default values of the parameters .

- Code word = 'TITLE'

  This option card must be followed by a card giving a run title, which will be reproduced in the output.

- Code word = 'COMMENT'

  This option allows to add comments to the input file at arbitrary positions.

  WHAT(1): number of comment cards following this card.
  default : 1.0

- Code word = 'PROJPAR'

  This card defines the type of the projectile;
  if given it has to be included before the MOMENTUM/ENERGY option(s).

  SDUM: defines the projectile to be a hadron if given; for naming conventions see Table 2.
  If SDUM is given WHAT(1) and WHAT(2) need no specification; for projectile nuclei SDUM has no meaning.

  WHAT(1): mass number of projectile nucleus - IP

  WHAT(2): atomic number of projectile nucleus - IPZ

  default: incident proton (IP=1, IPZ=1).

- Code word = 'TARPAR'

  This card defines the type of the target nucleus.

  WHAT(1): mass number of projectile nucleus - IT

  WHAT(2): atomic number of projectile nucleus - ITZ

  default: Nitrogen N target (IT=14, ITZ=7)

- Code word = 'GLAUBERI'

  Requests the initialization of the Glauber formalism for hadron–nucleus interactions;
  the target nucleus has to be defined by the code word TARPAR in advance;
  tables of impact parameter distributions for b–sampling are written to unit 47 for several momenta ($p_{lab} = \sqrt{10}^{(i+1)}; i = 1, ..., 24$) and different projectiles (p, π^+);
  WHAT(1) = JGLAUB JGLAUB = 1 Calculation of cross sections JGLAUB = 2 Calculation GLAUBTAR.DAT file (default)

- Code word = 'GLAUBERA'

  Requests the initialization of the Glauber formalism for nucleus–nucleus interactions;
  the target nucleus has to be defined by the code word TARPAR in advance;
  the projectile nucleus has to be defined by the code word PROJPAR in advance;
  tables of impact parameter distributions for b–sampling are written to unit 47 for several momenta ($p_{lab} = \sqrt{10}^{(i+1)}; i = 1, ..., 24$) and different projectiles ;
  WHAT(1) = JGLAUB JGLAUB = 1 Calculation of cross sections JGLAUB = 2 Calculation GLAUBTAR.DAT file (default)

- Code word = 'HADRONIZ'

Selects BAMJET or JETSET fragmentation of soft chains

WHAT(1): IHADRZ (default: 2)
IHADRZ = 1 selects BAMJET fragmentation,
IHADRZ = 2 selects JETSET fragmentation.
IHADRZ = 11 selects an alternative JETSET fragmentation.

- Code word = 'ENERGY'

  This card defines the energy of the projectile in the target rest system. For incident nuclei the energy per nucleon is expected.
  NOTE: only one of the ENERGY and the MOMENTUM options is necessary, the last defined option is applied; both these options are to be given after the PROJPAR definition.

  WHAT(1): projectile energy in *GeV*

- Code word = 'MOMENTUM'

  This card defines the momentum of the projectile in the target rest system. For incident nuclei the momentum per nucleon is expected.
  NOTE: only one of the ENERGY and the MOMENTUM options is necessary, the last defined option is applied; both these options are to be given after the PROJPAR definition.

  WHAT(1): projectile momentum in *GeV/c*;
  Default: 100 000 GeV/c

- Code word = 'CENTRAL'

  This code word forces central nucleus-nucleus collisions, i.e. most nucleons of the projectile nucleus are forced to interact. The actual requirement depends on the atomic number of both the projectile and the target nuclei and is defined in the subroutine KKEVT (source file DPMNUC2, after CALL SHMAKO). Furthermore, the actual impact parameter is set near to zero for this case in subroutine MODB (source file DPMTCBSH).

  WHAT(1): central collisions forced for WHAT(1)= 1.0;
  default: 0.0, i.e. no forcing.

  Please note: The definition of central collisions is not unique, see the actual definitions in routine KKEVT (DPMNUC2.f). The same parameter with values different from 0. or 1. might als be used in order to define other special types of collisions, i.e. peripheral collisions.

- Code word = 'TAUFOR'

  This option defines the formation time parameter controlling the intranuclear cascade. Additionally it allows to restrict the number of generations of secondary cascade interactions.

  WHAT(1): formation time in fm/c; default: 105 fm/c
  WHAT(2): maximum number of allowed generations of secondary interactions; default: 0
  WHAT(3): monitors the definition of the formation time actually applied (comp. Subsects. 2.3 and 3.3.3):
  WHAT(3)=1 : $p_\perp$–dependent formation time , (default)
  WHAT(3)=2 : constant formation time

  Please note, for h–h interactions, one should use WHAT(2) = 0. ! The default corresponds to a supression of the formation zone cascade. To apply the formation zone cascade, the recommended values are (TAUFOR 5. 25. 1.).

- Code word = 'SEADISTR'

  This option card defines properties of the quark distributions, which are of the general form $q(x) \propto x^{-\alpha}(1-x)^{\beta}$.

  WHAT(1): no meaning, α^{sea} is now controlled by the SEAQUARK card. (default $\alpha^{sea} = 0.5$)
  default : $\alpha^{sea} = 1.0$

WHAT(2): β^{nuc} for valence-quark distributions of nucleons;
default : $\beta^{nuc} = 3.5$

WHAT(3): β^{mes} for valence-quark distributions of mesons;
default : $\beta^{mes} = 1.1$

WHAT(4): no meaning;

NOTE: for reasons of the sampling efficiency the parameters for the sea distribution are fixed to α^{sea}=either 1.0 or 0.5 and $\beta^{sea} = 0.0$ in the present version of the subroutine XKSAMP and cannot be changed easily by the user.

- Code word = 'SEAQUARK'

This option card defines properties of the quark distributions, which are of the general form $q(x) \propto x^{-\alpha}(1-x)^{\beta}$.

WHAT(1): α^{sea} for sea-quark distributions possible values: 0.5 and 1.;
default : $\alpha^{sea} = 0.5$

NOTE: for reasons of the sampling efficiency the parameters for the sea distribution are fixed to α^{sea}=either 1.0 or 0.5 and $\beta^{sea} = 0.0$ in the present version of the subroutine XKSAMP and cannot be changed easily by the user. While $\alpha^{sea} = 0.5$ is fine for hadron–light nucleus collisions, $\alpha^{sea} = 1.0$ should be used as soon as heavy nuclei are involved as target or projectile.

- Code word = 'SEASU3'

This option determines the strange quark fraction s^{sea} at the sea–quark chain ends.

WHAT(1): s^{sea},
default: 0.5

- Code word = 'POPCORN'

This option determines the popcorn mechanism for BAMJET as well as JETSET fragmentation.

WHAT(1): PDB,
default: 0.20
BAMJET and JETSET: PDB gives the fraction of diquarks fragmenting directly into baryons.
PDB = 0 switches off the popcorn mechanism.

NOTE: POPCORN should appear before the HADRONIZE card.

- Code word = 'CRONINPT'

This option determines the Cronin effect.

WHAT(1): MKCRON,
default: 1.
MKCRON = 0 switches off the Cronin effect.

WHAT(2): CRONCO,
default: 0.64
CRONCO is the parameter in the parton multiple scattering formula.

- Code word = 'XCUTS'

This option redefines the lower cuts for the sampling of x-values to ensure minimum chain masses for hadronization (used in XKSAMP).

WHAT(1) = CVQ ; $(x_q^{val})^{min} = \mathrm{CVQ}/\sqrt{s}$,
lower cut for valence quarks; default : CVQ = 2.0

WHAT(2) = CDQ ; $(x_{qq}^{val})^{min} = \mathrm{CDQ}/\sqrt{s}$,
lower cut for valence diquarks; default : CDQ = 2.0

WHAT(3) = CSEA; $(x_{q/\bar{q}}^{sea})^{min} = \mathrm{CSEA}/\sqrt{s}$,
lower cut for sea quarks; default : CSEA = 0.3

WHAT(4) = SSMIMA; $(x_{q/\bar{q}}^{sea})^{target} \cdot (x_{q/\bar{q}}^{sea})^{project.} \cdot s \geq (SSMIMA)^2$,
lower cut for the mass of sea-sea chains applied in XKSAMP;
default : SSMIMA = 0.9 *GeV*.

- Code word = 'FERMI'

  WHAT(1): Inclusion of Fermi momenta for nucleons if WHAT(1)= 1.0 (default)

  WHAT(2): FERMOD - scale factor for Fermi momentum as calculated from zero temperature Fermi distribution of nucleons;
  default: FERMOD = 0.6.

  WHAT(3): use zero temperature Fermi momentum distribution if WHAT(3)= 1.0 (default); use distribution according to Ref.[115] for WHAT(3)=2.

- Code word = 'START'

  This option starts the generation of events in h–h, h–A and A–A collisions including the output of standard histograms.

  WHAT(1): number of events to be sampled; default: 100

  WHAT(2): the Glauber initialization is forced to be calculated in SHMAKI,
  i.e. no data read from file GLAUBTAR.DAT, if WHAT(2) = 1.0

- Code word = 'NEUTRINO'

  This option starts the generation of events for quasi elastic (qel) neutrino–nucleus collisions including the output of standard histograms.

  WHAT(1): number of events to be sampled; default: 100

  WHAT(2): neutrino type as defined in qel (1=ν_e, 2=$\bar{\nu}_e$, 3=ν_μ, 4=$\bar{\nu}_\mu$, 5=ν_τ, 6=$\bar{\nu}_\tau$)

- Code word = 'LEPTOEVT' (only available in DPMJET–II.4)

  This option starts the generation of events for deep inelastic (lepto) neutrino–nucleus collisions including the output of standard histograms.

  WHAT(1): number of events to be sampled; default: 100

  WHAT(2): neutrino type as defined in lepto (12=ν_e, -12=$\bar{\nu}_e$, 14=ν_μ, -14=$\bar{\nu}_\mu$)

- Code word = 'SINGDIFF'

  This option controls the generation of single diffractive events.

  WHAT(1): ISINGD;
  ISINGD=1: Single diffraction included,
  ISINGD=0: Single diffraction supressed,
  ISINGD=2: Only single diffraction,
  ISINGD=3: Only single diffraction, target excited,
  ISINGD=4: Only single diffraction, projectile excited.
  default: 0

- Code word = 'SINGLECH'

  WHAT(1): ISICHA;
  ISINGD=1: include Regge (single chain) contributions,
  ISINGD=0: single chains supressed,
  ISINGD=2: Only single contribution,
  default: 0

  Please note: The single chain (Regge) contributions are only essential at low energies. they are at present only implemented for antibaryon and meson projectiles.

- Code word = 'EVAPORAT'

  Evaporation is performed if the EVAPORAT card is present Default:No evaporation

what (1) = i1
i1 = 1: evaporation is performed
i1 = 0: no evaporation

what (2) = ig + 10 * if (ig and if must have the same sign)
ig = -1 = deexcitation gammas are not produced (if the evaporation step is not performed they are never produced)
if = -1 = Fermi Break Up is not invoked (if the evaporation step is not performed it is never invoked)
The default is: deexcitation gamma produced and Fermi break up activated for the new preequilibrium, not activated otherwise.

- Code word = 'PARTICLE'

  This card triggers a printout of all the particles defined in the BAMJET-DECAY chain fragmentation, including name conventions, quantum numbers and decay channels.

- Code word = 'POMTABLE'

  Only if the files dpm977pom.f and dpm97lap.f are linked instead of the files dtu97pom.f and dtu97lap.f.

  WHAT(1): 0 (default) the file pomtab.dat is written. :1 The file pomtab.dat is read.

- Code word = 'STOP'

  This option stops the execution of the program.

A.2: Sample Input

In the following several typical examples of input data are reproduced. In general we give all input cards, even if most of the parameters given agree with the default parameters.

One of the examples demonstrates the use of the test program to generate the input data for the Glauber formalism in A–N collisions.

6.0.9 Hadron-Hadron collisions

Note: The NOFINALE and EVAPORATE options suppress evaporation and evaluation of the residual nucleus, which does not exst in this case. The TAUFOR card assures that no FZIC is started. SINGDIFF includes diffractive events.

```
TITLE
DPMJET--II.3 p-p 200 GeV/c  w. Diffr.
PROJPAR                                                          PROTON
TARPAR          1.0          1.
MOMENTUM   200.
NOFINALE     1.
EVAPORATE    0.
OUTLEVEL    0.          0.          0.          -1.          0.          0.
RANDOMIZE           1.          7.         31.         77.         189.
STRUCFUN          222.          0.
SAMPT               4.
GLUSPLIT            1.          0.
SELHARD             0.          2.          0.          0.          3.          3.
SIGMAPOM            0.         10.        482.         30.        100.         2.
PSHOWER             1.
CENTRAL             0.
CMHISTO             0.
SEASU3           0.50
RECOMBIN            1.
SINGDIFF            1.          0.          1.
CRONINPT            1.        0.64
POPCORN          0.20
TAUFOR          105.0          0.
SEADISTR         1.00        3.50        1.11         5.0
XCUTS            2.00         2.0        0.30       1.201
PAULI               1.          0.
FERMI               1.         0.6
INTPT               1.
ALLPART             1.
HADRONIZE           2.
START          200000.          1.
STOP
```

Hadron-Nucleus collisions

Note: Here the NOFINALE and EVAPORATE optiond assure evaporation and the working out of the residual nucleus. If this is required, then also the TAUFOR card is needed in a form as given to perform the FZIC. In hadron–nucleus collisions diffractive events might be demanded like in the example or might be supressed.

```
TITLE
DPMJET-II.3 p-N  20 TeV LAB  w. Diffr. FZIC and evaporation
PROJPAR                                                          PROTON
```

```
TARPAR          14.0        7.
MOMENTUM       20000.
NOFINALE           0.
EVAPORATE          1.
OUTLEVEL           0.          0.          0.          -1.          0.          0.
RANDOMIZE          1.          7.         31.          77.         189.
STRUCFUN         222.          0.
SAMPT              4.
GLUSPLIT           1.          0.
SELHARD            0.          2.          0.          0.          3.          3.
SIGMAPOM           0.         10.        482.         30.        100.          2.
PSHOWER            1.
CENTRAL            0.
CMHISTO            0.
SEASU3          0.80
RECOMBIN           1.
SINGDIFF           1.          0.          1.
CRONINPT           1.        0.64
POPCORN         0.20
TAUFOR            5.0        25.
SEADISTR          1.0        3.50        1.11         5.0
XCUTS           2.00         2.0        0.30       0.901
PAULI              1.          0.
FERMI              1.         0.6
INTPT              1.
ALLPART            1.
HADRONIZE          2.
START          10000.          1.
STOP
```

Nucleus-Nucleus collisions

Note: In nucleus-nucleus collisions diffractive events, which are not yet reliably implemented should always be excluded like in the two examples given. In both examples the FZIC and evaporation is demanded (TAUFOR, NOFINALE, EVAPORATE options) It is also possible to run nucleus–nucleus collisions without FZIC and evaporation.

```
TITLE
DPMJET-II.3 central S-S 200 GeV/c FZIC and evaporation
PROJPAR         32.0        16.
TARPAR          32.0        16.
MOMENTUM         200.
NOFINALE           0.
EVAPORATE          1.
OUTLEVEL           0.          0.          0.          -1.          0.          0.
RANDOMIZE          1.          7.         31.          77.         189.
STRUCFUN         222.          0.
SAMPT              4.
GLUSPLIT           1.          0.
SELHARD            0.          2.          0.          0.          3.          3.
SIGMAPOM           0.         10.        482.         30.        100.          2.
PSHOWER            1.
CENTRAL            1.
CMHISTO            0.
SEASU3          0.50
RECOMBIN           1.
SINGDIFF           0.          0.          0.
```

```
CRONINPT          0.      0.00
POPCORN         0.20
TAUFOR           5.0      25.
SEADISTR         1.0      3.50      1.11       5.0
XCUTS           2.00      2.0      0.30     1.201
PAULI            1.        0.
FERMI            1.       0.6
INTPT            1.
ALLPART          1.
HADRONIZE        2.
START         1000.        1.
STOP


TITLE
DPMJET-II.3 Fe-N cms energy (nucleon-nucleon) 1000 TeV FZIC and evaporation
PROJPAR          56.        26.
TARPAR         14.0         7.
CMENERGY    1000000.
NOFINALE         0.
EVAPORATE        1.
OUTLEVEL         0.         0.        0.       -1.        0.         0.
RANDOMIZE        1.         7.       31.       77.       189.
STRUCFUN       222.         0.
SAMPT            4.
GLUSPLIT         1.         0.
SELHARD          0.         2.        0.        0.        3.         3.
SIGMAPOM         0.        10.      482.       30.      100.         2.
PSHOWER          1.
CENTRAL          0.
CMHISTO          0.
SEASU3         0.80
RECOMBIN         1.
SINGDIFF         0.        0.        0.
CRONINPT         0.      0.00
POPCORN        0.20
TAUFOR           5.0      25.
SEADISTR         1.0      3.50      1.11       5.0
XCUTS           2.00      2.0      0.30     0.901
PAULI            1.        0.
FERMI            1.      0.60
INTPT            1.
ALLPART          1.
HADRONIZE        2.
START         1000.        1.
STOP
```

Input data for Glauber formalism

```
TITLE
DPMJET-II Prepare Glauber data for different nucleus-N collisions
PROJPAR          1.         1.
TARPAR         14.0         7.
GLAUBERI
PROJPAR          4.         2.
TARPAR         14.0         7.
```

```
GLAUBERA
PROJPAR        12.         6.
TARPAR         14.0         7.
GLAUBERA
PROJPAR        14.         7.
TARPAR         14.0         7.
GLAUBERA
PROJPAR        24.         12.
TARPAR         14.0         7.
GLAUBERA
PROJPAR        28.         14.
TARPAR         14.0         7.
GLAUBERA
PROJPAR        40.         20.
TARPAR         14.0         7.
GLAUBERA
PROJPAR        48.         22.
TARPAR         14.0         7.
GLAUBERA
PROJPAR        56.0        26.
TARPAR         14.0         7.
GLAUBERA
STOP
```

qel neutrino interactions in DPMJET–II.3

Please note: DPMJET does not consider neutrinos as projectile particles, therefore, we use PROJPAR = PROTON. This is of course not used later on.

```
TITLE
 DPMJET-II.3 5 GeV Neutrino(nu-e)-Ar  quasi-elastic interaction
PROJPAR                                                          PROTON
TARPAR          40.0        18.
MOMENTUM          5.
NOFINALE          0.
EVAPORATE         1.
OUTLEVEL          0.          0.        0.          -1.        0.         0.
RANDOMIZE         1.          7.        31.      77.        189.
TAUFOR           5.0        25.
PAULI             1.          0.
FERMI             1.         0.6
NEUTRINO        1000.        1.
STOP
```

Please note: DPMJET does not consider neutrinos as projectile particles, therefore, we use PROJPAR = PROTON. This is of course not used later on.

Deep inelastic (lepto) neutrino-nucleus interaction in DPMJET–II.4

```
TITLE
 DPMJET Deep inelastic Neutrino(nu-e)-Ar using lepto
PROJPAR                                                          PROTON
TARPAR          40.0        18.
MOMENTUM          50.
```

```
NOFINALE          0.
EVAPORATE         1.
OUTLEVEL          0.          0.          0.          -1.          0.          0.
RANDOMIZE         1.          7.          31.         77.          189.
TAUFOR            5.0         25.
PAULI             1.          0.
FERMI             1.          0.6
LEPTOEVT          1000.       12.
STOP
```

Appendix B :
Event history and the common blocks /HKKEVT/ and /EXTEVT/

B.1: Structure of the common blocks

During the generation of individual events several entries are scored in the common blocks /HKKEVT/ and /EXTEVT/ characterizing subsequent stages of the sampling process. Scored entries are, for instance, initial state nucleons, partons and parton chains, decaying resonances as well as final state particles. These entries are characterized by their type, 4-momenta and coordinates; additional pointers define 'parents' and 'daughters' of the actual entry (if any). The structure of the /HKKEVT/ common block closely follows the suggestions of Ref. [111, 112]. Within the code there are extensive comments explaining the variables used in this common block. Below the common blocks are reproduced together with these comments.
Note that for interactions potentially resulting in high multiplicities of secondaries (i.e. very high energies and/or heavy ion–ion collisions) it may become necessary to increase the dimension NMXHKK, the maximum number of entries for a given event.

```
      PARAMETER (NMXHKK=49998)
      COMMON /HKKEVT/ NHKK,NEVHKK,ISTHKK(NMXHKK),IDHKK(NMXHKK),
     &                JMOHKK(2,NMXHKK),JDAHKK(2,NMXHKK),
     &                PHKK(5,NMXHKK),VHKK(4,NMXHKK),WHKK(4,NMXHKK)
      COMMON /EXTEVT/ IDRES(NMXHKK),IDXRES(NMXHKK),NOBAM(NMXHKK),
     &                IDBAM(NMXHKK),IDCH(NMXHKK),NPOINT(10)
C
C  Based on the proposed standard COMMON block (Sjostrand Memo 17.3,89)
C
C NMXHKK: maximum numbers of entries (partons/particles) that can be
C    stored in the common block.
C
C NHKK: the actual number of entries stored in current event. These are
C    found in the first NHKK positions of the respective arrays below.
C    Index IHKK, 1 <= IHKK <= NHKK, is used below to denote a given
C    entry.
C
C ISTHKK(IHKK): status code for entry IHKK, with following meanings:
C    = 0 : null entry.
C    = 1 : an existing entry, which has not decayed or fragmented.
C          This is the main class of entries which represents the
C          "final state" given by the generator.
C    = 2 : an entry which has decayed or fragmented and therefore
C          is not appearing in the final state, but is retained for
C          event history information.
C    = 3 : a documentation line, defined separately from the event
C          history. (incoming reacting
C          particles, etc.)
C    = 4 - 10 : undefined, but reserved for future standards.
C    = 11 - 20 : at the disposal of each model builder for constructs
C          specific to his program, but equivalent to a null line in the
C          context of any other program. One example is the cone defining
C          vector of HERWIG, another cluster or event axes of the JETSET
C          analysis routines.
C    = 21 - : at the disposal of users, in particular for event tracking
C          in the detector.
C
C IDHKK(IHKK) : particle identity, according to the Particle Data Group
C    standard.
C
C JMOHKK(1,IHKK) : pointer to the position where the mother is stored.
C    The value is 0 for initial entries.
```

```
C
C JMOHKK(2,IHKK) : pointer to position of second mother. Normally only
C    one mother exist, in which case the value 0 is used. In cluster
C    fragmentation models, the two mothers would correspond to the q
C    and qbar which join to form a cluster. In string fragmentation,
C    the two mothers of a particle produced in the fragmentation would
C    be the two endpoints of the string (with the range in between
C    implied).
C
C JDAHKK(1,IHKK) : pointer to the position of the first daughter. If an
C    entry has not decayed, this is 0.
C
C JDAHKK(2,IHKK) : pointer to the position of the last daughter. If an
C    entry has not decayed, this is 0. It is assumed that the daughters
C    of a particle (or cluster or string) are stored sequentially, so
C    that the whole range JDAHKK(1,IHKK) - JDAHKK(2,IHKK) contains
C    daughters. Even in cases where only one daughter is defined (e.g.
C    K0 -> K0S) both values should be defined, to make for a uniform
C    approach in terms of loop constructions.
C
C PHKK(1,IHKK) : momentum in the x direction, in GeV/c.
C PHKK(2,IHKK) : momentum in the y direction, in GeV/c.
C PHKK(3,IHKK) : momentum in the z direction, in GeV/c.
C PHKK(4,IHKK) : energy, in GeV.
C PHKK(5,IHKK) : mass, in GeV/c**2. For spacelike partons, it is allowed
C    to use a negative mass, according to PHKK(5,IHKK) = -sqrt(-m**2).
C
C VHKK(1,IHKK) : production vertex x position, in mm.
C VHKK(2,IHKK) : production vertex y position, in mm.
C VHKK(3,IHKK) : production vertex z position, in mm.
C VHKK(4,IHKK) : production time, in mm/c (= 3.33*10**(-12) s).
C
C WHKK(I,IHKK) gives positions and times in projectile frame,
C    the chains are created on the positions of the projectile nucleons
C    in the projectile frame (target nucleons in target frame);
C    both positions are threfore not completely consistent.
C    The times in the projectile frame ,however, are obtained by
C    a Lorentz transformtion from the lab system.
C
C         Entries to the /EXTEVT/ COMMON block
C
C IDRES(IHKK) gives the Mass number A in case of nuclear
C     fragments or residual nuclei (IDHKK(IHKK)=80000)
C
C IDXRES(IHKK) gives the charge Z in case of nuclear
C     fragments or residual nuclei (IDHKK(IHKK)=80000)
C
C NOBAM(IHKK) = 1 for particles resulting from projectile fragmentation
C             = 2 for particles resulting from target fragmentation
C
C IDBAM(IHKK) gives the internal dpmjet particle code (BAMJET code)
```

B.2: Conventions for the scoring of the event history in /HKKEVT/

In the following we briefly characterize the subsequent entries to /HKKEVT/ together with the most important conventions for their classification.

- projectile hadron/nucleons;
  for projectile nuclei Fermi momenta in the projectile rest frame and coordinates within the nucleus are stored in the arrays PHKK and VHKK, resp., by the subroutine KKEVT;
  interacting and non-interacting nucleons have the status ISTHKK=11 and 13, resp.;
  nucleons wounded by the formation zone intranuclear cascade get status 17.

- target nucleons;
  Fermi momenta in the target rest frame and coordinates within the nucleus are defined in PHKK and VHKK, resp. (KKEVT);
  interacting and non-interacting nucleons have the status ISTHKK=12 and 14, resp.;
  nucleons wounded by the formation zone intranuclear cascade get status 18.

- valence quarks / diquarks from the interacting projectile hadron/nucleon(s) defined in the subroutine XKSAMP (total number IXPV);
  PHKK(3,...)=PHKK(4,...) contains the actual momentum fraction, VHKK the position of the 'mother' hadron;
  defined status ISTHKK=21;

- sea quarks from interacting projectile hadrons defined in XKSAMP (total number IXPS);
  PHKK(3,...)=PHKK(4,...) contains the actual momentum fraction, VHKK the position of the 'mother' hadron;
  defined status ISTHKK=31;

- valence quarks / diquarks from interacting target nucleons defined in XKSAMP (number IXTV);
  PHKK(3,...)=PHKK(4,...) contains the actual momentum fraction, VHKK the position of the 'mother' hadron;
  defined status ISTHKK=22;

- sea quarks from interacting target nucleons defined in XKSAMP (number IXTS);
  PHKK(3,...)=PHKK(4,...) contains the actual momentum fraction, VHKK the position of the 'mother' hadron;
  defined status ISTHKK=32;

- characteristics of the individual parton-parton chains (before hadronization) from subroutines KKEVVV, KKEVSV, KKEVVS and KKEVSS; for each chain there are three entries:
  (1) two entries for the quark systems forming the chain;
  PHKK gives their 4-momenta; the status of the corresponding quark system is increased by 100 as compared to the previous entry from the subroutine XKSAMP (i.e. ISTHKK=121,122,131 or 132 ,resp.);
  (2) one entry for the complete chain;
  PHKK gives the total 4-momentum, the 'particle' type for chains is defined to be IDHKK=88888;
  the actual status ISTHKK points to the chain generating subroutine:
  ISTHKK=3 for chains from KKEVVV (constructed from valence quark systems),
  ISTHKK=4 for chains from subroutine KKEVSV (sea-valence chains),
  ISTHKK=5 for chains from subroutine KKEVVS (valence-sea chains),
  ISTHKK=6 for chains from subroutine KKEVSS (sea-sea chains);

- hadrons from the hadronization of chains, entries from subroutines HADRSS, HADRVS, HADRSV, HADRVV;
  assignment of values to all arrays of /HKKEVT/, status ISTHKK=1;

- hadrons from resonance decay in JETSET or in subroutine DECHKK
  (presently called after completion of the primary interaction of the projectile treated in KKEVT);
  the status of decaying hadrons is changed to ISTHKK=2, added decay products have ISTHKK=1;

- hadrons from intranuclear cascade interactions (monitored by FOZOKL):
  the status of interacting secondary is changed to ISTHKK=2; interacting target nucleons get ISTHKK=12, interacting projectile nucleons with ISTHKK=11; final state hadrons have the status ISTHKK=1.
  Particular cases:

  (i) If a given secondary interaction is found to be forbidden because of the Pauli principle the initial state particles are stored in /HKKEVT/ with their original properties, but the actual position; so they may participate in further intranuclear interactions.

  (ii) One (or two) nucleons from a secondary interaction cannot escape from the nuclear potential, but the particular collision is <u>not</u> forbidden by Pauli's principle (i.e. several nucleons knocked out of the nucleus already):
  Store the nucleon(s) with the actually generated momentum at the collision site, assigning the status ISTHKK=15 (16) for interactions in the target (projectile) nucleus. Those nucleons are available as target (projectile) nucleons in subsequent steps of the intranuclear cascade development.

  (iii) Negative particles with energies too low to escape from the potential are forced to be absorbed within the nucleus (comp. Section 2 and Appendix); absorbed π^-, K^- and $\bar{p}$ are characterized by the status ISTHKK=19.

- Evaporation nucleons, nuclear fragments and residual target nuclei from the interface to the evaporation mudule.

  (i) The excited residual nuclei before the evaporation step get ISTHKK(i)=1000 and IDHKK(i)=80000 , the mass number A and charge Z of the nucleus are given by IDRES(i) and IDXRES(i).

  (ii) The evaporation protons and neutrons are stored with ISTHKK(i)=-1.

  (iii) The nuclear fragments from evaporation are stored with ISTHKK(i)=-1 and IDHKK(i)=80000, the mass number A and charge Z of the nucleus are given by IDRES(i) and IDXRES(i).

  (iv) The deexcitation photons are stored with ISTHKK(i)=-1.

  (v) The stable residual nuclei after the evaporation step are stored with ISTHKK(i)=1001 and IDHKK(i)=80000, the mass number A and charge Z of the nucleus are given by IDRES(i) and IDXRES(i).

The information from this common block allows a rather detailed reconstruction of the actual event history, and is particularly useful for consistency tests and debugging. An example is discussed in Subsection B.3.

B.3: Sample event history from the common block /HKKEVT/

In this subsection we discuss a typical event history as stored in the common block /HKKEVT/ according to the conventions discussed in the preceding subsection B.2. The corresponding event was sampled for the interaction of a 200 *GeV* proton with a Argon nucleus. The following quantities from the common are listed for each entry: the number i of the entry, its status ISTHKK(i) and type IDHKK(i), the pointers JMOHKK(2,i) and JDAHKK(2,i) to the 'mother' and 'daughter' particles, resp., and the array PHKK(5,i), for final state particles containing the 4-momentum and their mass. The last 4 integers are IDRES(i), IDXRES(i), NOBAM(i) and IDBAM(i).
The first 41 entries are made in the subroutine KKEVT for the incident proton and the 40 nucleons from the Argon nucleus. According to our conventions interacting hadrons get the status 11 (projectile) and 12 (target) - there are two target nucleons participating in the primary interaction (entries 13 and 18, i.e one proton and one neutron). There are some target nucleons which got the status ISTHKK(i)=18, this are target nucleons participating in the formation zone intranuclear cascade.

1	11	2212	0	0	50	53	.00E+00	.00E+00	.00E+00	9.38E-01	9.38E-01	0	0	0	1
2	14	2112	0	0	130	0	1.07E-01	6.71E-02	1.38E-02	9.48E-01	9.40E-01	0	0	0	8
3	14	2112	0	0	0	0	7.20E-03	-1.30E-01	1.15E-03	9.49E-01	9.40E-01	0	0	0	8
4	14	2212	0	0	0	0	5.72E-02	-4.81E-02	-1.27E-01	9.50E-01	9.38E-01	0	0	0	1
5	14	2112	0	0	0	0	7.68E-02	-5.42E-02	-5.65E-02	9.46E-01	9.40E-01	0	0	0	8
6	14	2212	0	0	0	0	-8.12E-02	9.59E-02	-3.86E-02	9.47E-01	9.38E-01	0	0	0	1
7	14	2212	0	0	0	0	-1.20E-01	1.79E-02	1.24E-01	9.54E-01	9.38E-01	0	0	0	1
8	14	2212	0	0	0	0	-5.77E-02	6.06E-02	2.97E-02	9.42E-01	9.38E-01	0	0	0	1
9	14	2112	0	0	0	0	1.55E-01	-7.62E-02	2.05E-02	9.56E-01	9.40E-01	0	0	0	8
10	14	2212	0	0	0	0	-5.32E-02	1.06E-01	-5.12E-02	9.47E-01	9.38E-01	0	0	0	1
11	14	2212	0	0	0	0	1.29E-01	4.02E-02	-1.89E-02	9.48E-01	9.38E-01	0	0	0	1
12	14	2112	0	0	0	0	-3.86E-02	-6.17E-02	1.29E-01	9.51E-01	9.40E-01	0	0	0	8
13	12	2212	0	0	57	60	7.66E-02	1.18E-01	5.54E-02	9.50E-01	9.38E-01	0	0	0	1
14	14	2212	0	0	0	0	-3.16E-02	1.46E-01	-2.18E-02	9.50E-01	9.38E-01	0	0	0	1
15	14	2212	0	0	0	0	-4.24E-02	-2.12E-02	-1.66E-01	9.54E-01	9.38E-01	0	0	0	1
16	18	2112	0	0	120	121	-1.79E-01	9.23E-02	3.48E-03	9.61E-01	9.40E-01	0	0	0	8
17	14	2112	0	0	0	0	-1.34E-01	1.61E-01	5.86E-02	9.64E-01	9.40E-01	0	0	0	8
18	12	2112	0	0	51	54	2.76E-02	-7.15E-02	-3.55E-02	9.43E-01	9.40E-01	0	0	0	8
19	14	2212	0	0	0	0	5.03E-02	-3.53E-02	-5.74E-02	9.42E-01	9.38E-01	0	0	0	1
20	14	2212	0	0	0	0	1.15E-02	1.36E-03	1.72E-01	9.54E-01	9.38E-01	0	0	0	1
21	14	2112	0	0	0	0	-5.74E-02	-9.46E-02	6.57E-02	9.48E-01	9.40E-01	0	0	0	8
22	18	2212	0	0	114	116	6.50E-02	-1.05E-01	8.23E-02	9.50E-01	9.38E-01	0	0	0	1
23	14	2112	0	0	0	0	5.38E-02	7.01E-02	-1.52E-01	9.56E-01	9.40E-01	0	0	0	8
24	14	2112	0	0	0	0	-1.47E-02	-1.96E-02	1.10E-01	9.46E-01	9.40E-01	0	0	0	8
25	14	2212	0	0	0	0	-2.35E-02	-6.03E-03	-5.20E-02	9.40E-01	9.38E-01	0	0	0	1
26	14	2112	0	0	0	0	-1.76E-01	-4.48E-02	7.64E-03	9.57E-01	9.40E-01	0	0	0	8
27	14	2112	0	0	0	0	5.42E-02	-1.38E-02	1.39E-01	9.51E-01	9.40E-01	0	0	0	8
28	14	2112	0	0	0	0	1.16E-01	8.57E-02	-8.47E-02	9.54E-01	9.40E-01	0	0	0	8
29	14	2112	0	0	0	0	5.37E-03	-2.36E-03	-1.62E-01	9.53E-01	9.40E-01	0	0	0	8
30	18	2112	0	0	117	119	-6.65E-02	4.65E-02	-1.43E-01	9.54E-01	9.40E-01	0	0	0	8
31	14	2112	0	0	0	0	-1.99E-02	-1.23E-01	5.37E-02	9.49E-01	9.40E-01	0	0	0	8
32	18	2212	0	0	122	123	3.09E-02	1.12E-01	9.08E-02	9.50E-01	9.38E-01	0	0	0	1
33	14	2112	0	0	0	0	1.72E-02	-2.86E-02	9.12E-02	9.45E-01	9.40E-01	0	0	0	8
34	14	2112	0	0	0	0	3.73E-02	1.28E-01	5.68E-02	9.51E-01	9.40E-01	0	0	0	8
35	18	2212	0	0	124	125	4.83E-03	-4.50E-02	-1.51E-01	9.51E-01	9.38E-01	0	0	0	1
36	14	2112	0	0	0	0	1.37E-02	-1.60E-01	-5.46E-02	9.55E-01	9.40E-01	0	0	0	8
37	14	2212	0	0	0	0	-8.33E-02	-3.15E-02	-1.10E-01	9.49E-01	9.38E-01	0	0	0	1
38	18	2212	0	0	126	127	1.26E-01	-4.03E-03	1.52E-02	9.47E-01	9.38E-01	0	0	0	1
39	14	2212	0	0	0	0	7.30E-02	-2.90E-02	1.54E-01	9.54E-01	9.38E-01	0	0	0	1
40	18	2112	0	0	128	129	-4.31E-02	-4.22E-02	-6.67E-02	9.44E-01	9.40E-01	0	0	0	8
41	14	2112	0	0	0	0	-7.35E-02	-9.86E-02	7.55E-02	9.51E-01	9.40E-01	0	0	0	8

The next entries come from the subroutines XKSAMP and FLKSAM (in module DPMNUC3) assigning x values and flavor to the quarks participating in the interaction: The projectile proton is split into a d valence

quark, an valence diquark (uu) (both with status ISTHKK=21), and two quarks s and $\bar{s}$ from a colorless sea pair (status ISTHKK=31). The interacting target nucleons are split in valence quark-diquark systems: the neutron (entry 18) into d-(ud), the proton (entry 13) into u-(ud). The x values given for each quark system as PHKK(3,i)=PHKK(4,i) add up to one for each individual hadron.

```
42  21     1   1   0  56  56   .00E+00   .00E+00  2.69E-01  2.69E-01   .00E+00  0  0  0 391
43  21  2203   1   0  59  59   .00E+00   .00E+00  1.77E-01  1.77E-01   .00E+00  0  0  0 410
44  31     3   1   0  50  50   .00E+00   .00E+00  1.61E-01  1.61E-01   .00E+00  0  0  0 395
45  31    -3   1   0  53  53   .00E+00   .00E+00  3.93E-01  3.93E-01   .00E+00  0  0  0 396
46  22     2  13   0  60  60   .00E+00   .00E+00  3.11E-01  3.11E-01   .00E+00  0  0  0 393
47  22  2103  13   0  57  57   .00E+00   .00E+00  6.89E-01  6.89E-01   .00E+00  0  0  0 410
48  22     1  18   0  54  54   .00E+00   .00E+00  3.82E-01  3.82E-01   .00E+00  0  0  0 391
49  22  2103  18   0  51  51   .00E+00   .00E+00  6.18E-01  6.18E-01   .00E+00  0  0  0 410
```

The following entries come from the routines constructing the colorless parton-parton chains. First the chains are considered (in subroutine KKEVSV) which are composed from projectile sea quarks and target valence quarks. In this example there are two such chains: s-(ud) and $\bar{s}$-u. The entries are made subsequently for the partons forming the chain and the constructed chain itself, with the array PHKK(5,i) containing the corresponding 4-momenta and the mass, resp. The 4-momenta are defined in the cms system of the incident hadron and a single nucleon (without Fermi momentum). By definition these chains get the status ISTHKK=4, the status of quarks/quark systems at chain ends is increased by 100 compared to their previous entries.

Please note: quarks, diquarks and chains have no BAMJET code, therefore the last entry in the line (IDBAM(i)) picks up values without significance

```
50 131     3  44   1  52  52  4.47E-01  1.25E-01  1.04E+00  1.61E+00   .00E+00  0  0  0 395
51 122  2103  49  18  52  52  1.10E-01 -5.04E-02 -5.77E+00  6.26E+00   .00E+00  0  0  0 410
52   4 88888  50  51  62  74  5.57E-01  7.44E-02 -4.72E+00  7.87E+00  6.27E+00  0  0  0   0
53 131    -3  45   1  55  55 -8.24E-02 -2.11E-02 -3.55E+00  3.87E+00   .00E+00  0  0  0 396
54 122     1  48  18  55  55  1.39E-01 -2.70E-01  3.49E+00  3.82E+00   .00E+00  0  0  0 391
55   4 88888  53  54  75  91  5.67E-02 -2.91E-01 -6.25E-02  7.69E+00  7.68E+00  0  0  0   0
```

In the same manner the next entries describe the chains constructed from valence quark systems of both the projectile and a target nucleon (proton in this example) in the subroutine KKEVVV. Entries for all chains are marked by the identity IDHKK=88888, valence-valence chains get the status ISTHKK=3.

```
56 121     1  42   1  58  58  1.77E-01  5.50E-01  2.01E+00  2.63E+00   .00E+00  0  0  0 391
57 122  2103  47  13  58  58  9.89E-02  3.07E-01 -5.78E+00  6.39E+00   .00E+00  0  0  0 410
58   3 88888  56  57  92 105  2.76E-01  8.57E-01 -3.76E+00  9.01E+00  8.14E+00  0  0  0   0
59 121  2203  43   1  61  61 -2.23E-02 -1.89E-01 -1.95E+00  2.88E+00   .00E+00  0  0  0 410
60 122     2  46  13  61  61  2.35E-01 -8.85E-01  7.26E-01  1.79E+00   .00E+00  0  0  0 393
61   3 88888  59  60 106 113  2.13E-01 -1.07E+00 -1.22E+00  4.66E+00  4.36E+00  0  0  0   0
```

The next entries are generated by the routines HADRxx monitoring the chain decay.

First the decay of the (two) sea-valence chains is handled via HADRSV. With ISTHKK(i)=1 we find the final stable hadrons, with ISTHKK(i)=2 we find the resonances, which have decayed already within the JETSET fragmentation code. Also stable hadrons might have ISTHKK(i)=2, in this case they have interacted subsequently in the formation zone cascade.

After event completion the 4-momenta are given in the laboratory system.

```
62   2   211  52   0 106 108  5.32E-01 -1.49E-01  2.83E+00  2.89E+00  1.40E-01  0  0  0  13
63   1  2112  52   0   0   0  7.20E-02  2.42E-01  8.46E-01  1.29E+00  9.40E-01  0  0  2   8
64   1   310  52   0   0   0  2.64E-02 -1.56E-01  5.93E+00  5.96E+00  4.98E-01  0  0  2  19
65   1  -211  52   0   0   0 -9.31E-03  2.37E-01  2.30E+00  2.31E+00  1.40E-01  0  0  2  14
66   1   111  52   0   0   0  3.24E-03  1.13E-01  1.80E+01  1.80E+01  1.35E-01  0  0  2  23
67   1    22  52   0   0   0 -4.55E-02 -3.65E-02  9.03E-02  1.08E-01  2.63E-09  0  0  0   7
68   1   211  52   0   0   0  9.86E-02 -6.37E-02  1.63E+00  1.64E+00  1.40E-01  0  0  2  13
69   1  -211  52   0   0   0 -1.24E-01 -1.24E-01  4.44E-01  4.98E-01  1.40E-01  0  0  2  14
70   2  -311  52   0   0   0  2.64E-02 -1.56E-01  5.93E+00  5.96E+00  4.98E-01  0  0  0  25
71   2  -213  52   0   0   0 -6.07E-03  3.50E-01  2.03E+01  2.03E+01  7.61E-01  0  0  0  34
72   2   221  52   0   0   0 -7.12E-02 -2.24E-01  2.17E+00  2.25E+00  5.49E-01  0  0  0  31
```

73	1	-211	55	0	0	0	1.53E-01	-1.69E-01	2.52E-01	3.68E-01	1.40E-01	0	0	0	14
74	1	321	55	0	0	0	4.12E-01	-4.39E-01	1.11E+01	1.11E+01	4.94E-01	0	0	2	15
75	1	111	55	0	0	0	1.72E-02	6.53E-02	1.58E-01	2.18E-01	1.35E-01	0	0	0	23
76	1	111	55	0	0	0	3.70E-02	-1.24E-01	7.65E-01	7.87E-01	1.35E-01	0	0	2	23
77	1	310	55	0	0	0	-5.80E-01	-8.91E-02	5.04E+00	5.09E+00	4.98E-01	0	0	0	19
78	1	111	55	0	0	0	-1.30E-01	-1.27E-01	1.47E+01	1.47E+01	1.35E-01	0	0	2	23
79	1	211	55	0	0	0	1.07E-01	1.68E-02	3.59E-01	4.00E-01	1.40E-01	0	0	0	13
80	1	-211	55	0	0	0	-6.77E-02	-8.59E-02	5.71E-01	5.98E-01	1.40E-01	0	0	2	14
81	1	111	55	0	0	0	-2.73E-02	7.09E-02	8.76E-01	8.90E-01	1.35E-01	0	0	2	23
82	1	310	55	0	0	0	1.32E-01	5.92E-01	4.48E+01	4.48E+01	4.98E-01	0	0	2	19
83	2	331	55	0	0	0	6.69E-02	-5.56E-02	2.73E+00	2.90E+00	9.58E-01	0	0	0	95
84	2	-311	55	0	0	0	-5.80E-01	-8.91E-02	5.04E+00	5.09E+00	4.98E-01	0	0	0	25
85	2	313	55	0	0	0	1.78E-03	4.65E-01	5.95E+01	5.95E+01	9.00E-01	0	0	0	37
86	2	221	55	0	0	0	1.24E-02	1.88E-03	1.81E+00	1.89E+00	5.49E-01	0	0	0	31
87	2	311	55	0	0	0	1.32E-01	5.92E-01	4.48E+01	4.48E+01	4.98E-01	0	0	0	24
88	1	-211	58	0	0	0	3.16E-02	-1.71E-02	1.27E+01	1.27E+01	1.40E-01	0	0	2	14
89	2	-211	58	0	109	111	3.16E-01	6.96E-03	8.12E-01	8.82E-01	1.40E-01	0	0	0	14
90	1	2212	58	0	0	0	9.25E-02	3.89E-01	9.24E-01	1.38E+00	9.38E-01	0	0	2	1
91	1	211	58	0	0	0	2.26E-01	3.80E-01	1.14E+01	1.14E+01	1.40E-01	0	0	2	13
92	1	111	58	0	0	0	1.25E-01	-1.04E-01	1.61E+01	1.61E+01	1.35E-01	0	0	2	23
93	2	-211	58	0	112	113	-4.66E-02	-9.81E-03	3.74E-01	4.02E-01	1.40E-01	0	0	0	14
94	1	111	58	0	0	0	1.24E-01	7.43E-02	5.40E+00	5.40E+00	1.35E-01	0	0	2	23
95	1	211	58	0	0	0	-3.45E-01	-1.16E-01	4.67E+00	4.68E+00	1.40E-01	0	0	0	13
96	1	111	58	0	0	0	-2.52E-01	2.37E-01	1.56E+00	1.61E+00	1.35E-01	0	0	0	23
97	2	213	58	0	0	0	3.52E-01	2.77E-01	2.81E+01	2.81E+01	7.67E-01	0	0	0	32
98	2	-213	58	0	0	0	7.73E-02	6.45E-02	7.50E+00	7.54E+00	7.67E-01	0	0	0	34
99	2	213	58	0	0	0	-5.97E-01	1.21E-01	7.35E+00	7.41E+00	7.67E-01	0	0	0	32
100	1	111	61	0	0	0	6.28E-01	-4.76E-01	2.01E+00	2.16E+00	1.35E-01	0	0	2	23
101	1	2112	61	0	0	0	3.12E-01	-5.54E-03	1.10E+01	1.11E+01	9.40E-01	0	0	0	8
102	1	211	61	0	0	0	-5.12E-01	-4.63E-01	1.65E+01	1.65E+01	1.40E-01	0	0	0	13
103	1	211	61	0	0	0	-5.26E-03	-2.73E-01	7.02E-01	7.66E-01	1.40E-01	0	0	0	13
104	1	111	61	0	0	0	-2.10E-01	1.44E-01	5.12E+00	5.13E+00	1.35E-01	0	0	2	23
105	2	213	61	0	0	0	-2.16E-01	-1.30E-01	4.80E+00	4.86E+00	7.67E-01	0	0	0	32

Next we find the entries from the formation zone cascade in subroutine FOZOKL. For instance the pion from entry 48 interacts with the target nucleon from entry 10, three hadrons result from this collision but one (entry 92) interacts later again. The status of the initial state target nucleon is changed to ISTHKK=2.

In some of the entries we find the status code ISTHKK(i)=16. This are nucleons fron secondary interactions not able to escape from the nucleus. These nucleons are available as targets for subsequent collisions.

106	1	111	62	22	0	0	3.99E-02	-2.70E-01	1.95E-01	3.61E-01	1.35E-01	0	0	0	23
107	1	2212	62	22	0	0	7.63E-02	1.16E-01	2.13E-01	9.72E-01	9.38E-01	0	0	0	1
108	1	211	62	22	0	0	4.51E-01	-1.44E-01	2.42E+00	2.47E+00	1.40E-01	0	0	0	13
109	2	-211	89	30	114	115	2.97E-01	-3.94E-02	1.21E-01	3.52E-01	1.40E-01	0	0	0	14
110	1	2112	89	30	0	0	-2.40E-01	7.32E-02	1.37E-01	9.82E-01	9.40E-01	0	0	0	8
111	1	111	89	30	0	0	2.65E-01	-2.55E-03	3.66E-01	4.72E-01	1.35E-01	0	0	0	23
112	1	-211	93	16	0	0	-1.53E-01	-2.30E-01	8.24E-02	3.20E-01	1.40E-01	0	0	0	14
113	2	2112	93	16	116	117	-6.90E-02	3.18E-01	2.93E-01	1.04E+00	9.40E-01	0	0	0	8
114	1	-211	109	32	0	0	2.36E-01	-1.03E-01	1.63E-01	3.35E-01	1.40E-01	0	0	0	14
115	16	2212	109	32	0	0	8.60E-02	1.78E-01	4.57E-02	9.60E-01	9.38E-01	0	0	0	1
116	1	2112	113	35	0	0	-2.18E-01	8.13E-02	9.36E-03	9.68E-01	9.40E-01	0	0	0	8
117	2	2212	113	35	118	119	2.47E-01	1.57E-01	1.29E-01	9.91E-01	9.38E-01	0	0	0	1
118	2	2212	117	38	120	121	2.17E-01	1.81E-01	3.63E-02	9.81E-01	9.38E-01	0	0	0	1
119	16	2212	117	38	0	0	1.56E-01	-2.77E-02	1.08E-01	9.58E-01	9.38E-01	0	0	0	1
120	16	2212	118	40	122	0	8.07E-03	-4.02E-02	-1.32E-01	9.48E-01	9.38E-01	0	0	0	1
121	1	2112	118	40	0	0	7.57E-02	8.15E-02	4.63E-02	9.47E-01	9.40E-01	0	0	0	8

The final entries in the COMMON block refer to the evaporation step of the excited residual target nucleus. With status code ISTHKK(i)=1000 we find the excited residual nucleus. Evaporation nucleons, deexcitation

photons and nuclear fragments follow with status code ISTHKK(i)=-1 and the stable residual nuclei follows with status code ISTHKK(i)=1001.

```
1221000 80000    2 120 123 133  1.76E-01  2.24E-01  1.81E-01  3.18E+01  3.18E+01 34 16  0  0
123   -1  2112 122   0   0   0 -3.47E-02 -4.91E-02 -1.05E-02  9.42E-01  9.40E-01  0  0  2  8
124   -1  2112 122   0   0   0 -6.45E-02  9.39E-02 -3.79E-02  9.47E-01  9.40E-01  0  0  2  8
125   -1  2112 122   0   0   0  7.39E-02 -1.42E-02 -3.79E-02  9.43E-01  9.40E-01  0  0  2  8
126   -1  2112 122   0   0   0  2.90E-03  4.85E-03 -3.86E-03  9.40E-01  9.40E-01  0  0  2  8
127   -1  2212 122   0   0   0  7.99E-02  1.92E-02 -8.41E-02  9.46E-01  9.38E-01  0  0  2  1
128   -1  2212 122   0   0   0 -9.46E-03  3.00E-02  1.17E-01  9.46E-01  9.38E-01  0  0  2  1
129   -1  2212 122   0   0   0  7.64E-02 -6.67E-02  2.71E-02  9.44E-01  9.38E-01  0  0  2  1
130   -1    22 122   0   0   0  1.65E-03 -1.64E-03  9.02E-04  2.50E-03  3.39E-10  0  0  2  7
131   -1    22 122   0   0   0 -9.27E-04  1.22E-03  3.42E-03  3.75E-03  2.16E-10  0  0  2  7
132   -1 80000 122   0   0   0 -2.53E-01  4.54E-02 -1.07E-02  2.82E+00  2.81E+00  3  1  2  0
1331001 80000 122   0   0   0  3.04E-01  1.61E-01  2.16E-01  2.23E+01  2.23E+01 24 12  2  0
```

Eventually the actual final state hadrons, photons and nuclei are obtained from the common block /HKKEVT/ by picking up all particles with the status ISTHKK=1, ISTHKK=-1 and ISTHKK=1001.

Appendix C : Further options for internal use

- Code word = 'CMENERGY'

  Same as for code word 'ENERGY', but WHAT(1) defines the energy in the hadron/nucleon–nucleon c.m. system.

- Code word = 'PAULI'

  This option monitors the inclusion of Pauli's principle for the intranuclear cascade.

  WHAT(1) : Pauli principle active for 1.0 (default)

  WHAT(2) : triggers test prints for debugging if greater than 0.0;
  default : 0.0, i.e. no additional printout.

- Code word = 'INTPT'

  This option monitors the additional sampling of transverse momenta for partons;

  WHAT(1) : 1.0 activates the sampling of parton p_t values (default).

- Code word = 'TECALBAM'

  This option triggers tests of the hadronization routines; additional input cards are required (see subroutine TECALB), to be given immediately after the code word definition; WHAT parameters have no meaning.

- Code word = 'HADRIN'

  Via this option the secondary interactions generated from FHAD may be forced to be all inelastic/elastic ones.

  WHAT(1) = 0 : inelastic/elastic as monitored by FOZOKL
  1 : inelastic collisions forced
  2 : elastic collisions forced.

- Code word = 'OUTLEVEL'

  This option monitors the printout of intermediate results for diagnostics;

  WHAT(I) $\geq$ **1:** diagnostics for remaining minor problems is printed (mainly consistency/ accuracy problems in kinematical calculations).

Table 3: Additional options read by the main program

Option	Description
CMENERGY	c.m. energy (GeV per nucleon)
SEADISTR	monitors the x-behaviour of the quark distributions
FERMI	monitors assignment of Fermi momenta to nucleons
PAULI	monitors inclusion of Pauli principle
COULOMB	monitors treatment of Coulomb potential
SEASU3	changes the probability of sea chain end s quarks
COMBIJET	controls the chain fusion option
INTPT	monitors assignment of intrinsic p_t to partons
ALLPART	forces the decay of all chains
VALVAL	forces the decay of valence-valence chains
SEAVAL	forces the decay of sea-valence chains
VALSEA	forces the decay of valence-sea chains
SEASEA	forces the decay of sea-sea chains
PARTEV	additional histograms for parton-level events
DIQUARKS	to switcj off diquarks at sea–chain ends
PROJKASK	inclusion of the cascade within the projectile
OUTLEVEL	monitors printout for debugging
HBOOKHIS	serves to switch off HBOOK histograms
CMHISTO	event scoring in the nucleon-nucleon cms
TECALBAM	test run for BAMJET requested
SIGTEST	tables and double-log plots of cross sections
HADRIN	force inelastic/elastic collisions in FHAD
NOFINALE	Skip call of the routine FICONF
COMBIJET	Implement the chain fusion option of DPMJET–II
RECOMBIN	Combinatorics of sea and valence chain endsa
FLUCTUAT	introduce cross section fluctuations

- Code word = 'NOFINALE'

  This option skips the call of the routine FICONF, for instance in heavy ion collisions;
  WHAT(I) = 1. : no FICONF call, Default: 0.:

- Code word = 'COMBIJET'

  Call the chain fusion option of DPMJET–II (see Ref. [116] .
  WHAT(1) = 0 no chain fusion, Default: 0. :
  What(1) = 1 chain fusion implemented.
  WHAT(2) = NCUTOF = : minimum number of uncombined chains
  from single projectile or target nucleon.

- Code word = 'RECOMBIN'

  Combinatoric transformation of s–s and v–v chains into s–v and v–s chains
  WHAT(1) = 0 no recombination,
  What(1) = 1 recombination implemented.
  Default: 1.

- Code word = 'FLUCTUAT'

implement cross section fluctuation (see Ref. [117, 118, 119])

WHAT(1) = 0 no fluctuations,
What(1) = 1 fluctuations implemented.
Default: 0.

Appendix D : Further options from the DTUJET–97 code

Table 4: DTUJET options read by the main program

Option	Description
STRUCFUN	deep inelastic structure functions
PSHOWER	demands parton showering
GLUESPLIT	prevents splitting of gluons
SELHARD	defines the sampling of hard scattering
SIGMAPOM	defines options for the DTU unitarization
SAMPT	defines options for intrinsic pt of soft chains

- Code word: STRUCFUN

  Defines the structure functions used in the sampling of hard constituent scattering [120, 45, 121]
  .

  WHAT(1): = ISTRUF
  ISTRUF = 3 : Martin, Roberts, Stirling:Set 1
  ISTRUF = 9 Kwiecinski,Martin, Roberts, Stirling: Set B0
  ISTRUF = 10 : Kwiecinski,Martin, Roberts, Stirling: Set B_-
  ISTRUF = 11 : Kwiecinski,Martin, Roberts, Stirling: Set B_{-2}
  ISTRUF = 12 : Kwiecinski,Martin, Roberts, Stirling: Set B_{-5}
  ISTRUF = 13 : Martin, Roberts, Stirling (1992): Set S0
  ISTRUF = 14 : Martin, Roberts, Stirling (1992): Set D0
  ISTRUF = 15 : Martin, Roberts, Stirling (1992): Set D_-
  ISTRUF = 16 : CTEQ Collaboration (1993): Set 1M
  ISTRUF = 17 : CTEQ Collaboration (1993): Set 1MS
  ISTRUF = 18 : CTEQ Collaboration (1993): Set 1ML
  ISTRUF = 19 : CTEQ Collaboration (1993): Set 1D
  ISTRUF = 20 : CTEQ Collaboration (1993): Set 1L
  The last 3 exist only as 221, 222 and 223
  ISTRUF = 21 : Glueck,Reya,Vogt with K = 1: GRV94LO
  ISTRUF = 22 : Glueck,Reya,Vogt with K = 2: GRV94LO
  ISTRUF = 23 : CTEQ Collaboration (1996): CTEQ96
  ISTRUF = 210 .. 223 : as above with energy dependent $p_\perp$ threshold value
  The default is 222 .

  The hard process contributes above a $p_\perp$ threshold. The threshold is set for less than three digits ISTRUF values to 3 GeV by default. This option was used in the earlier DTUJET–92 version of the program. An energy dependent cutoff[5] can avoid a hard scattering cross section too large to be treated in our simple eikonal approximation. To use this new option the number 200 has to be added to the chosen ISTRUF value.

- Code word: PSHOWER

  This card determines whether hard partons initiate showers and is only recognized in connection with JETSET fragmentation. As the BAMJET option presently contains no parton showering it does not reproduce the $p_\perp$–distribution as well as the JETSET option.

WHAT(1): = IPSHOW
IPSHOW = 0 : Generation of hard parton showers suppressed.
IPSHOW = 1 :Hard parton showers are included.
The default is 1.

- Code word: GLUESPLIT

Prevents splitting of gluons into quark–antiquark pairs.

WHAT(1): = NUGLUU, Default: 1
NUGLUU=1 :Only one jet in hard gluon scattering.
Recommended: NUGLUU=1.

WHAT(2): = NSGLUU, Default: 0
NSGLUU=1 :Only one jet in soft sea gluon jets.
Recommended: NSGLUU=0.

- Code word: SELHARD

Defines the sampling of hard scattering of constituents and/or demands a test run.

WHAT(5): = PTTHR, Default: 3
Threshold $p_\perp$ for the hard scattering
of constituents in GeV/c

WHAT(6): = PTTHR,2 Default: 3
Threshold $p_\perp$ for the first hard scattering
of constituents in GeV/c

- Code word: SIGMAPOM

Defines options and/or demands a test run for the calculation of the DTU model unitarizing the soft and hard hadronic cross sections. The test run is for calculating the total and inelastic cross sections as functions of the collision energy as well as initializing and testing the sampling of multi-Pomeron events at some typical energies. Without the test run only the initialization at the energy defined in the run is done.

WHAT(1): = ITEST, test run for ITEST = 1.

WHAT(2) = ISIG, characterizes the soft and hard input cross sections for the unitarization (see SUBROUTINE SIGSHD).
Recommended and default: ISIG = 10

WHAT(3) = IPIM characterizes the method to calculate the distribution in the number of soft n_s and hard n_h Pomerons
Default and recommended: IPIM = 482

WHAT(4) = LMAX Default: 25
LMAX :Maximum considered number of soft Pomerons (Less than 26).

WHAT(5) = MMAX Default: 25
MMAX :Maximum considered number of hard Pomerons (Less than 26).

WHAT(5) = NMAX Default: 2
NMAX :Maximum considered number of triple–Pomerons (Less than 13).